

12-1995

Tectonic denudation of Mesozoic contractile structures by a low-angle normal fault and associated faults, southern White Pine Range, Nevada

Holly Langrock
University of Nevada, Las Vegas

Follow this and additional works at: <https://digitalscholarship.unlv.edu/thesesdissertations>



Part of the [Geology Commons](#), and the [Tectonics and Structure Commons](#)

Repository Citation

Langrock, Holly, "Tectonic denudation of Mesozoic contractile structures by a low-angle normal fault and associated faults, southern White Pine Range, Nevada" (1995). *UNLV Theses, Dissertations, Professional Papers, and Capstones*. 1420.
<http://dx.doi.org/10.34917/3339725>

This Thesis is protected by copyright and/or related rights. It has been brought to you by Digital Scholarship@UNLV with permission from the rights-holder(s). You are free to use this Thesis in any way that is permitted by the copyright and related rights legislation that applies to your use. For other uses you need to obtain permission from the rights-holder(s) directly, unless additional rights are indicated by a Creative Commons license in the record and/or on the work itself.

This Thesis has been accepted for inclusion in UNLV Theses, Dissertations, Professional Papers, and Capstones by an authorized administrator of Digital Scholarship@UNLV. For more information, please contact digitalscholarship@unlv.edu.

**TECTONIC DENUDATION OF MESOZOIC CONTRACTILE STRUCTURES
BY A LOW-ANGLE NORMAL FAULT AND ASSOCIATED FAULTS,
SOUTHERN WHITE PINE RANGE, NEVADA**

by

Holly Langrock

A thesis submitted in partial fulfillment
of the requirements for the degree of

Master of Science


in

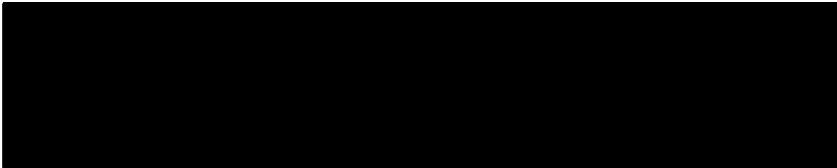
Geology

Department of Geoscience
University of Nevada, Las Vegas
December 1995

The thesis of Holly Langrock for the degree of Master of Science in Geology is approved.


Chairperson, Wanda J. Taylor, Ph.D.


Examining Committee Member, Margaret N. Rees, Ph.D.


Examining Committee Member, Eugene I. Smith, Ph.D.


Graduate Faculty Representative, Kathleen Robins, Ph.D.


Interim Dean of the Graduate College, Cheryl L. Bowles, Ed.D.

University of Nevada, Las Vegas
December 1995

ABSTRACT

The Blackrock Canyon area in the southern White Pine Range, Nevada mostly consists of the highly extended upper plate of a low-angle normal fault, the Blackrock fault. The post-31.3 Ma Blackrock fault places upper Paleozoic sedimentary rocks and overlying Tertiary volcanic rocks of the Garret Ranch Group in its hangingwall against a 50° E-dipping homocline of Cambrian through Mississippian rocks in its footwall.

The 15 to 30°W-dipping Blackrock fault is non-planar and consists of two fault segments and a pronounced corrugation, the Bull Spring corrugation. These geometric irregularities suggest the slip direction on the fault was east-southeast or west-northwest. Additional geometric data such as dips of footwall strata and bedding-to-fault angles constrain the slip direction to west-northwest. This movement of the upper plate over the irregular Blackrock fault resulted in non-conservative deformation within the hangingwall block.

Blackrock upper plate faults with diverse attitudes are approximately synchronous and orthorhombically symmetrical. Classical Andersonian conjugate faulting theory, which employs two-dimensional (plane) strain cannot explain these geometric and temporal fault relationships. Rather, these data suggest that non-conjugate processes generated these faults and that they represent three-dimensional or non-plane strain. A kinematic model, which invokes movement of the hangingwall block over a geometrically irregular detachment, explains the non-conservative, three-dimensional deformation observed in the Blackrock upper plate.

In the Blackrock upper plate, Blackrock-related faults cut and Tertiary volcanic rocks cover Mesozoic contractile structures. Restored and retrodeformable cross sections allow the reconstruction of the pre-extensional structures. They indicate that normal movement on the Blackrock fault tectonically denuded and disrupted Mesozoic folds and a previously unrecognized thrust fault, which is here named the White Pine thrust.

A restored and retrodeformable cross section across the Pancake Range, Duckwater Hills, and the White Pine Range reveals large-scale folds and thrust faults that are part of the central Nevada thrust belt. These structures correlate with previously reported folds and thrust faults that crop out in surrounding areas and consist of the Pancake thrust, McClure Spring syncline, Duckwater thrust, and the Easy Ridge or Green Springs thrust (Pipkin, 1956; Humphrey, 1960; Nolan and others, 1974; Perry and Dixon, 1993; Carpenter and others, 1993). This regional step-wise balanced and restored cross section, for the first time, allows (1) documentation of central Nevada thrust belt geometry across northern Railroad Valley and (2) examination of Tertiary extensional structural styles and the distribution of extension across this part of the belt. Together these findings suggest that northern Railroad Valley is an excellent petroleum prospect.

TABLE OF CONTENTS

ABSTRACT	iii
LIST OF FIGURES	vii
LIST OF PLATES	viii
LIST OF TABLES	viii
ACKNOWLEDGEMENTS	ix
CHAPTER 1- INTRODUCTION	1
CHAPTER 2 REGIONAL GEOLOGY	4
Location	4
Geologic Background	4
CHAPTER 3 STRATIGRAPHY	14
CHAPTER 4 STRUCTURAL DESCRIPTIONS	19
Blackrock Fault	19
Hangingwall Structures	20
Fault Geometries and Spatial Relationships	20
Temporal Fault Relationships	21
Folds	22
Railroad Valley Fault	23
Footwall Structures	24
CHAPTER 5 STRUCTURAL INTERPRETATIONS	33
Relative Timing of the Blackrock fault	33
Kinematics of the Blackrock fault	34
Three-Dimensional Strain	37
Three Dimensional Strain in Extended Terranes	
A Kinematic Model	40
Evidence of Folding and Thrusting	41
Pre-Volcanic Folds	41
Paleo-relief	42
Thrust Faults	42
Central Nevada thrust belt	43
CHAPTER 6 REGIONAL STRUCTURES	52
Regional Retrodeformable Cross Section	52
Extension	53

Post-Volcanic Extension	54
Pre-Volcanic Extension	55
Central Nevada Thrust Belt Reconstruction	55
Pancake Range	56
Duckwater Hills	56
White Pine Range	57
Interpretation of the Regional Cross Section	59
Cenozoic Extensional Structural Styles and Distributions	59
Mesozoic Contractional Structural Styles and Distributions	60
CHAPTER 7 PETROLEUM POTENTIAL	63
Hydrocarbon Occurrence in the Great Basin	63
The Grant Canyon Field	
A Structural and Stratigraphic Analog	64
Stratigraphy	64
Structure	64
Petroleum Potential of the Blackrock Canyon Area	66
Stratigraphy	66
Structure	67
Oil Generation Potential	68
CHAPTER 8 SUMMARY AND CONCLUSIONS	73
APPENDIX A STRATIGRAPHIC DESCRIPTIONS	76
Paleozoic Sedimentary Formations	76
Tertiary Volcanic Units	82
APPENDIX B METHODS	94
Geologic Mapping	94
Cross Section Techniques	94
⁴⁰ Ar/ ³⁹ Ar Methods	95
X-ray Fluorescence Techniques	95
Point Count Analysis	96
REFERENCES CITED	98

LIST OF FIGURES

Figure 1. Location Map of the White Pine Range and the Study Area.....	10
Figure 2. Map of Tectonic Features of the Antler and Sonoran Orogenies	11
Figure 3. Map of Mesozoic Thrust Belts of the Cordillera	12
Figure 4. Map Showing Cenozoic Volcanism Patterns in the Great Basin	13
Figure 5. Paleozoic Stratigraphic Column	16
Figure 6. Tertiary Stratigraphic Column	18
Figure 7. Map of the Blackrock Fault in the Study Area	26
Figure 8. Structure Contour Map of the Blackrock Fault	27
Figure 9. Map of Blackrock Hangingwall Faults.....	28
Figure 10. Stereoplots of Spatial and Temporal Variations of Hangingwall ~Faults	29
Figure 11. Temporal Relationships Among Selected Hangingwall Faults	30
Figure 12. Map Showing Contractile Structures in the Study Area.....	31
Figure 13. Cross Sections Showing a Pre-Volcanic Fold Pair in the Blackrock Hangingwall	32
Figure 14. 3-D Block Diagram of Blackrock Fault Geometry	44
Figure 15. Two- and Three-Dimensional Strain Illustrations	45
Figure 16. Stereoplot of Poles to Selected Faults Illustrating Orthorhombic Symmetry	46
Figure 17. Stereoplot of Rotated Poles of All Post-Volcanic Hangingwall Faults.....	47
Figure 18. Cross Section Illustrating Paleo Relief	48
Figure 19. Deformed State and Restored Hangingwall Cross Sections of the Blackrock Fault	49
Figure 20. Nonrestorable Cross Section of the Blackrock Fault.....	50
Figure 21. Map of the Central Nevada Thrust Belt and Other Mesozoic Thrust Belts	51
Figure 22. Map Showing the Location of Structures Shown on the Regional Cross Section.....	62
Figure 23. Map of Oil Fields in Nevada	69
Figure 24. Cross Section of the Bacon Flat and Grant Canyon Oil Fields	70
Figure 25. Structure Contour Map Illustrating an Extension-Related Fold in the Grant Canyon Field	71
Figure 26. Structure Contour Map of the Railroad Valley Fault in the Grant Canyon	72
Figure 27. Cox Igneous Classification Diagram of the Blackrock andesite	91
Figure 28. Geochemical Plots of Andesites in the Duckwater Hills and White Pine Range Illustrating Similarities in Geochemistry	93

LIST OF PLATES

Plate 1. Geologic Map of the Blackrock Canyon Area, White Pine Range, Nevada.....	in pocket
Plate 2. Present Day and Restored Cross Sections of the Blackrock Canyon Area, White Pine Range.....	in pocket
Plate 3. Present Day and Restored Regional Cross Section.....	in pocket

LIST OF TABLES

Table 1. Modal and Volume Percentages of Constituents in Tertiary Volcanic Units.....	88
Table 2. $^{40}\text{Ar}/^{39}\text{Ar}$ Data of Sanidine Crystals From the Windous Butte Formation, Sample L94WP-307	90
Table 3. Major and Trace Element Concentrations of Andesite Collected in the Duckwater Hills (L94DH-3) and the Blackrock Canyon Area (L95WP-1).	92
Table 4. Standard Deviation, Precision, and Accuracy of Measurements Using Standards U.S.G.S. BIR-1, GIT-IWG BE-N, and U.S.G.S. MAG-1	97

ACKNOWLEDGEMENTS

First and foremost, I would like to thank my parents, Dave and Patti, for their endless love and support and my sister Heidi for encouraging me to have some fun along the way. I would also like to thank my advisor and friend, Dr. Wanda J. Taylor, for suggesting and funding this project and for her most appreciated patience, understanding, and assistance. I also greatly appreciate my committee members, Dr. Gene Smith, Dr. Margaret Rees, and Dr. Kathleen Robins for their helpful reviews and input and for their flexibility in working toward deadlines. Additionally, I thank Dr. Smith and Dr. Rees, for assistance with interpreting the geochemical data and in trilobite collection, respectively.

I acknowledge the following sources that granted funding for this project: American Chemical Society/Petroleum Research Fund grant #27576-GB2 to Dr. Wanda J. Taylor, American Association of Petroleum Geologists Research Grant, Geological Society of America Research Grant, Sigma Xi Grant-in-Aid of research, NSF-EPSCoR Summer Enhancement Grant and Research Assistantship, Anne F. Wyman Scholarship, Bernada E. French Scholarship, and Scrounger's Scholarship.

I would like to thank Jason Johnson for his cooking, mechanical, and story telling abilities and for keeping me safe and sane in the field. I thank Alex J. Sanchez and Shirley A. Morikawa (UNLV) for analyzing the XRF samples; Edna and Allen Forsgren of Duckwater, Nevada for their hospitality and jumper cables; Leigh Justet and Nate Stout for drafting assistance; Dr. Penny Amy, Dr. Margaret Rees, and Ms. Ellen Jacobson (UNLV, NSF-EPSCoR) for their assistance and support; Dr. Mike Taylor (U.S.

Geological Survey) for examining trilobite samples; Dr. William C. McIntosh (New Mexico Tech) for the $^{40}\text{Ar}/^{39}\text{Ar}$ age analysis; Chuck Henson and Mary Stahl (Apache Corporation) for aid in obtaining well data; Bob Bucola and Randy Stone for aid in interpreting well data; James A. Carpenter (Mobil) for insightful discussions on White Pine Range geology; and Dr. Barney Pipkin (University of Southern California) for lending me a personal copy of his geologic map.

I acknowledge each of the UNLV faculty and staff for their individual contributions and for creating a pleasant environment in which to work. I would particularly like to thank Kelly Rash for his wonderful friendship and support especially in the last months of completion. I wish to thank my good friends at UNLV; especially Meg Schramm, Kelly Boland, Shelly Cox, Gary Gin, Carole Farr, Alex Sanchez, and Jason Johnson for their support, smiling faces, and for the good times.

Last, but definitely not least, I thank Matthew J. Novak for his love, patience, understanding, reality checks, motivation, encouragement, editing skills, and a whole lot more. This one's for you, I couldn't have done it without you.

CHAPTER 1

INTRODUCTION

In well developed rifts, such as the Basin and Range Province, reconstruction of the pre-extensional structural framework is difficult because of severe extensional overprinting. In east-central Nevada, at the present latitude of the southern White Pine Range, the dominant pre-extensional structures are Mesozoic folds and thrust faults (Figure 1). These folds and thrust faults are disrupted by younger normal faults and covered by volcanic rocks that make reconstruction of the Mesozoic thrust belt difficult. The purpose of this study is to (1) reconstruct Mesozoic contractional deformation across the White Pine and Pancake Ranges, (2) document the Cenozoic extensional evolution of this area, and (3) analyze normal faulting processes and the development of three-dimensional strain.

Because of the lack of exposure of folds and thrust faults at this latitude, Armstrong (1968) designated central Nevada and parts of western Utah as the hinterland to the Sevier orogenic belt. This theory implies that this region only underwent minor contraction during the Mesozoic. However, several recent studies in central Nevada, including this one, document large-scale contractile structures indicating that this area underwent large-scale folding and thrusting in the Mesozoic (Nolan and others, 1974; Quinlivan and others, 1974; Fryxell, 1988, 1991; Camilleri, 1989, 1992; Bartley and Gleason, 1990; Perry, 1992; Armstrong and Bartley, 1993; Bartley and others, 1993; Taylor and others, 1993; Carpenter and others, 1993; Perry and Dixon, 1993). These large-scale folds and thrust faults crop out in the northern White Pine, Grant, Quinn

Canyon, and Pancake Ranges (Figure 1), and they typically are considered part of the central Nevada thrust belt (CNTB) (Speed and others, 1988; Bartley and others, 1993; Taylor and others, 1993).

In this thesis, I incorporate detailed geologic mapping and restored and retrodeformable cross sections of the southern White Pine Range and a regional cross section of the Pancake Range, Duckwater Hills, and the White Pine Range to deduce both the Mesozoic contractile and Cenozoic extensional development of this structurally complex area. These data yield reconstructions suggesting that the disrupted contractile structures, at this latitude, relate to folds and thrust faults exposed in the surrounding ranges, and thus, they represent part of the central Nevada thrust belt.

In the Basin and Range Province, low-angle and high-angle normal faults cut and displace pre-extensional thrust belts. Low-angle normal faults, widely documented in the Basin and Range Province, can accommodate a significant amount of extension (up to 400%) (Wernicke, 1992). In the southern White Pine Range, a low-angle normal fault (the Blackrock fault) and high-angle faults, exposed in the Pancake Range and Duckwater Hills, extended the Mesozoic thrust belt and nearly doubled its original width. In this study, detailed geometric and kinematic analyses of these normal faults provided the necessary data to reconstruct pre-extensional structures. Additionally, detailed structural analyses allow determination of extensional structural styles, distribution of extension, and faulting processes that generated the extension.

Here, I address faulting processes that generated faults in the vicinity of Blackrock Canyon, in the southern White Pine Range (Figure 1). Classically, researchers refer to Andersonian conjugate faulting theory to explain faults in rifts (e.g., Anderson, 1951; Ode', 1960; Varnes, 1962). However, geometrical and temporal fault relationships in several localities within the Basin and Range Province, including the southern White Pine Range, suggest that faults may also form by non-conjugate

processes, or non-plane strain (e.g., Donath, 1962; Thompson and Burke, 1973, Malone and others, 1975; Aydin and Reches, 1982; Smith, 1984; Langrock and Taylor, 1995). Recognition of these faulting processes in isolated localities is significant because it bears on our present understanding of large-scale extensional processes.

In the study area, faults with diverse attitudes crop out in the hangingwall of a low-angle normal fault. I employ detailed geologic mapping as well as geometrical and temporal analyses of these upper plate faults. The analyses suggest that the faults formed penecontemporaneously by non-conjugate faulting processes. Such non-conjugate faults, which reflect three-dimensional strain, are a documented part of many rifts (e.g., Donath, 1962; Thompson and Burke, 1973; Malone and others, 1975; Aydin, 1977; Aydin and Reches, 1982; Langrock and Taylor, 1995). Because such geometry is common, I combine southern White Pine Range data with geometric analysis of the controlling low-angle normal fault and propose a kinematic model that relates hangingwall faulting processes to the geometry of the controlling fault.

An additional incentive for studying the structural evolution of this region is to examine the petroleum potential of the area. The study area is located just 45 km (30 mi) northeast of Nevada's most productive oil fields. Several of Nevada's oil fields are structurally, stratigraphically, and thermally analogous to the study area. Structures and stratigraphy similar to that mapped in the range are in a fault block beneath the valley just west of the study area. The structures and strata necessary to promote hydrocarbon generation, migration, and entrapment appear to exist beneath northern Railroad Valley based on a comparison of the documented geology in the range and available well data.

CHAPTER 2

REGIONAL GEOLOGY

Location

The study area is located in the southern White Pine Range, White Pine County, Nevada (Figure 1). The White Pine Range is bounded on the west by Railroad Valley and on the east by White River Valley (Figure 1). The study area encompasses approximately 31 km² of the Currant Mtn., Duckwater NE, Green Springs, and Indian Garden Mtn. 7.5' topographic quadrangles and is in the vicinity of Blackrock Canyon.

Geologic Background

Throughout the Phanerozoic, much of the Basin and Range was subjected to (1) deposition of a thick succession of marine sedimentary rocks, (2) compressional orogeny during the Mesozoic, (3) magmatism, and (4) widespread extension mostly in Cenozoic time. The following simplified tectonic overview of the Basin and Range Province, particularly the Great Basin, puts rocks and structures in the study area into a regional context.

Subsequent to rifting in the Late Precambrian or earliest Cambrian (Levy and Christie-Blick, 1991), a westward-thickening wedge of dominantly carbonate strata was deposited from Cambrian to Devonian time along the passive continental margin of the western United States. The shallow carbonate shelf on which this thick package of rock was deposited is referred to as the Cordilleran miogeocline of western North America (Stewart and Poole, 1974; Stewart and Suczek, 1977). In the northeastern Great Basin,

Cambrian through Devonian miogeoclinal sediments have an estimated average thickness of 5000 m (Kellogg, 1963; Hose and Blake, 1976). Early Paleozoic sediments exposed in the study area include the Cambrian Windfall Formation, Ordovician Pogonip Group, Ordovician Eureka Quartzite, Ordovician Fish Haven Dolomite, Silurian Laketown Dolomite, and Devonian Guilmette Formation (Hague, 1883; Richardson, 1913; Nolan, 1935; Nolan and others, 1956).

During the first tectonic disturbance of this passive margin, the Late Devonian to Mississippian Antler Orogeny, basinal sediments and volcanic rocks were thrust eastward over shelf deposits along the Roberts Mountains thrust (Roberts and others, 1958; Silberling and Roberts, 1962; Miller and others, 1992) (Figure 2). The Antler Orogeny resulted in the uplift and partial erosion of the Roberts Mountains allochthon and the formation of an extensive foreland basin, the Antler foredeep. Deposition of both siliciclastic and carbonate sediments in the foredeep began during the Mississippian (Sadlick, 1960; Poole and Sandberg, 1977; Stevens, 1977). Antler foredeep deposits crop out throughout much of the Great Basin and include the Mississippian Chainman Shale, Diamond Peak Formation, and Joana Limestone in the White Pine Range (Hague, 1883; Spencer, 1917; Brew, 1961).

Following the Antler Orogeny, deposition of marine sedimentary rocks continued in the miogeocline. Pennsylvanian and Permian carbonates within the Basin and Range typically show significant facies variability and consist of greater amounts of siliciclastic sediment. These rock types and the presence of several intra-Permian disconformities suggest that this time interval was dominated by local uplifts and subsiding basins and that sediment accumulated in structurally controlled troughs (Carr and others, 1984; Stone and Stevens, 1984; Burchfiel and others, 1992). Pennsylvanian and Permian rocks that record this tectonism in the study area include the Ely Limestone, Reipe Spring

Formation, and Reipetown Formation (Lawson, 1906; Spencer, 1917; Steele, 1960; Bissell, 1964).

In latest Permian to earliest Triassic time, the continental margin underwent another major tectonic disturbance, the Sonoman orogeny. During this event, the Golconda thrust juxtaposed western basinal sediments and volcanic rocks against eastern shelf deposits and the Roberts Mountains allochthon (Figure 2) (Silberling and Roberts, 1962; Burchfiel and Davis, 1972; Speed, 1979; Gabrielse and others, 1983; Miller and others, 1992). Ultimately, this orogeny resulted in the accretion of the Klamath-Sierran island arc to western North America and the reconfiguration of the plate margin (Burchfiel and Davis, 1972; Speed, 1979; Miller and others, 1992; Saleeby and Busby-Spera, 1992). The extent of the Sonoman orogeny remains somewhat enigmatic and controversial due in part to the lack of associated foreland basin deposits and the extreme complexity of deformation within the Golconda allochthon. No structural or stratigraphic evidence suggests that this orogenic deformation extended as far east as the White Pine Range. However, recent studies by Perry (1994) suggest that Sonoman age contractile deformation may extend as far east as the Pancake Range (Figure 1).

This early Mesozoic reorganization of the western North American plate margin resulted in eastward subduction of oceanic lithosphere beneath the craton and the inception of an Andean-type continental arc. Near this time (post-Early Triassic) marine sedimentation in the miogeocline ceased (Saleeby and Busby-Spera, 1992). From the Triassic to the Middle Jurassic, the magmatic arc was restricted to a narrow band along the western edge of the continental margin and areas east of the arc were tectonically inactive. However, beginning in the Middle Jurassic, deformation and plutonism in the back arc region began to migrate eastward and eventually spread more than 1000 km into the craton (Burchfiel and others, 1992). This contraction is recorded in three major fold and thrust belts named, from west to east, the Luning-Fencemaker, Eureka or central

Nevada, and Sevier belts (Figure 3) (Armstrong, 1968; Oldow, 1983; Speed, 1983; Bartley and others, 1993; Taylor and others, 1993).

The Luning-Fencemaker allochthon or Winnemucca belt comprises a generally north-trending band of typically east-vergent and some west-vergent contractile structures in western Nevada (Figure 3) (Oldow, 1984; Speed and others, 1988). Deformation within the Luning-Fencemaker belt occurred between Middle(?) or Late Jurassic and Early Cretaceous (Oldow, 1984; Speed and others, 1988).

The Eureka belt, first defined by Speed (1983), is a belt of folds and thrust faults in the vicinity of Eureka, Nevada. The Eureka belt is a part of a continuous orogen called the central Nevada thrust belt (CNTB) that comprises a series of generally north-striking thrust faults and folds that extend from Eureka to Alamo, Nevada (Figure 3) (Bartley and others, 1993; Taylor and others, 1993). These ramp-flat type thrust faults mostly verge eastward, but west-vergent structures also crop out. Timing of deformation in the CNTB is widely bracketed between late Permian and 86 Ma (Bartley and Taylor, 1991; Bartley and others, 1993).

The Sevier orogenic belt extends from southeastern California into northern Canada (Figure 3). Deformation within this belt is bracketed between Late Jurassic (?) to late Late Cretaceous by Armstrong (1968) and from late Early Cretaceous to Late Cretaceous by Heller and others (1986). Thin-skinned east-vergent folds and thrust faults that exhibit ramp-flat geometries characterize the Sevier belt (Armstrong and Oriel, 1965; Allmendinger, 1992). Sevier thrusting and tectonic thickening resulted in the formation of an extensive foreland basin east of the orogenic front that contains up to 6 km of detritus (Armstrong and Oriel, 1965; Jordan, 1981; Burchfiel and others, 1992).

The White Pine Range lies along the eastern side of the central Nevada thrust belt and within the Sevier hinterland, as defined by Armstrong (1968) (Figure 3). No thrust faults crop out within the study area and only minor folds are exposed. However, a

north-trending fold train, the Illipah fold belt (Humphrey, 1960; Lumsden, 1964; Hose and Blake, 1976; Tracy, 1980; Guerrero, 1983), lies just 3 km north and northeast of the study area and large stratigraphic separation thrust faults crop out in the northern White Pine, Pancake, and Grant Ranges (Figure 1) (Humphrey, 1960; Misch, 1960; Fryxell, 1988, 1991; Camilleri, 1989, 1992; Nolan and others, 1974; Quinlivan and others, 1974; Hose and Blake, 1976; Kleinhampl and Ziony, 1985; Gleason, 1989; Bartley and Gleason, 1990; Perry, 1992; Perry and Dixon, 1993; Carpenter and others, 1993). Cross sections, produced in this study, illustrate the presence of these Mesozoic contractile structures in the subsurface.

Thin-skinned thrusting in the back-arc region generally ended during the Eocene (Armstrong, 1968; Allmendinger, 1992). Widespread extension commenced in the Basin and Range, during the Eocene, and it continues into the Holocene (Crone and Harding, 1984; Bartley and others, 1988; Taylor and others, 1989; Wernicke, 1992). Numerous Cenozoic high- and low-angle ($<30^\circ$ dip) normal faults crop out in the Great Basin and such faults are well documented within the White Pine Range (Lumsden, 1964; Moores and others, 1968; Tracy, 1980; Guerrero, 1983; this study). The low-angle faults are typically viewed as older structures that are then cut by younger, high-angle faults that collectively result in the present Basin and Range topography (Burchfiel and others, 1992; Wernicke, 1992). Several low-angle normal faults crop out in, but are not restricted to, metamorphic core complexes throughout the Basin and Range. In these metamorphic core complexes, low-angle normal faults juxtapose unmetamorphosed, brittlely deformed, highly extended hangingwall rocks against medium- to high-grade metamorphosed footwall rocks (Wernicke, 1981; Miller and others, 1983; Spencer, 1984; Davis and Lister, 1988; Spencer and Reynolds, 1990). Although early studies of low-angle normal faults focused on metamorphic core complexes, many recent studies

document examples of entirely upper crustal low-angle normal faulting within the Great Basin (e.g., Fryxell, 1988; Axen and others, 1990; Camilleri, 1992; this study).

Widespread Cenozoic volcanism occurred within the Basin and Range Province (Stewart and Carlson, 1976; Best and others, 1989; Axen and others, 1993). Stewart and Carlson (1976) summarized Cenozoic Basin and Range volcanism as the (1) extrusion of andesitic and rhyolitic lavas from 43 to 34 Ma; (2) eruption of silicic ash-flow tuffs and intermediate calc-alkaline rocks from 34 to 20 Ma; (3) production of bimodal basalt and rhyolite from 17 to 6 Ma; and (4) localized eruptions of cinder cones after 6 Ma. Great Basin volcanism migrated southward with time, beginning with effusive eruptions in the north during the Eocene and ending in the south with Oligocene-Miocene ignimbrite eruptions from calderas that define an irregular belt (Stewart and Carlson, 1976; Best and others, 1989; Axen and others, 1993) (Figure 4). Volcanic rocks exposed in the White Pine Range presumably erupted from calderas during this southward sweep. Basaltic volcanism began approximately 6 Ma and did not follow the southward sweep, but 3 belts formed across the Great Basin: one on the east side, one on the west side, and one near the center.

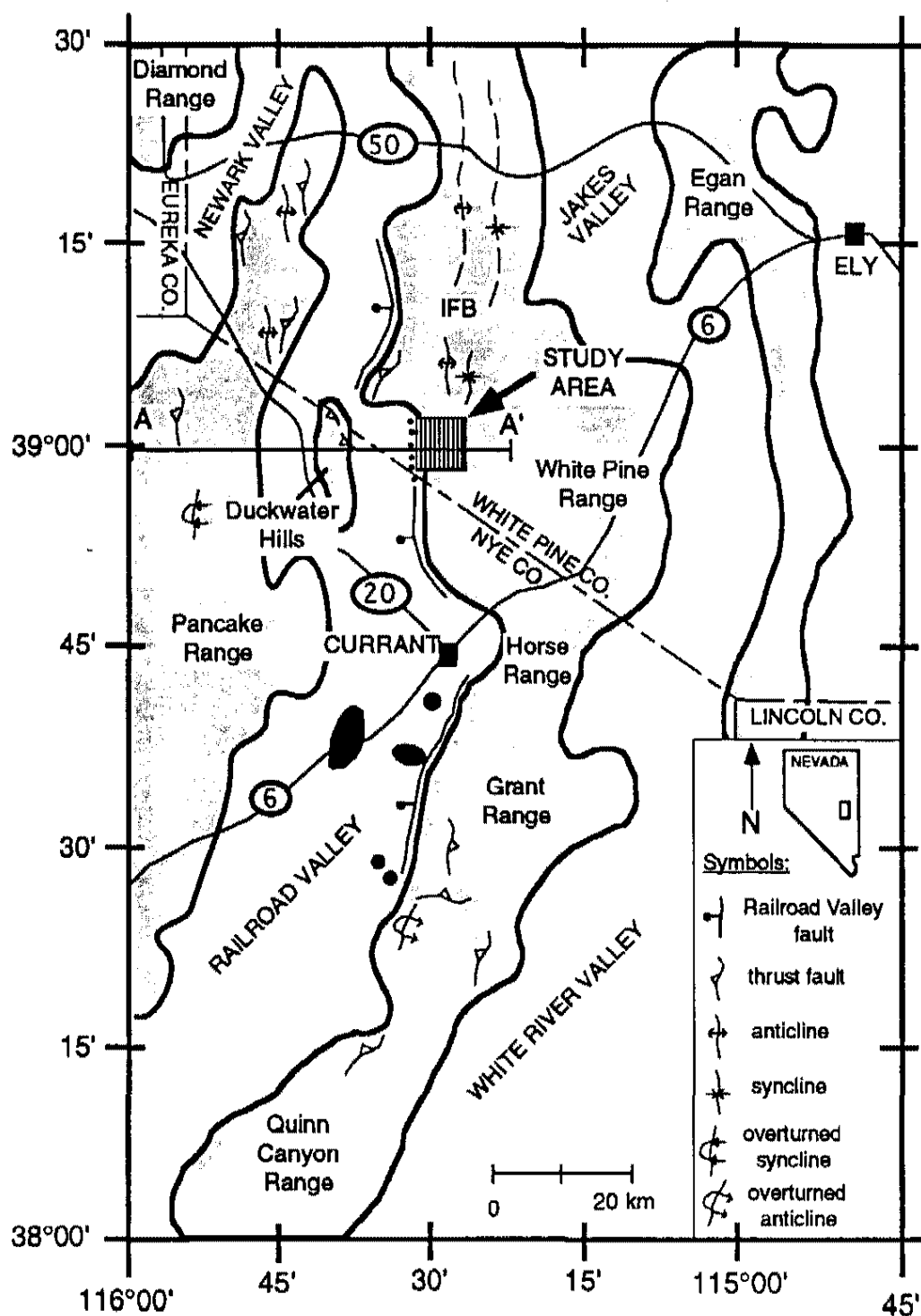


Figure 1. Location map of the White Pine Range and surrounding areas. The vertically ruled box indicates the study area. Oil fields are in black in Railroad Valley. A-A' shows the location of the regional cross section (Plate 3). Selected exposures of folds and thrust faults of the central Nevada thrust belt (CNTB) are shown and the Illipah fold belt is labeled IFB.

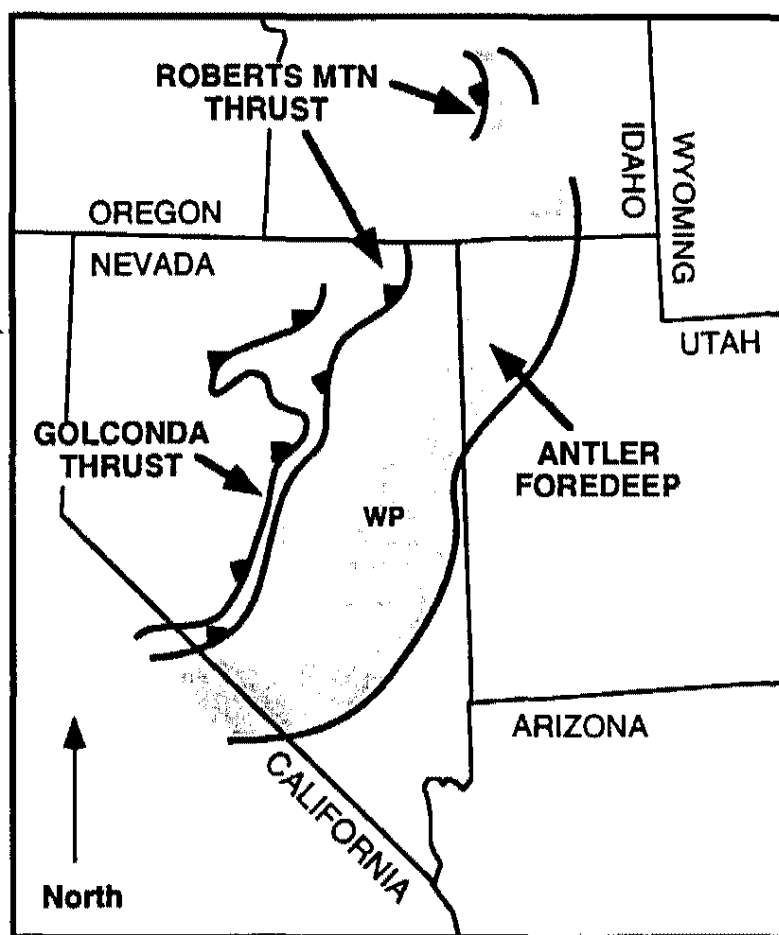


Figure 2. Map showing major tectonic features of the Antler and Sonoran orogenic belts. Eastern limits of the Roberts Mountain and Golconda thrusts are shown. The stippled region indicates the extent of the Antler foredeep during Mississippian time. WP denotes the location of the White Pine Range (modified from Burchfiel and others, 1992).

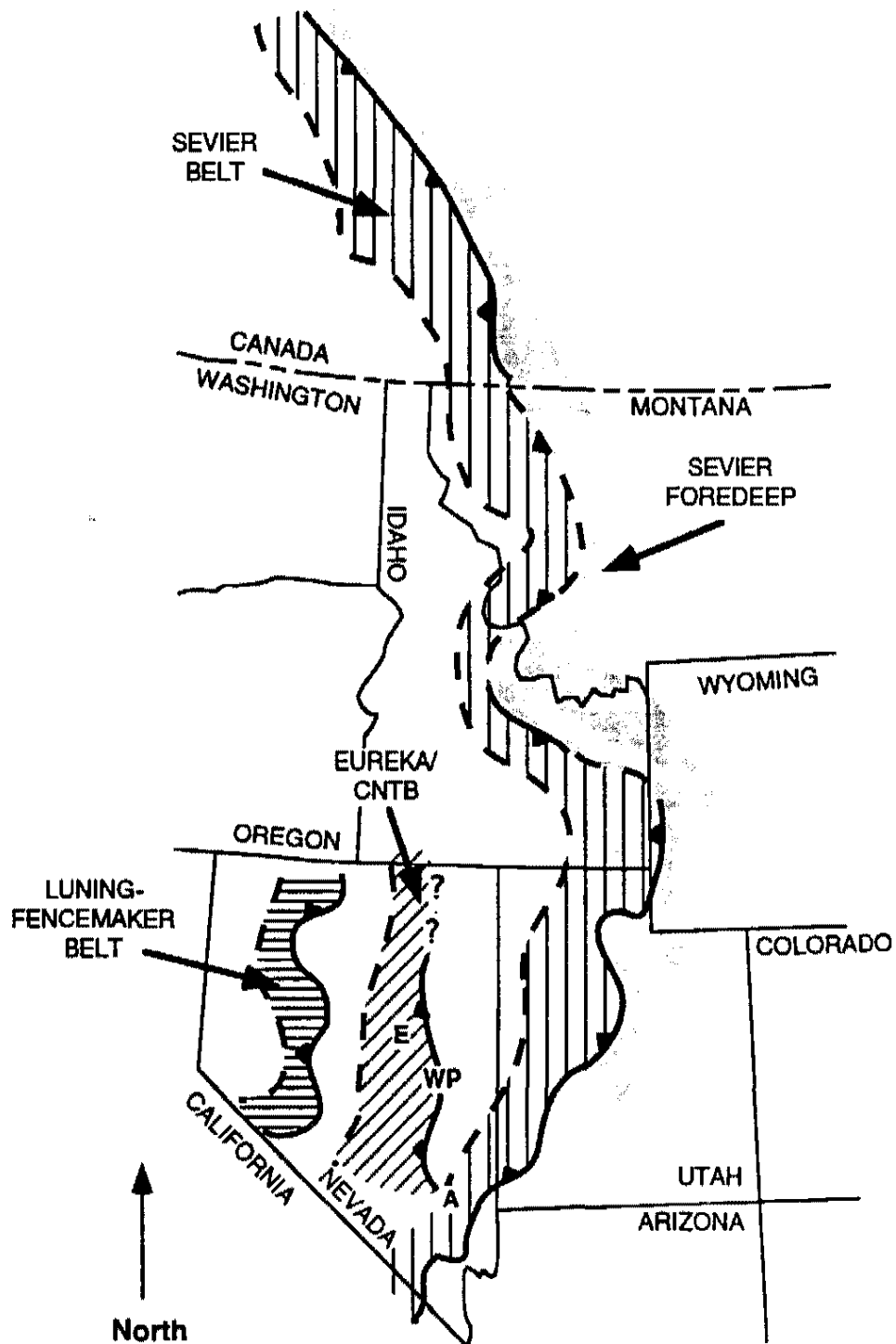


Figure 3. Map showing Mesozoic thrust belts of the Cordillera. WP denotes the location of the White Pine Range (modified from Burchfiel and others, 1992; Taylor and others, 1993) CNTB= central Nevada thrust belt, E= Eureka, A= Alamo.

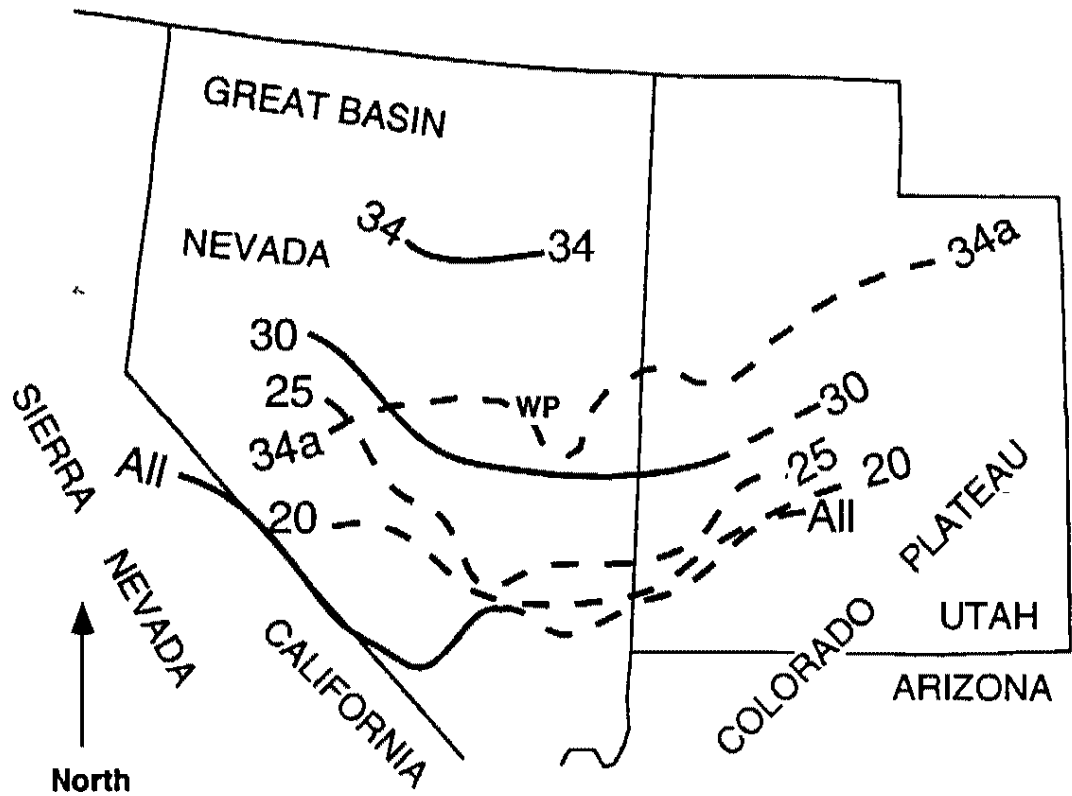


Figure 4. Map showing southward sweep of Tertiary volcanism with time across the Great Basin. Solid lines are the southernmost extent of calderas in Ma, except the southern limit of all calderas older than 5 Ma (All). The dashed line is the southern limit of >34 Ma andesite (34a). WP denotes the location of the White Pine Range (modified from Stewart and Carlson, 1976; Best and others, 1989; and Axen and others, 1993).

CHAPTER 3

STRATIGRAPHY

The stratigraphy in the study area consists of a thick sequence of Paleozoic carbonate and siliciclastic rocks that are unconformably overlain by Cenozoic volcanic and sedimentary rocks and Tertiary and Quaternary alluvium. No Mesozoic sedimentary rocks are present and neither metamorphic nor intrusive rocks crop out in the study area. Detailed descriptions and lithologic and temporal correlatives of each of the exposed units in the study area are in Appendix A.

The Paleozoic sequence in the study area is approximately 7200 m (24,600 feet) thick and is part of the miogeoclinal sedimentary section of the western North American passive margin (Humphrey, 1960; Lumsden, 1964; Hose and Blake, 1976). Cambrian through Permian limestones, dolostones, sandstones, and conglomerates crop out in the study area (Figure 5). Formation subdivisions used elsewhere in the Great Basin are employed here, and units exposed in the study area consist of Cambrian Windfall Formation; Ordovician Pogonip Group, Eureka Quartzite, and Fish Haven Dolomite; Silurian Laketown Dolomite; Devonian Guilmette Formation; Mississippian Diamond Peak Formation; Pennsylvanian Ely Limestone; and Permian Reipe Spring and Reipetown formations (e.g., King, 1878; Hague, 1883; Lawson, 1906; Richardson, 1913; Spencer, 1917; Pennebaker, 1932; Nolan, 1935; Steele, 1960). Those units that do not crop out in the study area but which are assumed to lie in the subsurface include Cambrian Prospect Mountain Quartzite, Pioche Shale, Pole Canyon Limestone, Lincoln Peak Formation, and Dunderberg Shale; Devonian Simonson and Sevy dolomites; and

the Mississippian Chainman Shale and Joana Limestone (e.g., Hague, 1883; Walcott, 1908; Spencer, 1917; Nolan, 1930; Nolan, 1935; Drewes and Palmer, 1957).

Tertiary volcanic and sedimentary rocks unconformably overlie Pennsylvanian and Permian strata. The unconformity in the study area is generally angular and nonplanar exhibiting paleo-relief in several localities. The Tertiary rocks consist of rhyolitic and dacitic ash-flow tuffs, tuffaceous sedimentary rocks, rhyolites, and a locally exposed andesite (Figure 6). The total estimated thickness of Tertiary rocks in the study area is approximately 1460 m (4800 feet). The ignimbrites are part of the Oligocene Garret Ranch Group that consists of the Stone Cabin Formation, Currant Tuff, and Windous Butte Formation (French, 1994). The volcanic sequence also appears to correlate with Oligocene volcanic rocks exposed in the Portuguese Mountain quadrangle in the northern Pancake Range (Quinlivan and others, 1974). Volcanic vents for these units have not been located. However, the source for the Stone Cabin Formation probably is buried beneath Railroad Valley in the vicinity of the Pancake Range and the Duckwater Hills (French and Freeman, 1979; Radke, 1992). The eruptive source for the thick rhyolites also should be nearby. Other detailed descriptions of these volcanic units and those in surrounding areas are provided by Lumsden (1964), Cook (1965), Scott (1965), Nolan and others (1974), Quinlivan and others (1974), Hose and Blake (1976), Best and others (1989), Radke (1992), and Best and others (1993).

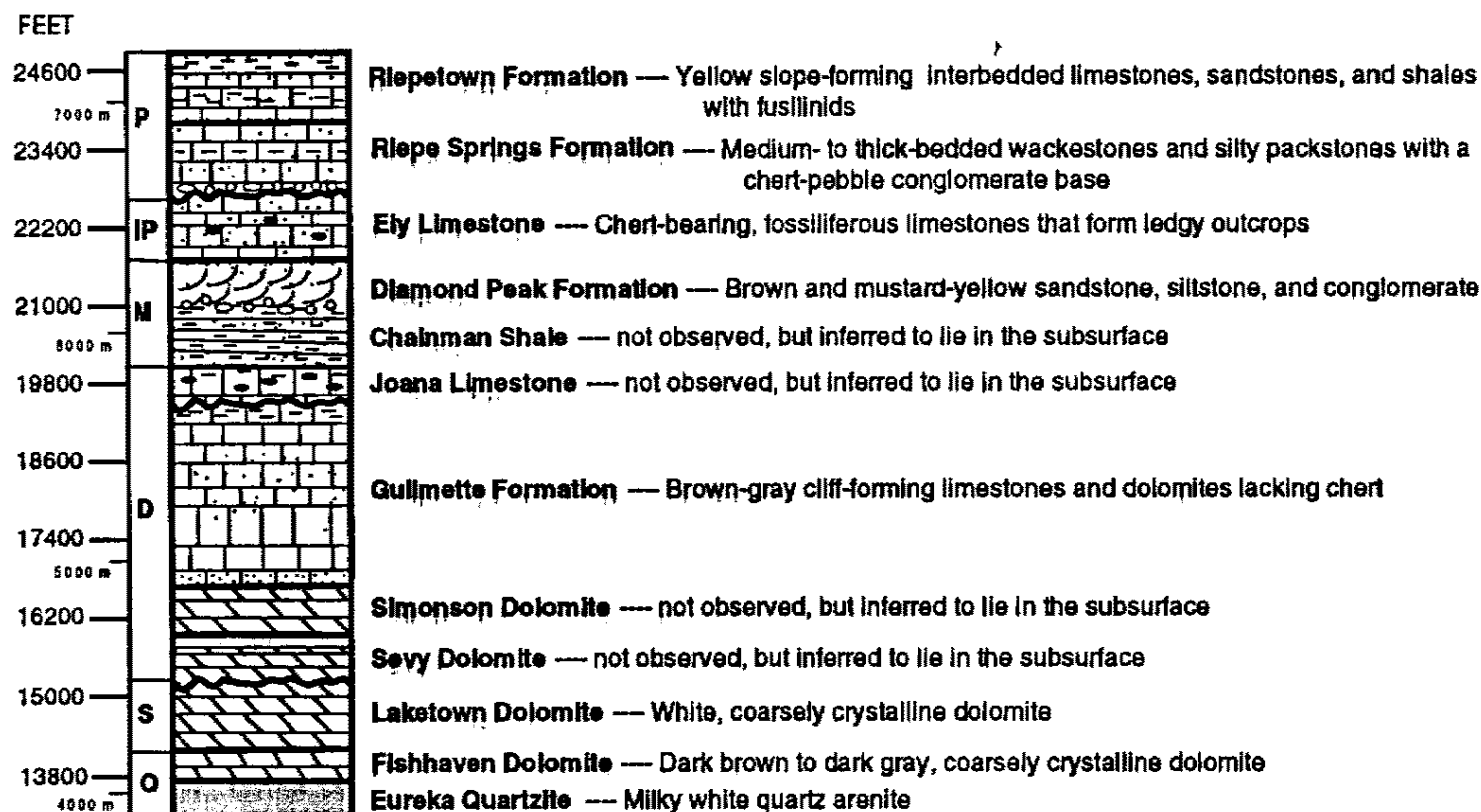


Figure 5a. Top part of the Paleozoic stratigraphic column of all units (both exposed and inferred) in the study area. Thicknesses are based on regional thicknesses combined with measured stratigraphic sections in the Blackrock Canyon area (Lumsden, 1964). Conventional letter abbreviations are used for Paleozoic ages. Rock types are shown by conventional symbols. Downward continuation of this column is shown in Figure 5b. See Appendix A for complete stratigraphic descriptions.

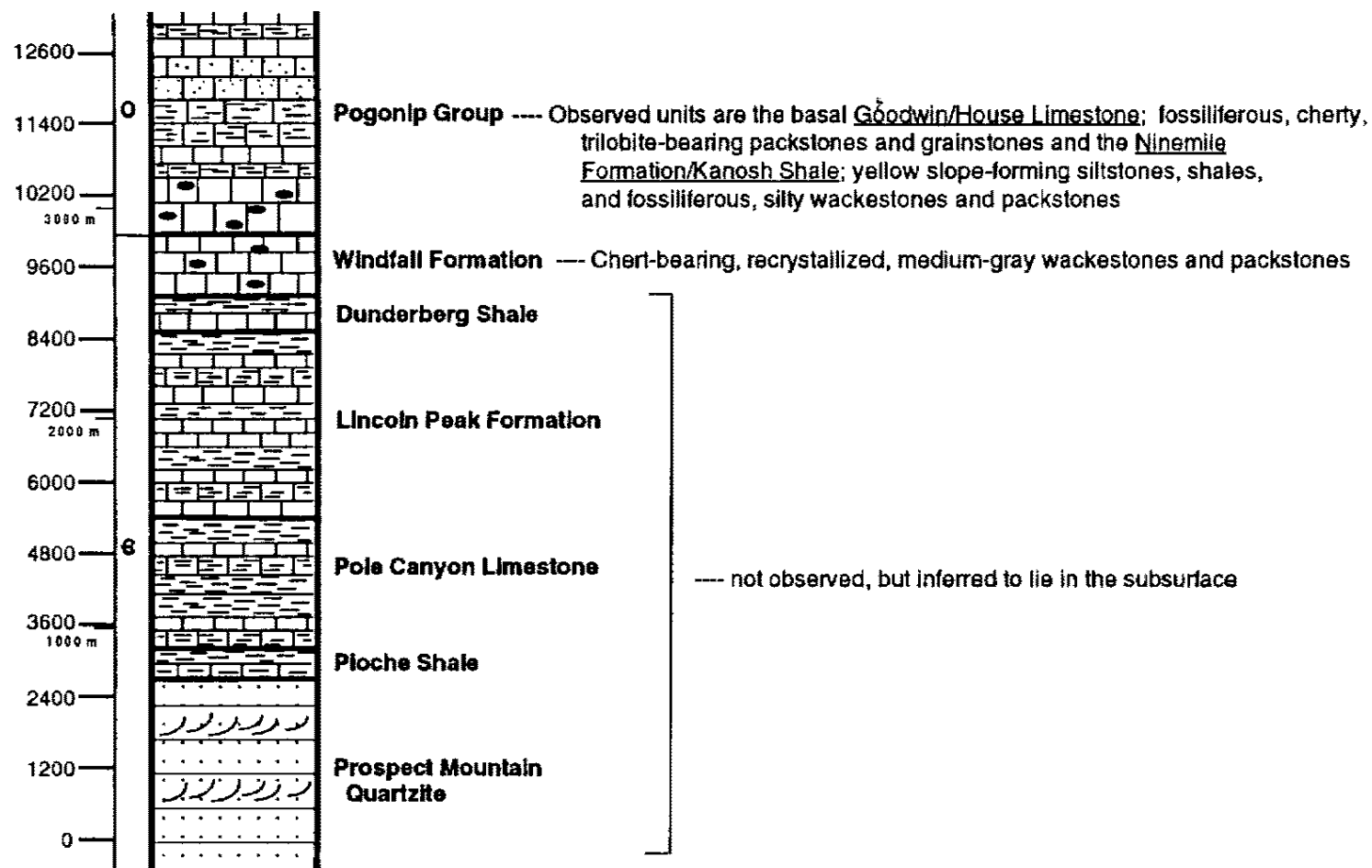


Figure 5b. Downward continuation of Paleozoic stratigraphic column of all units (both exposed and inferred) in the study area. Thicknesses are based on regional thicknesses combined with measured stratigraphic sections in the Blackrock Canyon area (Lumsden, 1964). Conventional letter abbreviations are used for Paleozoic ages. Rock types are shown by conventional symbols. See Appendix A for complete stratigraphic descriptions.

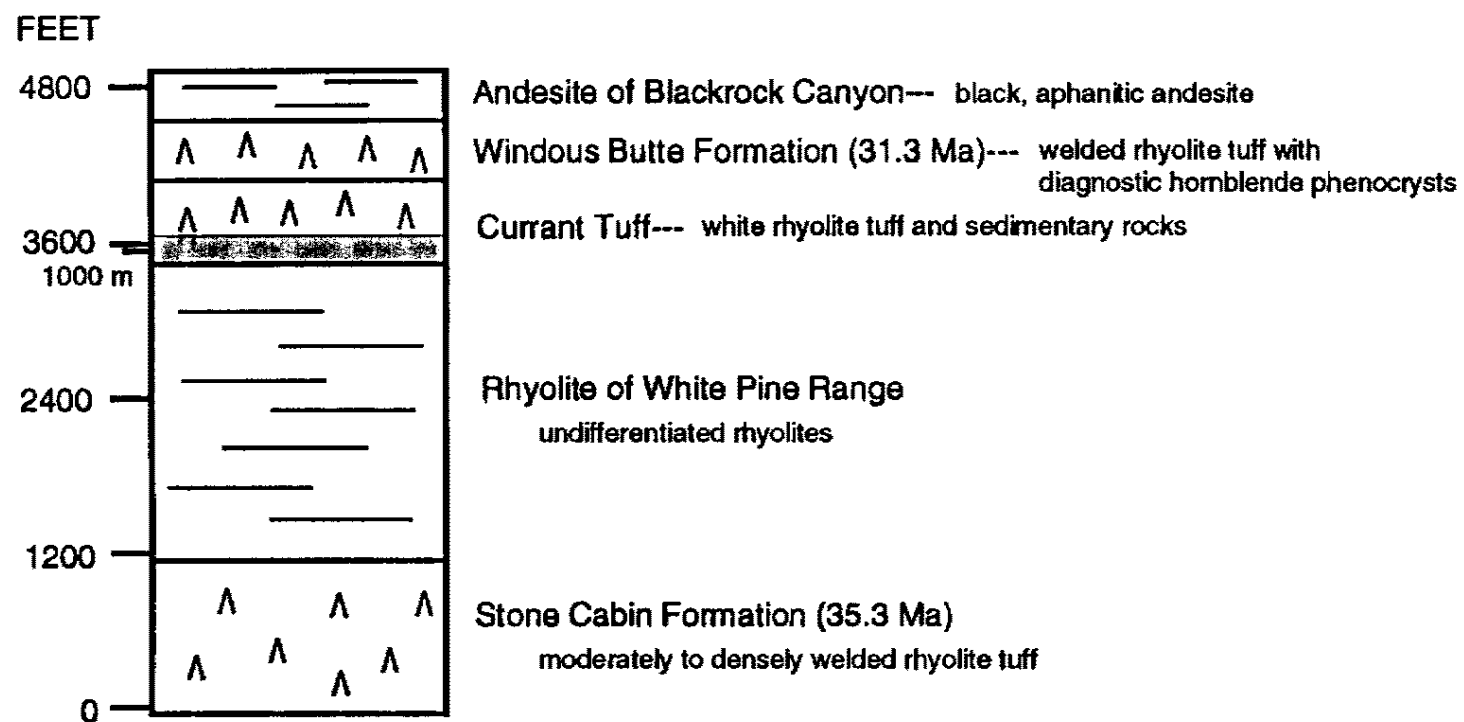


Figure 6. Tertiary stratigraphic column of volcanic and sedimentary units exposed in the study area. See text for references to ages. New, informal names used here are rhyolite of White Pine Range and andesite of Blackrock Canyon. Refer to Appendix A for complete unit descriptions.

CHAPTER 4

STRUCTURAL DESCRIPTIONS

The majority of the study area is underlain by the upper plate of a regionally widespread low-angle normal fault, the Blackrock fault (named by Lumsden, 1964). The Blackrock fault juxtaposes a brittlely deformed hangingwall that contains numerous normal faults, a few reverse faults, and folds against a less deformed footwall that is a steeply east-dipping homocline. New data from this study show that the Blackrock fault and its upper plate structures tectonically denuded pre-Oligocene contractile structures. The geometries and timing of structures exposed in the study area are described below.

Blackrock Fault

The Blackrock fault dominantly dips 15° to 30°W and can be traced for at least 20 km along strike on the western flank of the White Pine Range (Moore and others, 1968; Tracy 1980; Guerrero 1983; this study). The Blackrock fault omits ~3500 to 4800 m (~11,500 to 12,500 ft) of strata where the fault is a single strand and ~3500 to 4200 m (11,500 to 13,800 ft) where it is a fault zone.

In the study area, the Blackrock fault consists of both a north- and an east-striking segment that connect across a sharp bend (Figure 7). These segments represent two parts of the same fault because a fault of the same magnitude neither continues to the west or north. A fault segment is defined, for this study, as a section of the fault with a distinct geometry and fault strike. The most obvious changes in fault geometry occur

across the bend from the north-striking to the east-striking segment, an approximately 90° change in fault strike (Plate 1, Figure 7).

Along most of the north-striking segment, the Blackrock fault dips <30°W and places Pennsylvanian Ely Limestone and the overlying Tertiary Garret Ranch Group in its hangingwall against Cambrian Windfall Formation in its footwall (Plate 1). The north-striking segment is nonplanar and contains a pronounced corrugation that is here named the Bull Spring corrugation (Figure 7). This corrugation is apparent in fault contour maps and has implications for the sense and direction of slip on the Blackrock fault (Figure 8).

The east-striking segment is a fault zone in which the fault juxtaposes blocks of rock varying in age from Ordovician to Permian. This Blackrock fault zone contains chiefly nonplanar normal faults that strike east, northeast, and northwest and dip from 28° to vertical. These faults crop out over an ~1 km² area (Figure 7).

Hangingwall Structures

The Blackrock upper plate is complexly deformed and contains mostly normal faults, a few reverse faults, and folds. The gross sense of motion on each fault was determined by ages of juxtaposed strata and associated hangingwall and footwall structures. Due to the lack of kinematic indicators, the exact net-slip direction was impossible to assess for most faults.

Fault Geometries and Spatial Relationships

Hangingwall faults strike north, northeast, northwest, and east, and their dips range from 15° to vertical (Figure 9). Several of the faults are nonplanar, and most faults cut both the Paleozoic and overlying Tertiary volcanic rocks.

Normal faults are the most prevalent structures exposed within the Blackrock hangingwall (Figure 9). The collective amount of upper plate extension accommodated

on these faults is at least 950 m (1500 ft). Attitudes of the normal faults were plotted on equal-area lower hemisphere stereonet to assess their spatial distribution (Allmendinger, 1989). A plot of all normal faults in the hangingwall yields an apparently random distribution (Figure 10a). No systematic spatial variations of upper plate normal faults occur either across- or along-strike of the Blackrock fault. Also, no difference in the spatial distribution of high- versus low-angle normal faults is apparent.

Although most of the Blackrock fault-related deformation was extensional, limited contraction occurred along four upper plate reverse faults (Figure 9). Three of the reverse faults dip steeply ($>40^\circ$). The longest upper plate reverse fault dips 18° E at the surface, but hangingwall beds that dip east more gently than footwall beds geometrically require that this fault steepens with depth (Plates 1 and 2, Figure 9).

Three post-Oligocene reverse faults occur along the down-dip projection of the Bull Spring corrugation (Figure 9). This spatial relationship may suggest that the localized post-volcanic shortening in the Blackrock upper plate was caused by and related to the corrugation. The other reverse fault, north of the Bull Spring corrugation, is evidence of pre-Oligocene contraction because it is cut by a fault that is overlain by Oligocene volcanic rocks.

Temporal Fault Relationships

Cross-cutting relationships among all hangingwall faults suggest six timing sets, defined as fault sets 1 through 6 (Figure 9). Fault sets 3 through 6 are Oligocene or younger because they cut Oligocene volcanic rocks. The oldest two fault sets (1 and 2) are Oligocene or older because Oligocene volcanic rocks overlap these faults. The age of faults in the northeast corner of the study area (Figure 9) cannot precisely be determined from field observations. However, an ESE-striking fault (fault A on Figure 9) appears to be a continuation of an east-striking set 2 fault (fault B on Figure 9) suggesting that the northeasternmost faults are also Oligocene or older.

These fault sets were defined assuming the simplest cross-cutting relationships, and, therefore, the occurrence of timing inconsistencies are minimized. Even so, some cross-cutting relationships yield timing inconsistencies suggesting that the faults were roughly synchronous. These temporal relationships suggest that some upper plate fault sets were active at slightly different times, but deformation along the Blackrock fault and all upper plate faults collectively occurred over a prolonged period of time.

Fault attitudes in each of the six timing sets were plotted on equal-area stereonet (Allmendinger, 1989). Most of the timing sets have too few data points to evaluate statistically. However, faults in sets 3 and 4 exhibit distinct orientations (Figure 10b). One interpretation of these data is that these fault sets formed at distinctly different times and the extension direction possibly rotated through time. However, other inconsistent cross-cutting relationships suggest that the set 3 through set 6 faults were active at roughly the same time. One major example of these inconsistent relationships is documented where four fault sets intersect (Figure 11). In this example, a set 6 fault cuts an "older" set 4 fault at its southern tip, but the same set 6 fault is also cut by an "older" set 4 fault at its northern end (Figure 11). This type of timing inconsistency demands explanation and suggests that these faults were active at the same time.

Other examples of inconsistent cross-cutting relationships may occur within the Blackrock hangingwall. However, in order to document these examples, at least three faults must intersect one another. Few cases are exposed where more than two hangingwall faults intersect, and thus, other examples of temporal inconsistency cannot be unequivocally documented.

Folds

Folds in the Blackrock upper plate are difficult to recognize due to disruption by later normal faults and cover by younger volcanic rocks. Two map-scale folds crop out in the hangingwall of the Blackrock fault (Plate 1, Figure 12). The western fold (fold A

on Figure 12) is an upright, open syncline exposed in Pennsylvanian Ely Limestone and cored by Permian Reipe Spring Formation. The fold plunges 11° and trends 195° and is unconformably overlain by the Tertiary rhyolite of White Pine Range.

The eastern fold (fold B on Figure 12) is an open, upright anticline that lies near much of the surface trace of the Blackrock fault within the study area (Figure 12). Only the east-dipping limb of this fold is exposed, and the anticline is not readily apparent in the field. However, a number of restored cross sections along the entire length of the Blackrock fault geometrically require the presence of the anticline (Figure 13, Plate 2). The exposed fold limb crops out in Mississippian and Pennsylvanian rocks and is unconformably overlain by the Tertiary Stone Cabin Formation (Plate 1).

Additionally, several restored cross sections of the study area (Plate 2) geometrically require the presence of a third fold (fold C on Figure 12). This fold, an upright, open syncline, is entirely covered by Tertiary volcanic rocks and thus, cannot be observed in the field (Plate 1). However, the approximate location of the axial surface trace can be projected from the different cross sections and is dashed on Figure 12.

These folds reflect pre-Oligocene contraction because they are overlain by nonfolded Tertiary rocks. The timing of folding is bracketed between Permian and Oligocene because the youngest folded rocks belong to the Permian Reipe Spring Formation, and the oldest unit that overlaps the folds is the Oligocene Stone Cabin Formation. Furthermore, a Mesozoic age of folding is consistent with the regional geology (see Chapter 1).

Railroad Valley Fault

The youngest fault in the region is a range-bounding high-angle normal fault, the Railroad Valley fault. The west-dipping Railroad Valley fault is at least 50 km long and can be traced southward along the Grant Range (Figure 1) (Moore and others, 1968;

Dohrenwend and others, 1991). Offset alluvial terraces in Railroad Valley indicate that the Railroad Valley fault experienced some Quaternary slip (Lumsden, 1964; Dohrenwend and others, 1991). This fault has no surface expression in the study area. The Railroad Valley fault, however, must continue beneath alluvium within the study area because active fault scarps crop out to the north and south (Dohrenwend and others, 1991). Therefore, the Railroad Valley fault probably dropped the Blackrock fault and its upper plate structures down and they are now covered by valley fill.

Footwall Structures

Previous geologic mapping suggests that the Blackrock footwall consists of a steeply east-dipping homocline of Cambrian through Mississippian rocks, which is consistent with this study (Lumsden, 1964; Moores and others, 1968; Tracy, 1980). The footwall homocline dips ~50°E, and only a few footwall faults and minor folds crop out in the study area.

The most obvious footwall fault in the study area is here named the Limerock Spring fault (Plate 1, Figure 7). This fault crops out for more than 4.5 km along strike. A dark red-brown jasperoid, up to 15 m (50 feet) thick, crops out along most of the fault's length (Plate 1). The jasperoid is commonly brecciated and contains numerous subsidiary faults within it.

The Limerock Spring fault dips 40° to 50°E along most of its surface trace, except in the southern part of the study area where it is nearly horizontal and cuts bedding at a high angle. The Limerock Spring fault is a normal fault that places a middle member of the Ordovician Pogonip Group (Kanosh Shale or upper Ninemile Formation) in its hangingwall against the basal part of the Pogonip Group (Goodwin or House Limestone) in its footwall. It omits ~330 m (1000 ft) of Ordovician strata at its northern end and ~830 m (2500 ft) in the southern part of the mapped area (Plate 1). Stratigraphic

separation across the fault is approximate because calculations are based on regional thicknesses.

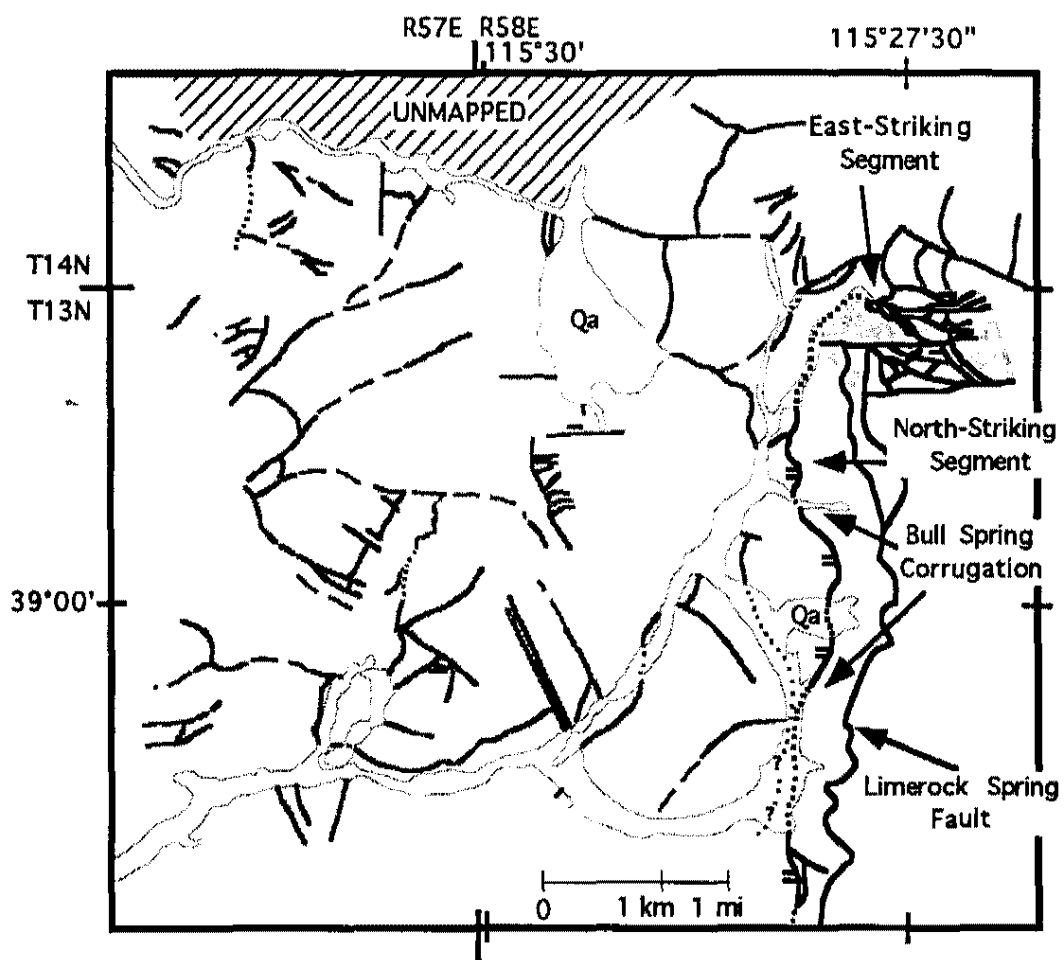


Figure 7. Map of all faults in the study area (dark gray and heavy weight black lines). Quaternary alluvium is outlined with a light weight, light gray line for reference. The more continuous faults are shown as black lines and are labeled. Geometric constituents of the Blackrock fault (double hatchur) are labeled. The stipple pattern defines the Blackrock fault zone.

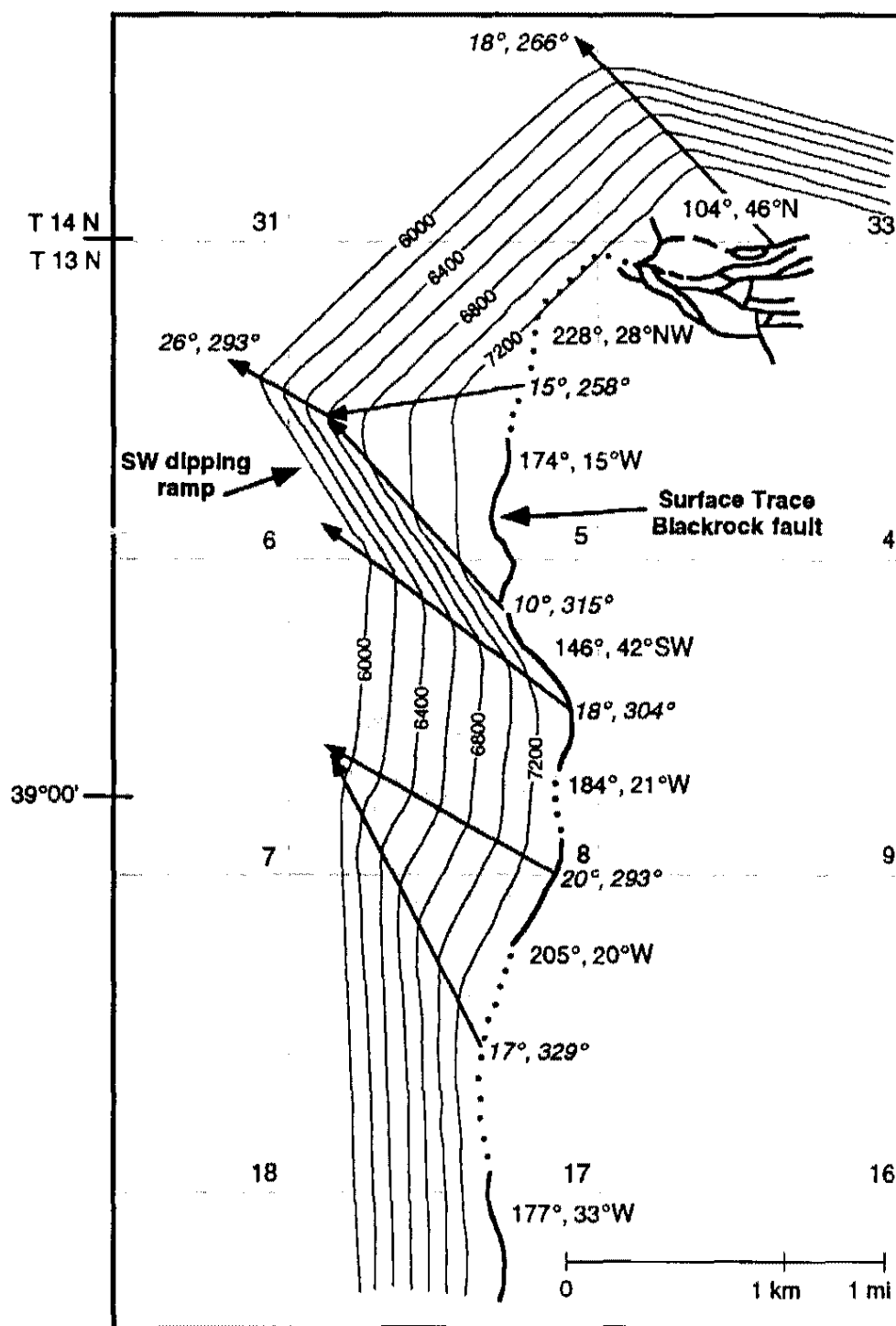


Figure 8. Structure contour map of the Blackrock fault. Contour interval is 200 feet. Arrows are intersection lines between fault segments and sections of the Bull Spring corrugation (stipple pattern). Attitudes of fault sections (plain text) and intersection lines (italics) are shown. Dashed, gray lines are section boundaries.

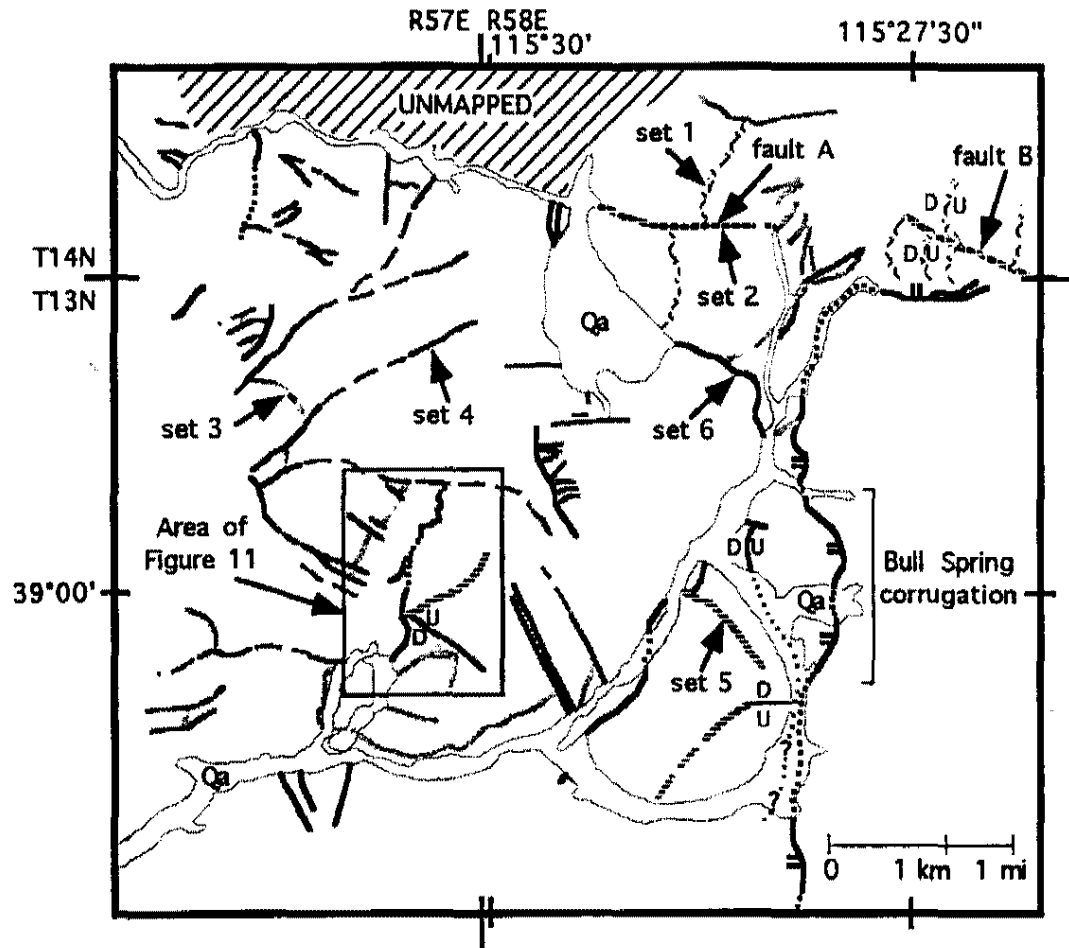


Figure 9. Map of hangingwall faults. The Blackrock fault is designated by the double hatchure. Reverse faults are shown by D/U where U indicates the upthrown block; the remaining faults are normal faults. Faults are grouped into six timing domains. They are from oldest to youngest, set 1 through set 6 and are shown by different pen patterns. Faults A and B appear to represent the same pre-Oligocene fault.

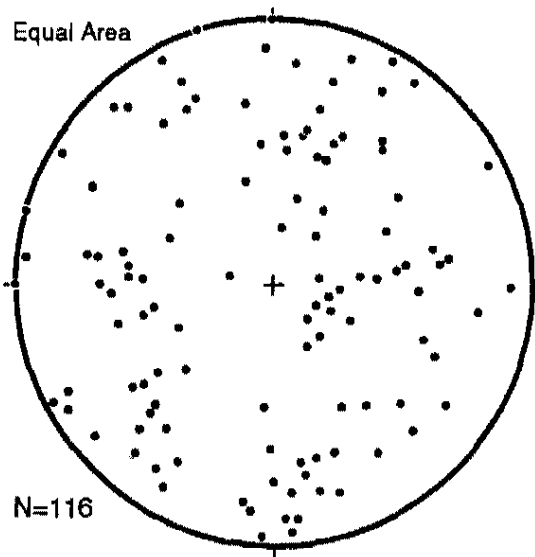


Figure 10a. Stereoplot of poles to all hangingwall normal faults. This plot suggests an apparent random orientation of these faults.

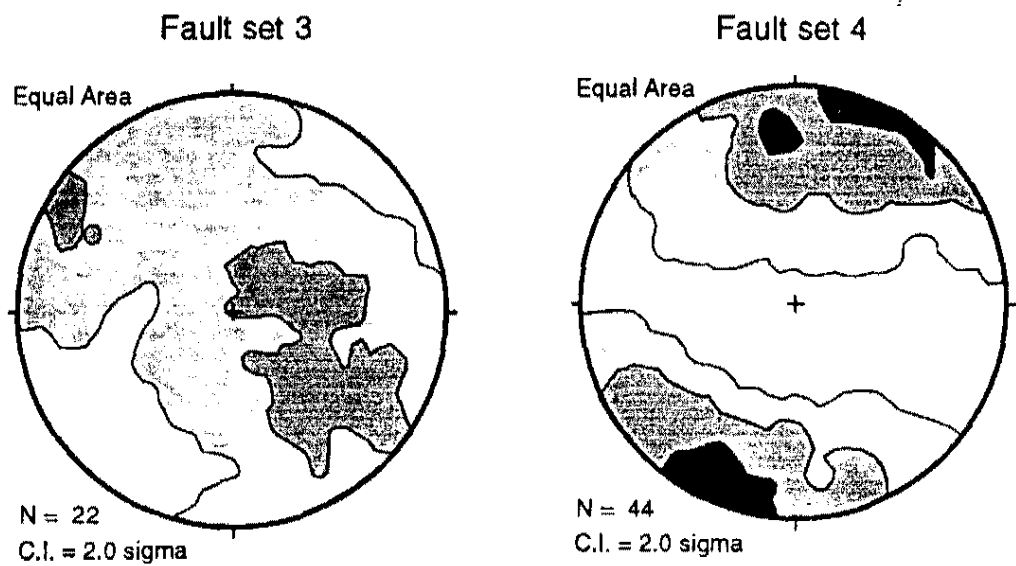


Figure 10b. Kamb contours of poles to faults for set 3 and set 4 faults. The faults in each set show consistent orientations. The preferred orientation of poles in fault set 3 is NW and in fault set 4 is NNE.

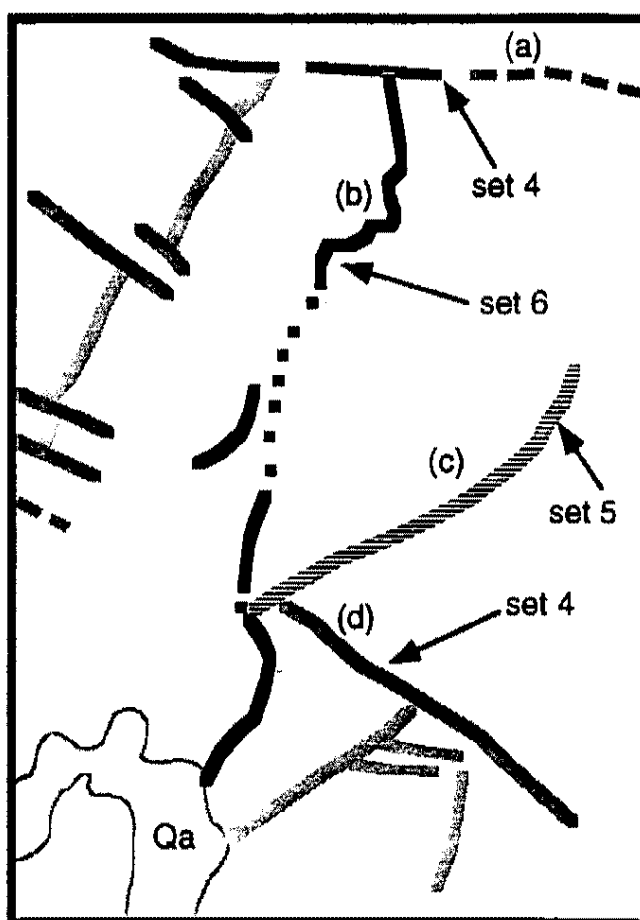


Figure 11. Map showing inconsistent timing relationships among hangingwall faults. At its southern end, a set 6 fault (b) cuts an "older" set 5 (c) fault which, in turn, cuts a set 4 (d) fault. However, the set 6 fault is cut by an "older" set 4 (a) fault at its northern tip. These relationships suggest that these faults were active at roughly the same time. Letters (a) through (d) reference the faults plotted in Figure 18. The location of this map is shown on Figure 9.

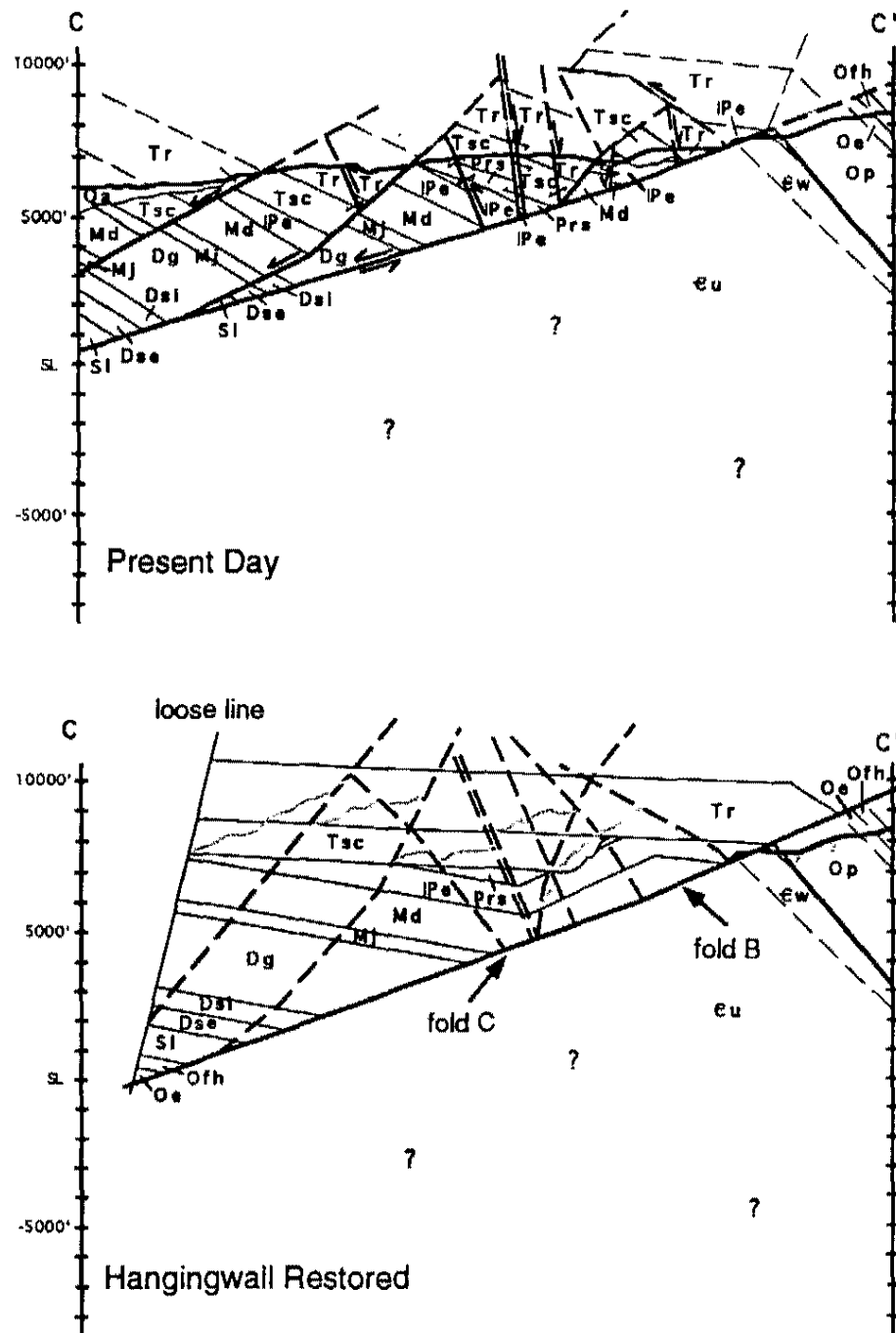


Figure 13. Present day (top) and hangingwall restored (bottom) cross sections. Location of cross section line C-C' is shown on Figure 12. The restored cross section shows a pre-volcanic fold pair in the Blackrock upper plate. A loose line shown on the restored cross section is used for balancing purposes. Question marks indicate where footwall geology is poorly constrained. Refer to Plate 1 for geologic units. Topography (light weight patterned line) shifts with the faulted block when restored.

CHAPTER 5

STRUCTURAL INTERPRETATIONS

The Blackrock fault and its associated hangingwall faults tectonically denuded Mesozoic folds and thrust faults since the Oligocene. Field and geometric data of the Blackrock fault and associated faults allow reconstruction of pre-extensional contractile structures, delineation of slip and extension directions, and description of faulting processes.

Relative Timing of the Blackrock fault

Cross-cutting relationships among Blackrock hangingwall faults constrain the relative timing of deformation related to the Blackrock fault. Most hangingwall faults cut Oligocene volcanic rocks. Although no direct field relationships yield the age of oldest movement on the Blackrock fault, the hangingwall faults most likely record the entire deformational history and suggest that the Blackrock fault is Oligocene or younger.

The complete absence of volcanic rocks in the Blackrock footwall further supports this timing of deformation related to the Blackrock fault. The complete absence of these rocks suggests that (1) the footwall underwent extreme erosion (~1460 m or 4800 ft), (2) the footwall was a barrier to the emplacement of volcanic flows, or (3) the footwall rocks were not yet at the surface during emplacement of the volcanic rocks. The first option is omitted because up to 1460 m (4800') of volcanic rocks crop out in the Blackrock hangingwall and their presence would require an unrealistic amount of

differential erosion of the hangingwall and footwall blocks. The second hypothesis can be ruled out because the both the Stone Cabin and Windous Butte Formations crop out on the western and eastern sides of the White Pine Range and the source areas for both tuffs lie west of the range. Thus, the units flowed over the area where the footwall is currently exposed and were not blocked by it. Consequently, the last option is probably most reasonable and suggests that the Blackrock fault tectonically removed the volcanic rocks and was not active until after 31.3 Ma, the age of the youngest unit cut.

The timing of youngest movement on the Blackrock fault cannot be constrained. Cross cutting relationships, in the study area, however, suggest that the fault experienced no Quaternary motion. The Blackrock fault neither cuts Tertiary or Quaternary alluvium nor does it form scarps in these younger sediments.

Kinematics of the Blackrock fault

The orientations and geometries of fault bends and corrugations can constrain the slip direction on the Blackrock fault as either west-northwest or east-southeast. In addition, geometric data, such as dips of footwall strata and bedding-to-fault angles, further constrain the slip direction as west-northwest.

Fault mullions can be used as kinematic indicators and define the direction of fault motion, such that the long axis of a fault mullion is roughly parallel to the fault slip direction (c.f., Burchfiel and others, 1995). Fault corrugations can be used in a similar manner to suggest fault slip direction. The Bull Spring corrugation constrains the fault slip direction because it is a set of primary fault bends. If the bends were secondary, and formed by later folding of the fault, hangingwall and footwall beds would also be folded and their attitudes would mimic the orientation of the corrugation. The orientations of hangingwall and footwall beds across strike of the corrugation reflect no systematic change and, thus, the fault corrugation is primary.

The WNW-trending Bull Spring corrugation (Figure 8, Figure 14) suggests that the slip vector along the Blackrock fault, in the study area, is approximately west-northwest or east-southeast. Furthermore, the intersection lines between each subsection of the Bull Spring Corrugation are subparallel and trend roughly northwest or southeast (Figure 8).

The intersection lines between the fault segments and the sections of the Bull Spring corrugation trend approximately northwest and are subparallel to each other (Figure 8). The slip direction on the Blackrock fault appears to be approximately parallel to these intersections because (1) the orientations of all these intersection lines are similar and (2) nearly opposing fault dip directions across the intersection lines suggest that slip at a high angle to these lines would require that the Blackrock fault had normal slip in some places and had reverse slip elsewhere. The latter type of motion is kinematically difficult and thus, suggests that the slip direction approximately paralleled the trend of the intersection lines.

The northern margin of the Bull Spring corrugation, a 42°SW-dipping fault ramp, lies just southwest of the boundary between the north- and east-striking fault segments (Figure 8). This ramp could be either a transport parallel ramp or a lateral ramp. If the ramp was transport parallel, then motion would occur in the dip direction of the ramp requiring down and up movement of the Blackrock hangingwall across the Bull Spring corrugation. Bedding and compaction foliation attitudes, however, do not oppose each other across the Bull Spring corrugation and, thus, do not record dip-slip movement along fault sections with opposite dip directions. Furthermore, this type of hangingwall movement is unlikely and a north-northeast or south-southwest slip direction is highly improbable. Thus, I suggest that the ramp is a lateral ramp that accommodated slip to the west-northwest or east-southeast.

The attitude of the intersection line between the north- and east-striking fault segments further supports a west-northwest or east-southeast slip direction (Figure 8). At the surface, the intersection line between these fault segments plunges 15° toward 258° . The intersection line persists to a depth of ~ 245 m (800 ft) with that attitude (Figure 8). However, ~ 245 m down the intersection line assumes a more northwesterly orientation of 26° , 293° . This approximately west-northwest orientation suggests that slip along the Blackrock fault, if conserved, occurred in a roughly west-northwest or east-southeast direction.

All of the above mentioned data can constrain the Blackrock fault slip direction in a bi-directional sense (either west-northwest or east-southeast). Other geometric data, such as observed footwall dips, further constrain the slip direction to west-northwest. For example, an east-southeast slip direction would require doming or westward block tilting of the area because the Blackrock fault is a normal fault (omits section), and presently dips west in the study area. Doming typically occurs late in the development of a low-angle normal fault and, thus, affects both the hangingwall and footwall. Doming is not suggested by the geometric data. The Blackrock fault dips $\sim 10^\circ$ E, east of the study area (W.J. Taylor, unpublished data), and 15° to 30° W in the study area. Therefore, doming would have occurred about an approximately north-trending axis. Such doming requires shortening in the footwall, and up to 40° of systematic dip change in footwall strata. No systematic change is observed, and thus, doming of the Blackrock fault is rejected as an option (W.J. Taylor, unpublished data, this study).

Westward block tilt of the range, to tilt the fault from an east dip to its present west dip, requires a minimum of 25° to 30° of west tilt along a large-slip east-dipping normal fault. No such normal fault is observed in the region for approximately 100 km across strike from the western Pancake Range to the eastern Egan Range (Figure 1). Because no fault exists to tilt the Blackrock fault the correct amount in the appropriate

direction, large-scale block tilt to re-orient the fault from an original east dip to the present west dip is ruled out.

Footwall bedding-to-fault angles are additional geometric data that suggest movement on the Blackrock fault occurred in a west-northwest direction. In the study area, bedding-to-fault angles between footwall beds and the Blackrock fault are roughly 70° (Plate 1, Figure 13). These footwall bedding-to-fault angles should remain roughly constant regardless of later deformation and tilting because the 50°E dips in the footwall homocline persist for a great distance (≥ 5 km) from the fault. Also, younger faults block tilt the area eastward. A hypothetical scenario in which the Blackrock fault originally dipped shallowly ($\sim 25^\circ$) east and cut across the footwall beds with their approximately present attitude, yields bedding-to-fault angles of $\sim 20^\circ$. These angles are nowhere near the currently observed angles of 70° and, thus, suggest that the Blackrock fault must have slipped as a shallowly W-dipping fault. These data, combined with the linear and geometric data, constrain the Blackrock fault slip direction as west-northwest. This west-northwest slip direction suggests that both the north- and east-striking segments accommodated normal-oblique slip.

Three-Dimensional Strain

Multiple orientations of faults, which typically result in an orthorhombic map pattern, commonly occur in rifts (e.g. Donath, 1962; Thompson and Burke, 1973; Aydin and Reches, 1982; Scott and others, 1992). Orthorhombic fault patterns exist within upper plates of low-angle normal faults in the Basin and Range Province (Smith, 1984; Langrock and Taylor, 1995). Despite the widespread observation of these complex fault patterns few studies attempt to explain faulting processes within upper plates in extended terranes. Classically, researchers suggest that these multiple fault sets were active at different times and that the complex geometries resulted from changes in the orientation

of the stress field over time. However, several studies document multiple fault sets that were active simultaneously (e.g., Malone and others, 1975; Aydin and Reches, 1982; Langrock and Taylor, 1995). These synchronous faults with diverse attitudes cannot be explained by the "classical" conjugate faulting theory originally proposed by Anderson (1951). Alternatively, more recently proposed faulting models suggest that these faults represent three-dimensional strain.

Anderson (1951), Ode' (1960), and Varnes (1962) employed Mohr Coulomb failure criterion to explain failure along faults. According to this theory, faulting occurs on a conjugate set of fault planes inclined 45° to the maximum compressive stress (σ_1). The intersection of the conjugate faults is in the direction of the intermediate compressive stress (σ_2) (Figure 15a). This widely accepted faulting theory requires plane (two-dimensional) strain that limits movement in the direction of intermediate strain or stress. Furthermore, this theory can only account for synchronous movement on a set of faults and fails to explain synchronous fault sets with multiple attitudes.

A number of researchers have modeled three-dimensional strain both experimentally and theoretically. Oertel (1965) subjected clay cakes to three-dimensional strain fields and observed orthorhombic fault sets. Reches and Dieterich (1983) deformed cubes of sandstone, limestone, and granite producing conjugate fault sets under plane strain conditions and typically four sets of faults in three-dimensional strain fields. Theoretical models agree well with the experimental data (Reches, 1978, 1983; Krantz, 1988, 1989). These faulting models demonstrate that at least four sets of synchronous faults in orthorhombic symmetry are necessary to accommodate three-dimensional strain (Figure 15b). The models apply to a number of field studies and explain complex structures that are impossible to explain by conjugate faulting theory (e.g., Aydin, 1977; Krantz, 1988, 1989; Scott and others, 1992; Langrock and Taylor, 1995).

Temporal relationships among post-volcanic faults exposed in the Blackrock upper plate cannot be explained by Andersonian conjugate faulting processes. Fault sets with four different strikes were active penecontemporaneously and suggest three-dimensional strain. Figure 11 depicts one example of penecontemporaneous hangingwall fault relationships.

A geometrical analysis of these same faults allows deduction of whether the fault sets formed according to Andersonian faulting theory and are symmetrically conjugate (2-D or plane strain) or are orthorhombic (3-D strain). Stereoplots illustrate the difference in fault symmetries (Figure 15). If the faults are conjugate, their poles will lie on one of the principal strain planes (XY, XZ, YZ) (Figure 15a). In contrast, if the faults display orthorhombic symmetry, their poles will lie between the principal planes (Figure 15b).

The post-volcanic Blackrock upper plate faults make up four geometric sets (e.g., Figure 11). The fault sets represent orthorhombic symmetry (3-D strain) as shown by the stereographic method of Reches (1983) and Reches and Dieterich (1983). Figure 16a shows a stereoplot of poles to the four synchronous faults in Figure 11. Each pole is rotated using the orthorhombic rule into one quadrant of the stereonet (Figure 16b). In this analysis, fault orientations are examined with respect to the principal strain/stress axes. Thus, any one of the quadrants can be used, but its boundaries are defined by the orientations of these axes (e.g., Figure 16b). I assume that the extension direction in the Blackrock upper plate is the same as that for the Blackrock fault. Thus, for this particular analysis, I use an extension direction or least principal stress axis (σ_3) of 293° . The maximum principal stress (σ_1) is assumed to be vertical, as is consistent with slip on near surface normal faults. If a pole lies within the selected quadrant, then it will remain stationary. Poles that lie outside of the quadrant are rotated into the quadrant by rotating them to their mirror images. Some poles must be rotated twice. After rotating the poles,

an average pole, representative of all faults in the analysis, is calculated. If the average pole lies on one of the principal strain planes (XY, XZ, or YZ), then it suggests a set of two conjugate faults (2-D strain), but if the average pole lies between the principal planes, then it suggests fault sets in orthorhombic symmetry (3-D strain) (Reches 1983; Reches and Dieterich, 1983). The average pole in this data set does not lie on any of the principal planes suggesting that these faults record three-dimensional strain.

The orthorhombic fault pattern of the entire Blackrock upper plate geometrically suggests that nearly all of the post-volcanic hangingwall faults formed by three-dimensional strain. Though in specific localities, cross-cutting relationships show that hangingwall faults are synchronous, the exact temporal relationships among all of the post-volcanic hangingwall faults cannot be precisely determined. However, a plot of all rotated poles, using the stereographic method described above, shows that nearly all of these faults together display orthorhombic symmetry (Figure 17). Only four of the 86 faults (Figure 17) are conjugately summetrical. This geometric analysis suggests that nearly all of the post-volcanic faults collectively formed by non-conjugate faulting processes, and they represent three-dimensional strain.

Three Dimensional Strain in Extended Terranes: A Kinematic Model

Given data from the Blackrock fault, I propose a kinematic model in which orthorhombic, synchronous faults represent three-dimensional strain and result from movement of the upper plate across a non-planar and irregular low-angle normal fault. In this model, I suggest that slip above a non-planar, irregular, basal fault does not permit conservation of upper plate volume unless fault bends are oriented perpendicular to the slip direction. Therefore, three-dimensional strain could consistently be generated in cases where the controlling fault is non-planar or where fault bends are not oriented perpendicular to the fault slip direction.

The geometric, temporal, and kinematic data of the Blackrock fault permit this kinematic model. The slip direction of the Blackrock fault is assumed to approximately parallel the intersection lines of the different fault segments and sections. However, the intersection lines between each of the Bull Spring corrugation sections is of a slightly different orientation (Figure 8). Thus, movement of the upper plate block over these irregularities should cause the block to deform in a non-conservative manner and result in the observed three-dimensional strain.

Similar orthorhombic and synchronous faults occur in the upper plates of other low-angle normal faults, such as the Saddle Island detachment fault, Nevada (Smith, 1984). In the Saddle Island hangingwall, upper plate faults appear to be conjugate (2-D strain) where the controlling, low-angle detachment is planar, but appear to be orthorhombic (3-D strain) where the surface trace of the detachment is irregular (Smith, personal communication).

Evidence of Folding and Thrusting

Neogene extensional structures disrupted and obscured the evidence of a pre-Tertiary thrust belt in the southern White Pine Range. However, new detailed geologic mapping and restored cross sections of the study area reveal that the Blackrock fault and associated hangingwall faults tectonically denuded folds and thrust faults. New evidence of folding and thrusting in the White Pine Range includes pre-volcanic folds, significant paleo-relief, and a large-scale thrust fault. This new evidence of pre-Oligocene contraction is significant because only folding and not large-scale thrusting was documented in the range previously.

Pre-Volcanic Folds

A pre-volcanic fold pair, in the upper plate of the Blackrock fault, is evidence of pre-Oligocene contraction. Recognition of these folds is difficult because Tertiary

normal faults cut them and volcanic rocks cover them. Present day cross sections show how the highly extended Blackrock upper plate masks evidence of contraction (Figure 13, Plate 2). However, contractile structures are readily apparent in cross sections with hangingwalls restored to pre-extensional geometries (Figures 12 and 13, Plate 2). These cross-sections geometrically require the existence of a pre-volcanic fold pair. The folds occur along the entire length of the Blackrock fault, in the study area, and are unconformably overlain by the Oligocene volcanic sequence (Figure 13, Plate 2).

Paleo-relief

Paleo-relief also suggests pre-Oligocene deformation. Paleo-relief is documented by the non-planar geometry of the sub-Tertiary unconformity, and it is observed both in cross section and map view in several localities within the study area (Figure 18). Significant paleo-relief, in the study area, suggests that deformation or erosion (or both) occurred prior to the deposition of the Oligocene volcanic rocks. Based on other data described here, the deformation was most likely pre-Oligocene folding and thrusting.

Thrust Faults

The most compelling evidence of folding and thrusting, in the study area, is the documentation of a large-scale thrust fault. The thrust fault is not presently exposed because the Blackrock fault either cut it out or reactivated it. Step-wise restoration of the Blackrock fault and its associated upper plate structures (Figures 19 and 20) geometrically require the existence of this thrust. In this step-wise restoration, the hangingwall restores to its pre-extensional geometry by removing all post-volcanic Blackrock upper plate faults from the present day cross section (Figure 19). In the restored cross section evidence of contraction, such as pre-volcanic folds, is apparent. The geometries of the footwall and restored hangingwall structures preclude a simple restoration of the Blackrock fault. The geometry of the pre-volcanic fold pair in the

hangingwall drastically differs from the steeply dipping homocline in the footwall. Therefore, the fault cannot be simply restored by sliding the restored hangingwall units up the fault plane to meet their respective counterparts in the footwall (Figure 20). These geometric constraints require that the hangingwall and footwall blocks occupied different thrust plates, and consequently, suggest that the Blackrock fault either cut out or reactivated a thrust. This previously unrecognized thrust is here named the White Pine thrust and is described in detail in Chapter 6.

Central Nevada thrust belt

I suggest that newly discovered contractile structures, in the study area, are a part of the central Nevada thrust belt (CNTB) (Speed, 1983; Bartley and others, 1993; Taylor and others, 1993) (Figure 21). Overprinting by extensional structures makes reconstruction of the CNTB at the latitude of the White Pine Range difficult. However, the geometries and vergence of the pre-volcanic folds described above are consistent with the dominantly east-vergent, ramp-flat structures in the CNTB. Furthermore, the timing of contractile deformation in the study area permits correlation with the CNTB.

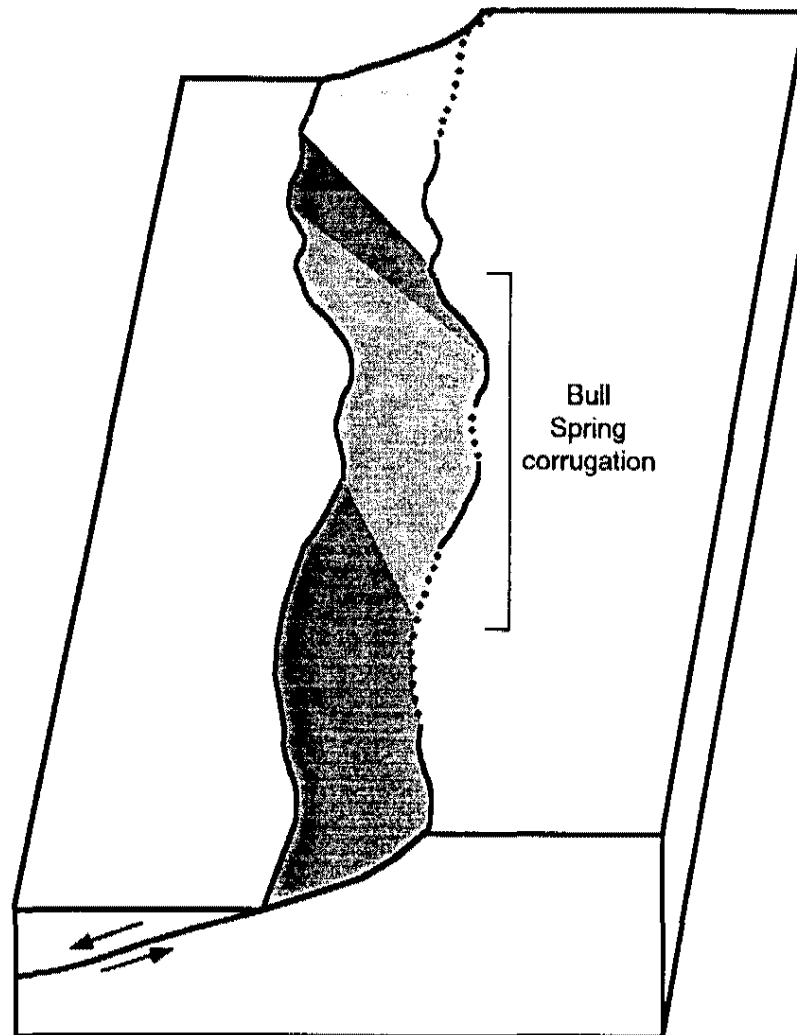


Figure 14. Three-dimensional block diagram illustrating the geometry of the north-striking segment of the Blackrock fault. Lighter shades indicate gentle dips and darker shades indicate moderate dips.

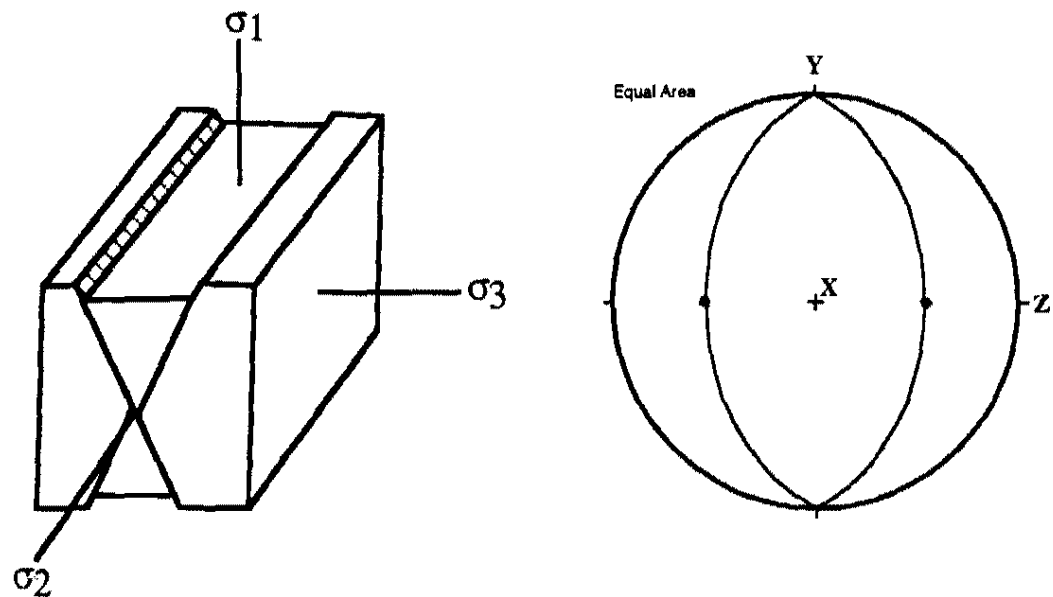


Figure 15a. Example of conjugate fault sets formed in two-dimensional strain. The principal stress axes (σ_1 , σ_2 , σ_3) correspond with principal strain axes (X , Y , Z). In this example, poles to the conjugate faults lie on the principal strain plane XZ .

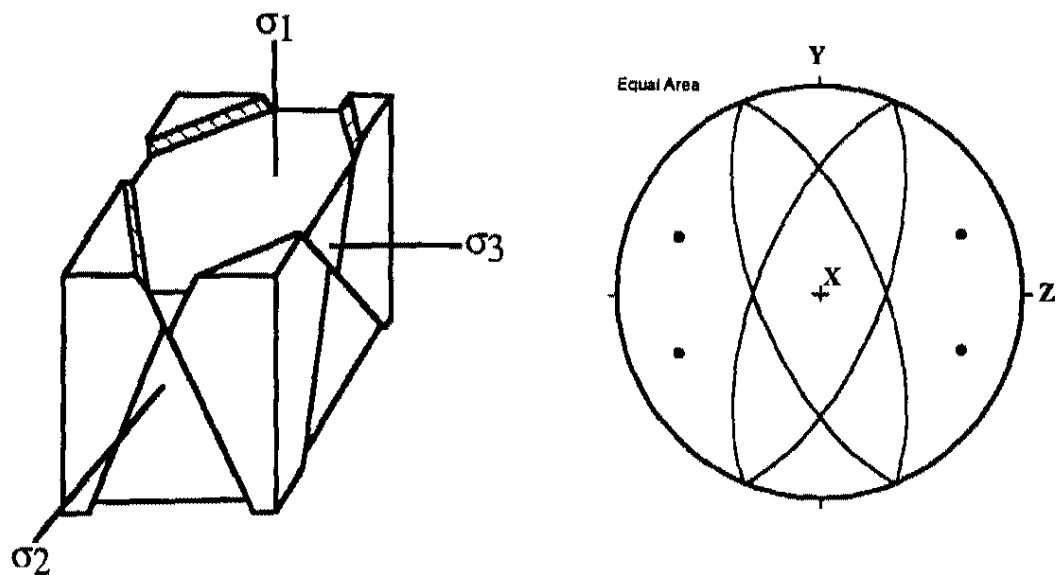


Figure 15b. Example of orthorhombic fault sets and three-dimensional strain. In this example, poles to the conjugate faults lie between the principal strain planes (XZ , YZ , XY).

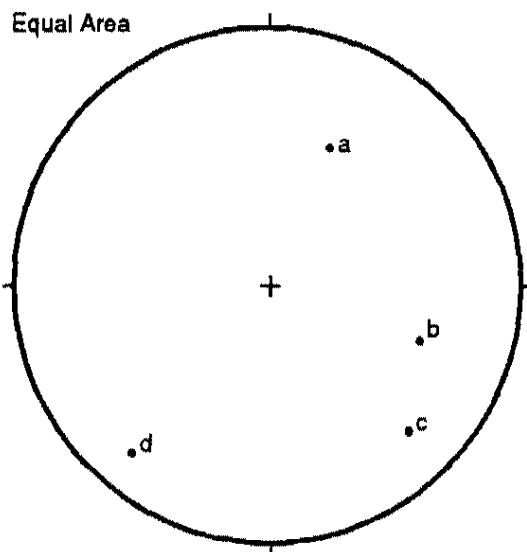


Figure 16a. Lower hemisphere stereoplot showing poles to the set 4, set 5, and set 6 faults shown in Figure 11.

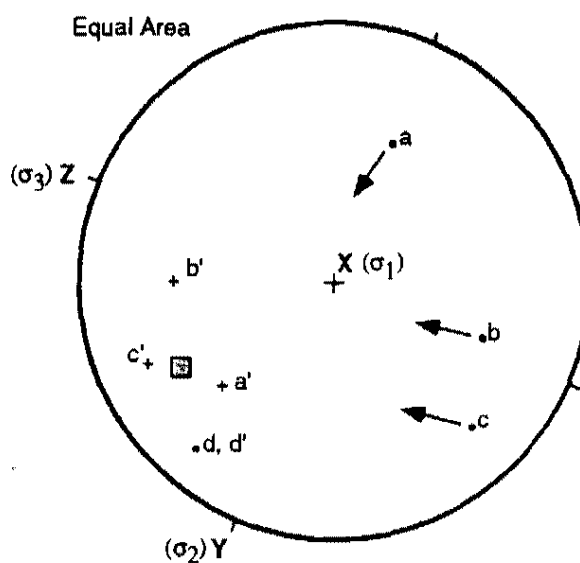


Figure 16b. Stereoplot of poles in Figure 16a rotated using the orthorhombic rule. The quadrant is defined by the principal strain axes X, Y, and Z. The average pole, shown by the box, does not lie on any of the principal strain or stress planes (XY, XZ, YZ) and indicates that these faults represent three-dimensional strain.

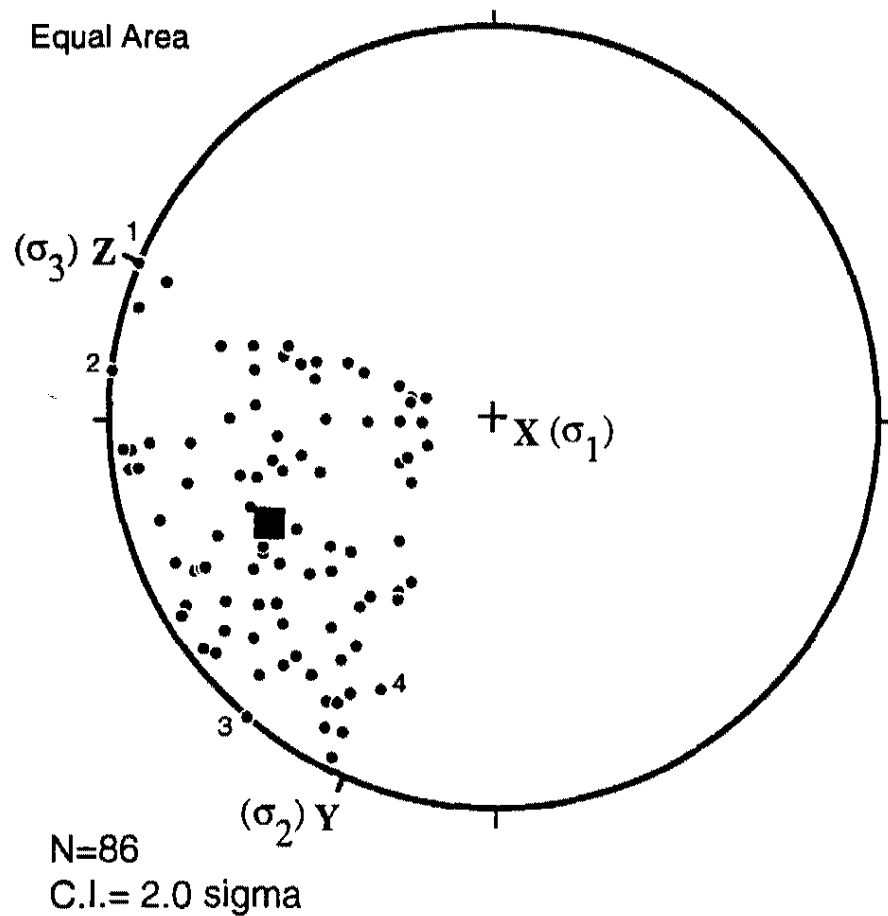


Figure 17. Stereoplot of rotated poles to all post-volcanic hangingwall faults, including the Blackrock fault. The faults collectively display orthorhombic symmetry. The average pole is shown by the box and does not lie on any of the principal strain planes. X, Y, and Z represent the principal strain axes. Only four (labeled 1 through 4) of the 86 faults are conjugately symmetrical.

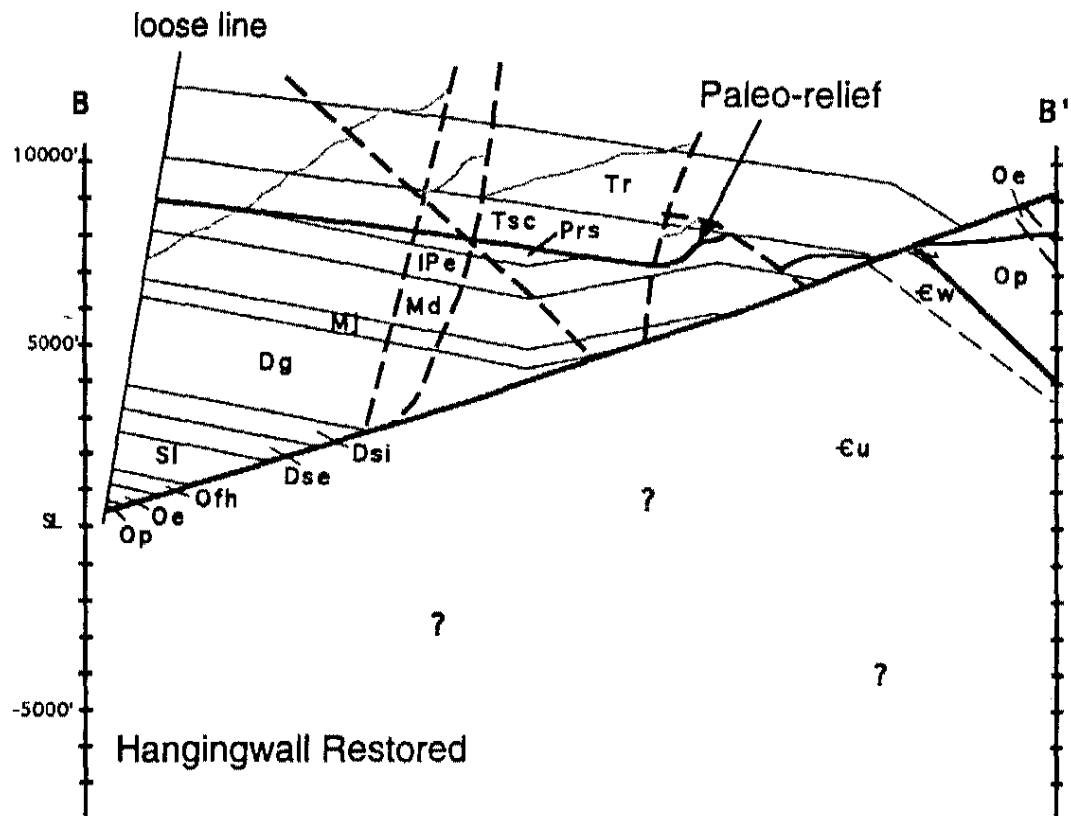


Figure 18. Paleo-relief is easily seen in this cross section where the hangingwall is restored to its pre-extensional geometry. Paleo-relief is indicated by the nonplanar geometry of the sub-Tertiary unconformity (bold). Paleo-relief is shown by the thinning of Pennsylvanian Ely Limestone (IPe) and the pinchout of the Tertiary Stone Cabin Formation (Tsc). The loose line is used for balancing purposes. Topography is shown by a light weight patterned line and it shifts with the faulted block when restored. Question marks indicate where the footwall geology cannot be constrained.

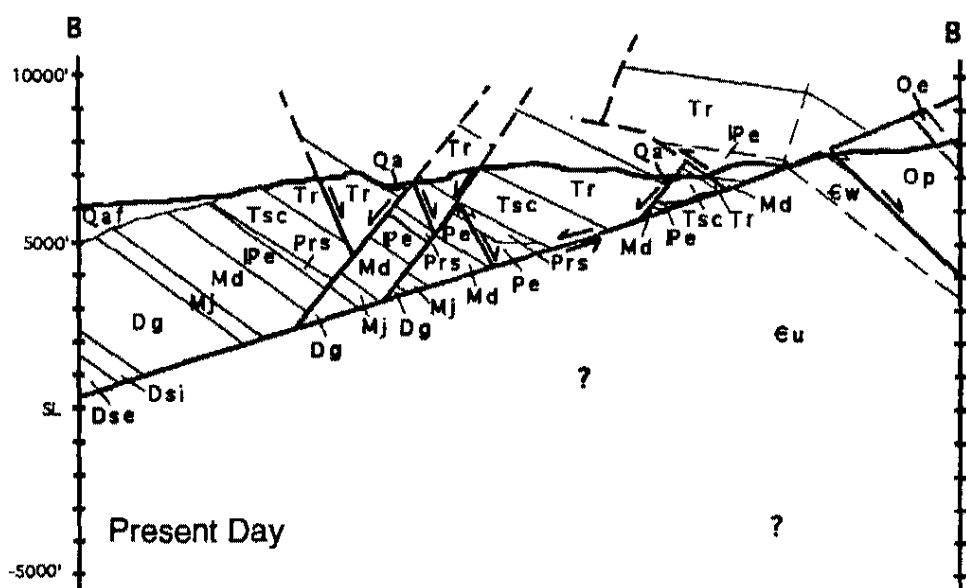


Figure 19a. Deformed state cross section that shows the Blackrock fault and its highly extended upper plate. Refer to Plate 1 for geologic units. Question marks indicate where footwall geology is poorly constrained. Figure 12 shows the location of cross-section line B-B'.

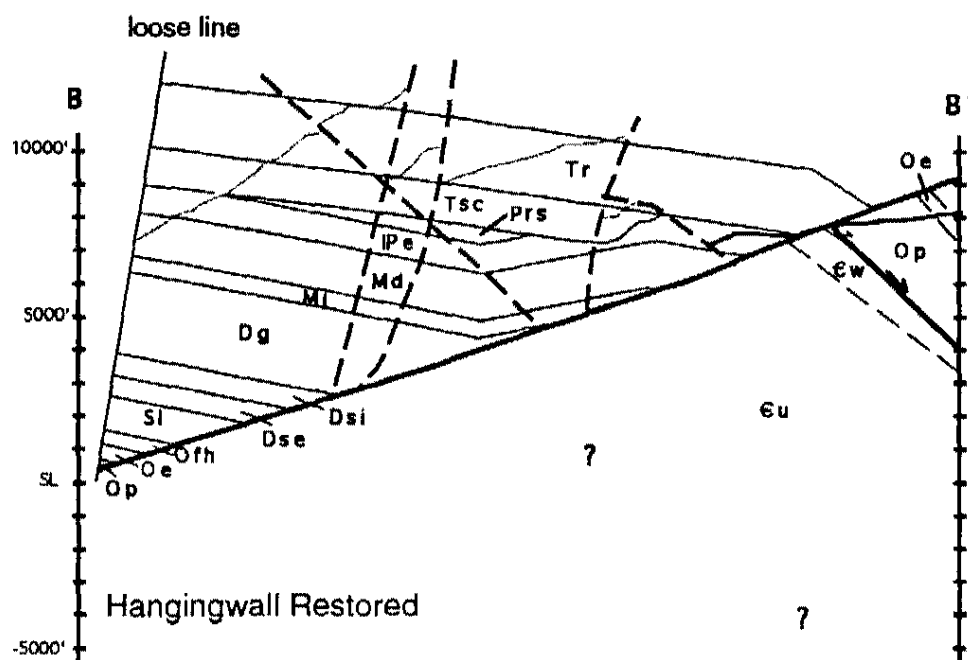


Figure 19b. The hangingwall is restored to its pre-extensional geometry. Original positions of faults are shown by the heavy weight dashed lines. Topography (light weight patterned line) shifts with the faulted block in the restoration. The loose line is used for balancing.

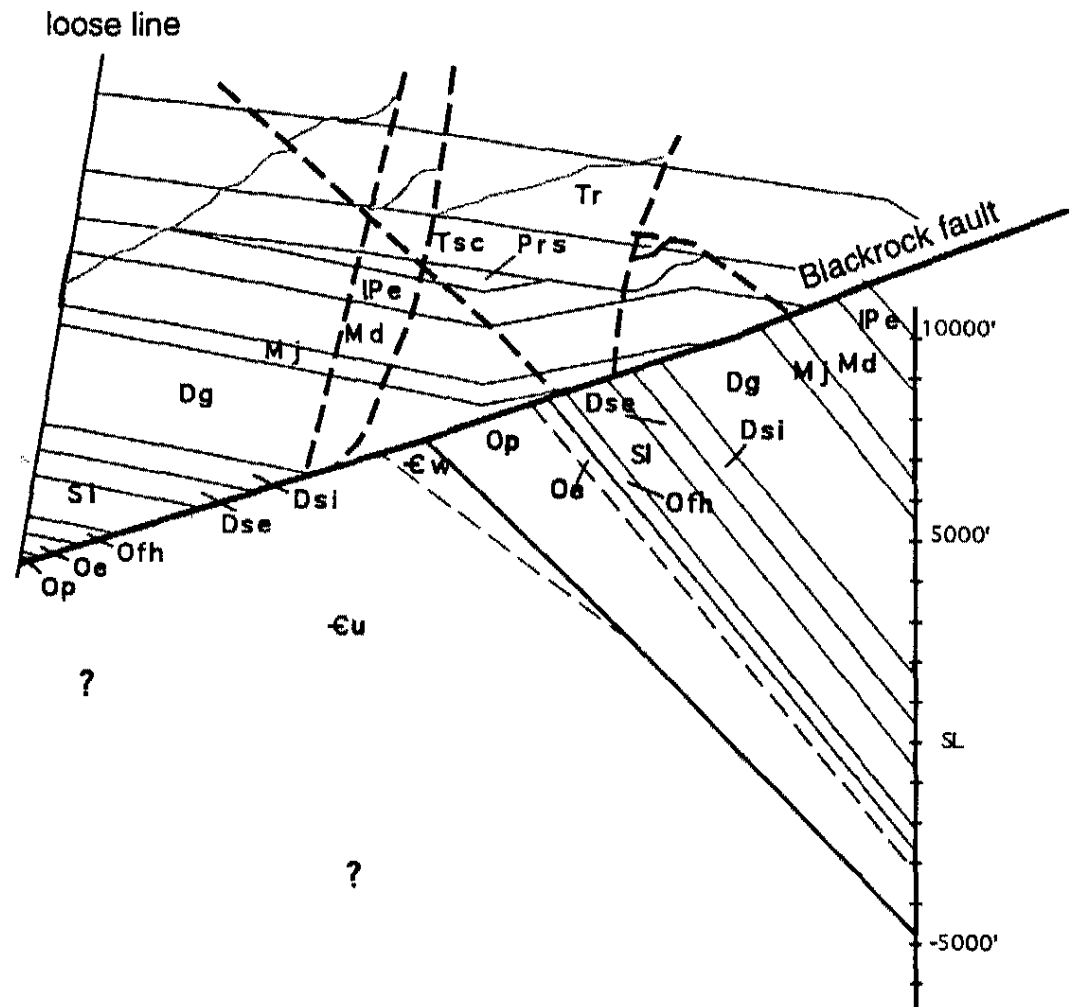


Figure 20. Blackrock hangingwall and footwall blocks are nonrestorable. The inconsistent geometries of these blocks require that the hangingwall and footwall were not continuous when the Blackrock fault became active and, thus, they occupied different thrust plates. The footwall geology is modified from Lumsden (1964) and Tracy (1980).

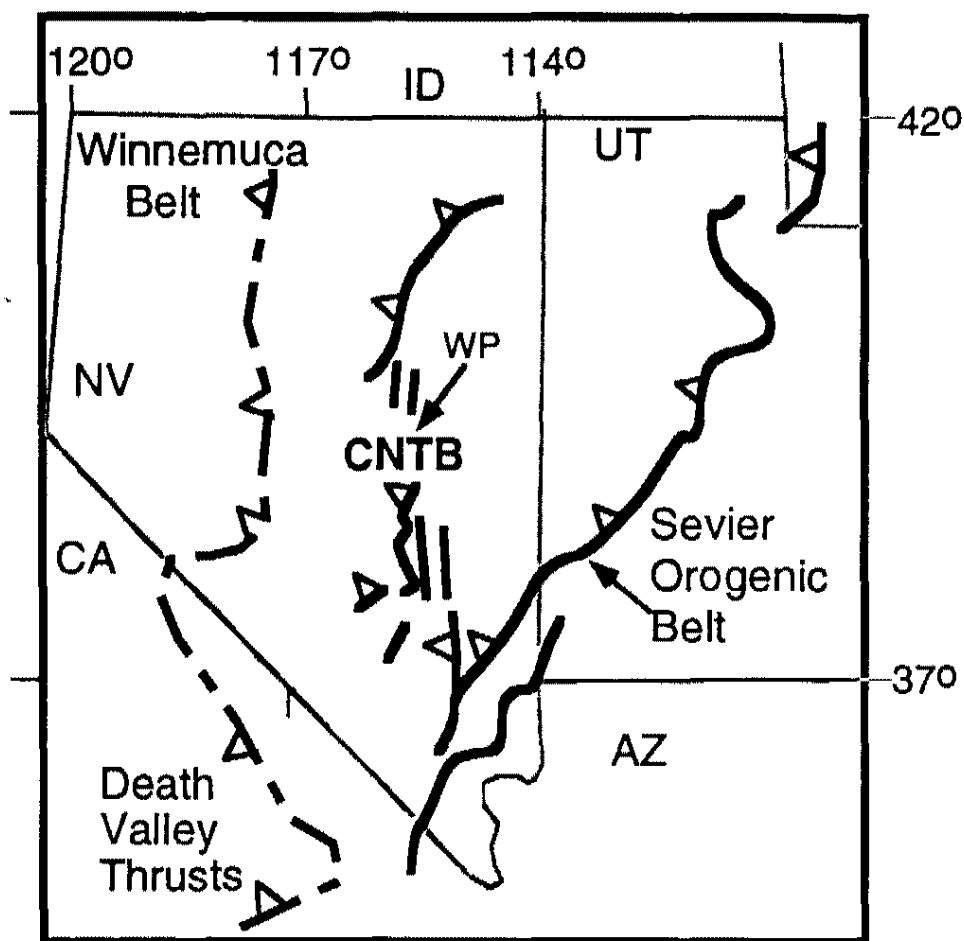


Figure 21. Locations of some of the pre-Tertiary thrust belts in the Basin and Range Province. The central Nevada thrust belt is labeled as CNTB. The location of the White Pine Range is indicated by WP (modified from Taylor and others, in preparation).

CHAPTER 6

REGIONAL STRUCTURES

Mesozoic contraction and Cenozoic extension define the regional structural framework of the Great Basin. At the present latitude of the southern White Pine Range, at least four episodes of normal faulting and widespread Cenozoic volcanism disrupted and obscured Mesozoic contractile structures. Detailed geologic mapping and cross-section restorations in the southern White Pine Range are required for and allow the documentation of a previously unrecognized thrust fault (see Chapter 5). These data, combined with existing data in the Pancake Range and Duckwater Hills, were used to reconstruct the regional Mesozoic thrust belt. Step-wise balanced and restored cross sections through the Pancake Range, Duckwater Hills, and the White Pine Range allow reconstruction and correlation of large-scale contractile structures and suggest that they are part of the central Nevada thrust belt (Figures 1 and 22, Plate 3). This reconstruction is significant because the geometry of the CNTB across northern Railroad Valley has never been documented. Furthermore, this regional cross section is used to determine extensional structural styles and the distribution of extension across northern Railroad Valley.

Regional Retrodeformable Cross Section

A regional retrodeformable cross section (at a scale of 1:62,500) at approximately 39°00' N latitude through the Pancake Range, Duckwater Hills, and White Pine Range (Figures 1 and 22, Plate 3) places the geology of the study area into a regional structural

context and allows examination of extension and reconstruction of the CNTB. To construct the cross section, I used data from published geologic maps (Pipkin, 1956; Lumsden, 1964; Hose and Blake, 1976; Kleinhampl and Ziony, 1985) of the Pancake Range, Duckwater Hills, and White Pine Range. My mapping and W.J. Taylor's unpublished mapping further constrains the geology in the White Pine Range. A combination of available well data (scout tickets and well logs) and surface geology aided in constraining valley-fill thicknesses and the geology beneath valley fill (Celsius Energy well 9-1; Apache Corporation well 12-34). The availability of subsurface data is limited, and therefore, the geology beneath the valleys is simplified. In some cases, unconstrained faults are geometrically required but are clearly marked on the cross section. I used basic cross-section balancing techniques that are briefly described in Appendix B.

The resultant cross section is restorable, retrodeformable and line-length balances between two loose lines within an error of $<1\%$ (Plate 3c). It is possible that the eastern loose line could be considered a pin line (where the units return to regional dip). However, the eastern extent of the CNTB at this latitude is poorly constrained, and thus, the line is more conservatively considered a loose line. Although balanced and restored cross sections yield non-unique solutions, this regional cross section provides both a viable and admissible interpretation of the available data.

Extension

At least four episodes of normal faulting occurred in the region between the Pancake Range and the White Pine Range at $39^{\circ}00'$ N latitude. These normal faults cut and down dropped Mesozoic folds and thrust faults and accommodated 14 km (45,750 ft) of extension across the entire cross section. Except within the study area, most normal faults in the region strike roughly north and dip moderately to steeply west, although some faults dip east (Plate 3a). Most faults cut the Oligocene Stone Cabin

Formation and are, therefore, Oligocene or younger (Pipkin, 1956; Lumsden, 1964; Hose and Blake, 1976; Kleinhampl and Ziony, 1985).

Post-Volcanic Extension

Cross cutting relationships among post-volcanic normal faults suggest that of the 4 episodes of extension at least 3 periods are post-Oligocene (Plate 3a). Most post-Oligocene faults dip 50° to 60°W, although in the Pancake Range the faults dip consistently east; and in the White Pine Range, the faults exhibit a wide range of strikes and dips (see Chapter 4). Four post-Oligocene faults were interpreted to exist in the valleys near the edges of the Duckwater Hills and the Pancake Range (Plate 3a). These unexposed faults lie beneath valley fill and are geometrically required. The projections of formations from ranges into the basin do not align, and the faults provide an explanation of the misalignment. Because these faults lie near the edges of the ranges and have large stratigraphic separations, I refer to them as range-bounding faults. Along the cross-section line, stratigraphic separations of range-bounding faults average 1800 m (5940 ft) and stratigraphic separations of faults that crop out in the range interiors average ~360 m (~1200 ft). However, the total heave or extension across the range interior and range-bounding faults (excluding the Blackrock fault) is only ~2200 m (7250 ft) and ~4400 m (14,500 ft), respectively.

Although most of the post-Oligocene faults are moderately to steeply dipping, a major part of the total extension across this region was accommodated by the low-angle Blackrock fault and associated high-angle faults that crop out in the southern White Pine Range (see Chapter 4, Plate 1, Plate 3a). The Blackrock fault and associated faults accommodated 7.6 km (25,000 ft) or ~55% of the total extension across the region. The Blackrock fault contains a bend, such that the fault dips 15° to 30°W on the western side of the range and ~20°E on the eastern side (Plate 3a). This bend in the fault is interpreted

as a primary fault bend. Geometric data do not support the hypothesis that this bend resulted from later doming or block tilting (see Chapter 5).

Pre-Volcanic Extension

The only pre-volcanic normal faults exposed near the regional cross section are those that crop out in the study area (see Chapter 4, Plate 1). However, in the Pancake Range, Pennsylvanian Ely Limestone and Devonian Guilmette Formation crop out beneath the sub-Tertiary unconformity, and the juxtaposition of these two units geometrically requires the presence of two pre-volcanic faults (Plate 3b). These faults are pre-Oligocene because they cut and down dropped the Pancake thrust and associated anticline prior to the deposition of the Oligocene Stone Cabin Formation (Plate 3b). Although geometrically unconstrained, these faults are drawn with originally steep dips (80°W) because pre-volcanic normal faults in the region are typically steeply dipping. Stratigraphic separations of ~1600 m (5250 ft) and 152 m (500 ft) are required across the eastern and western faults, respectively. The large amount of stratigraphic separation on the eastern fault is reasonable because Late Cretaceous-Eocene sedimentary rocks of the Sheep Pass Formation crop out in the central Pancake Range and occur in drill holes in Railroad Valley suggesting significant down dropping created a sedimentary depositional center during that time (Winfrey, 1960; Kleinhampl and Ziony, 1985).

Central Nevada Thrust Belt Reconstruction

Previously documented folds and thrust faults that are part of the central Nevada thrust belt at the present latitude of 39°00' N include the Pancake thrust, McClure Spring syncline, Duckwater thrust, and the Easy Ridge or Green Springs thrust (Figure 22, Plate 3) (Pipkin, 1956; Humphrey, 1960; Nolan and others, 1974; Carpenter and others, 1993; Perry and Dixon, 1993). Additionally, geologic mapping and restored and retrodeformable cross sections of the study area, reveal the presence of a previously

unrecognized thrust, the White Pine thrust. Each of these contractile structures is described below.

Pancake Range

The Pancake thrust and McClure Spring syncline crop out for at least 3 and 6 km, respectively, along strike in the central Pancake Range (Figure 22) (Carpenter and others, 1993; Perry and Dixon, 1993). Volcanic rocks cover and Tertiary normal faults cut the syncline and thrust fault along the cross-section line. These structures must be present along the cross-section line because the thrust fault crops out just 0.5 km to the north, and the syncline crops out just 2 km to the south. The Pancake thrust restores to a 60°W-dipping footwall and hangingwall ramp that places (at the paleosurface) Devonian Guilmette Formation on an overturned footwall syncline (McClure Spring syncline) of Mississippian Chainman Shale and Diamond Peak Formation and Pennsylvanian Ely Limestone (Plate 3c). Stratigraphic separation across the Pancake thrust is 770 m (2500 ft). The unusually steep dip of this thrust ramp is also calculated from Mobil Oil well DH-2, Black Point (Figure 22) (Carpenter and others, 1993), in the central Pancake Range. Long, steep ramps are typical of thrust faults in the CNTB (Taylor and others, 1993).

Duckwater Hills

In the Duckwater Hills, Tertiary rhyolites, andesite, and ash-flow tuffs unconformably overlie the Devonian Guilmette Formation, but just east of the hills in Railroad Valley, Pennsylvanian Ely Limestone crops out. The position of these rocks suggests that the Duckwater thrust (Flapjack thrust of Pipkin, 1956), which is documented ~5 km to the north (Carpenter and others, 1993), lies beneath the surface near the eastern edge of the Duckwater Hills (Figure 22, Plate 3a). The Duckwater thrust, where it is exposed north of the cross-section line, places Devonian Guilmette

Formation (part of a hangingwall ramp anticline) over Pennsylvanian Ely Limestone (Pipkin, 1956; Hose and Blake, 1976; Carpenter and others, 1993). The Duckwater thrust, in the line of the cross section, has a stratigraphic separation of 3280 m (10,750 ft) and restores to a 70°W-dipping footwall and hangingwall ramp (Plate 3c).

An upright anticline exposed in the Devonian Guilmette Formation crops out approximately 6 km north of the cross section line, in the valley between the Duckwater Hills and the Pancake Range (Figure 22, Plates 3a and 3c). The fold is west-vergent and is interpreted as a fault propagation fold that formed above a backthrust to the Duckwater thrust (Plate 3c). M. Chapin mapped a backthrust ~16 km to the north that places Ordovician and Silurian units over Devonian Guilmette Formation (Carpenter and others, 1993). Displacement along this backthrust apparently decreases southward, because at the latitude of the cross-section line the backthrust is required to have less than 200 m of stratigraphic separation (Plate 3c).

White Pine Range

Two west-dipping thrust faults crop out in the vicinity of the northwestern White Pine Range: the Easy Ridge and Green Springs thrusts (Figure 22) (Humphrey, 1960; Hose and Blake, 1976; Carpenter and others, 1993). At the surface, both thrust faults juxtapose Devonian Guilmette Formation in the hangingwall against Mississippian Diamond Peak and Pennsylvanian Ely Limestone in the footwall (Hose and Blake, 1976; Carpenter and others, 1993). The Easy Ridge thrust, where it is documented by Carpenter and others (1993), lies along the eastern edge of hills just north of the Duckwater Hills (Figure 22). Along the cross section line, however, the Easy Ridge thrust is interpreted to lie beneath northern Railroad Valley (Figure 22, Plates 3a and 3c). The Green Springs thrust crops out along the White Pine range front north of the cross-section line (Figure 22) (Humphrey, 1960).

Along the cross-section line, one thrust fault with the above mentioned juxtaposition is geometrically required beneath northern Railroad Valley. This particular thrust fault marks the eastern edge of a duplex (Plate 3c). It is the floor thrust of the duplex and the Duckwater thrust is the roof thrust. Along the cross-section line, the stratigraphic separation on this thrust fault is 1067 m (3500 ft). This thrust fault may correlate reasonably with either the Easy Ridge thrust or the Green Springs thrust. However, a direct correlation with only one of the thrust faults is indeterminable. In my interpretation, I suggest that either (1) the Easy Ridge and Green Springs thrusts merge into a single thrust or (2) one of the two faults dies out north of the cross-section line.

Geologic mapping and cross-section restorations suggest that, in the southern White Pine Range, the Blackrock fault reactivated or cut an unexposed thrust fault, the White Pine thrust (see Chapter 5). Conceptually, the Blackrock fault could cut out this thrust fault, but in this interpretation, the Blackrock fault reactivates the thrust fault because it provides an end-member geometry. Additionally, in this interpretation the Blackrock fault cuts away from the thrust at depth (Plate 3a). Reconstructions suggest that hangingwall folds (see Chapters 4 and 5) were thrust over an $\sim 50^\circ$ E-dipping homocline of Cambrian through Mississippian rocks (Plate 3c). These hangingwall folds are probably part of the Illipah fold belt that consists of approximately north-south trending, upright, open anticlines and synclines exposed in Devonian through Permian units (Figures 1 and 22, Plates 2 and 3c) (Hose and Blake, 1976; Tracy, 1980; Guerrero, 1983; W.J. Taylor, unpublished mapping). In the interpretation shown in the reconstruction, which minimizes slip along the White Pine thrust, the fault places (at the paleosurface) Pennsylvanian Ely Limestone over Permian Reipetown Formation (Plate 3c) and has a stratigraphic separation of 1067 m (3500 ft). Following thrusting and the emplacement of Oligocene volcanic rocks, the Blackrock fault reactivated the White

Pine thrust down dropping the hangingwall folds to their present position against the footwall homocline (Plates 1, 2, and 3a).

A literature review provided no possible correlative thrust fault to the White Pine thrust exposed either to the north or south. The White Pine thrust does not lie along strike of the Green Springs thrust and, thus, probably does not correlate with it (Figure 22). Also, the Illipah fold belt appears to lie in the footwall of the Green Springs thrust, but in the hangingwall of the White Pine thrust (Humphrey, 1960; Carpenter and others, 1993). Because the White Pine thrust underlies the Illipah folds and additional folds are exposed north and northeast of the study area (Tracy, 1980; Guerrero, 1983; W.J. Taylor unpublished mapping), the White Pine thrust may underlie much of the northern White Pine Range.

Interpretation of the Regional Cross Section

A restored and balanced cross section through this region allows (1) documentation of extensional structural styles and distributions of extension, (2) restoration of the Mesozoic central Nevada thrust belt, and (3) determinations of the amounts of shortening and extension across this part of the thrust belt.

Cenozoic Extensional Structural Styles and Distributions

Post-Oligocene extension in this region is unevenly distributed and probably reflects different extensional structural styles that were active at different times. The largest magnitude of post-Oligocene extension occurred in the southern White Pine Range, along the Blackrock fault and associated faults. Hangingwall faults to the Blackrock fault are more closely spaced (~1/2 km apart) than the range-bounding Basin and Range faults (~8 km apart) (Plate 3a). Therefore, the range-bounding Basin and Range faults and the Blackrock-related faults may either represent different styles of extension or suggest that a basal detachment for the Basin and Range faults lies deep in

the crust. If these faults represent two different extensional styles, then the older, post-Oligocene extensional style consists of low-angle normal faults and associated closely spaced hangingwall faults; and the younger Basin and Range style is one of widely spaced, steeply dipping faults.

Pre-Oligocene extension accounts for ~10% of the total extension along the cross-section line. Local known faults that accommodated this extension are restricted to the Pancake Range and the northeastern part of the map area in the southern White Pine Range (Plates 1 and 3b). These faults typically dip steeply. Although the faults are few, the magnitude of extension along each can be significant, up to 1600 m (5250 ft). Post-contractile, pre-Oligocene normal faults and related basinal deposits are documented in isolated localities throughout the Great Basin (e.g., Sheep Pass Basin) (Winfrey, 1960). Although the magnitude of pre-Oligocene extension is significant, the limited and isolated distribution of these faults and basins suggests that this part of the Basin and Range Province did not undergo widespread extension until the Oligocene (Axen and others, 1993).

Mesozoic Contractional Structural Styles and Distributions

It was possible to construct a geometrically and geologically reasonable and viable cross section across this region. Reconstructed folds and thrust faults across the region show a thrust belt geometry consistent with that documented elsewhere in the CNTB (Taylor and others, 1993). This geometry typically consists of long, steep ramps; large vertical uplift; and significant, but not extremely large, amounts of shortening. For example, folds and thrust faults in this part of the belt together accommodated 6 km (19,500 ft) of horizontal shortening and 6.3 km (20,750 ft) of throw (Plate 3c). This geometry and kinematics is similar to that seen elsewhere in the trailing edge of thrust belts (e.g., Boyer and Elliot, 1982). In addition, this geometry and position is consistent

with the interpretation that the CNTB is the western part of the Sevier orogenic belt (Taylor and others, in preparation).

Age constraints permit interpretations of the thrust faults and folds in the cross section as part of either one thrust belt or parts of two belts, with the older belt exposed on the western end of the section and the younger belt exposed on the eastern end. Perry and Dixon (1993) suggest that the Pancake thrust and McClure Spring syncline could be part of an older, separate thrust belt. However, the Pancake thrust and McClure Spring syncline do not exhibit a geometry indicative of the frontal part of a thrust belt, such as long flats and short ramps or a triangle zone. Furthermore, all of the folds and thrust faults exhibit a similar structural style that can be geometrically linked to represent one thrust belt. Therefore, I propose that the Pancake thrust and McClure Spring syncline are part of the same thrust belt as the Duckwater thrust, Easy Ridge or Green Springs thrust, and the White Pine thrust.

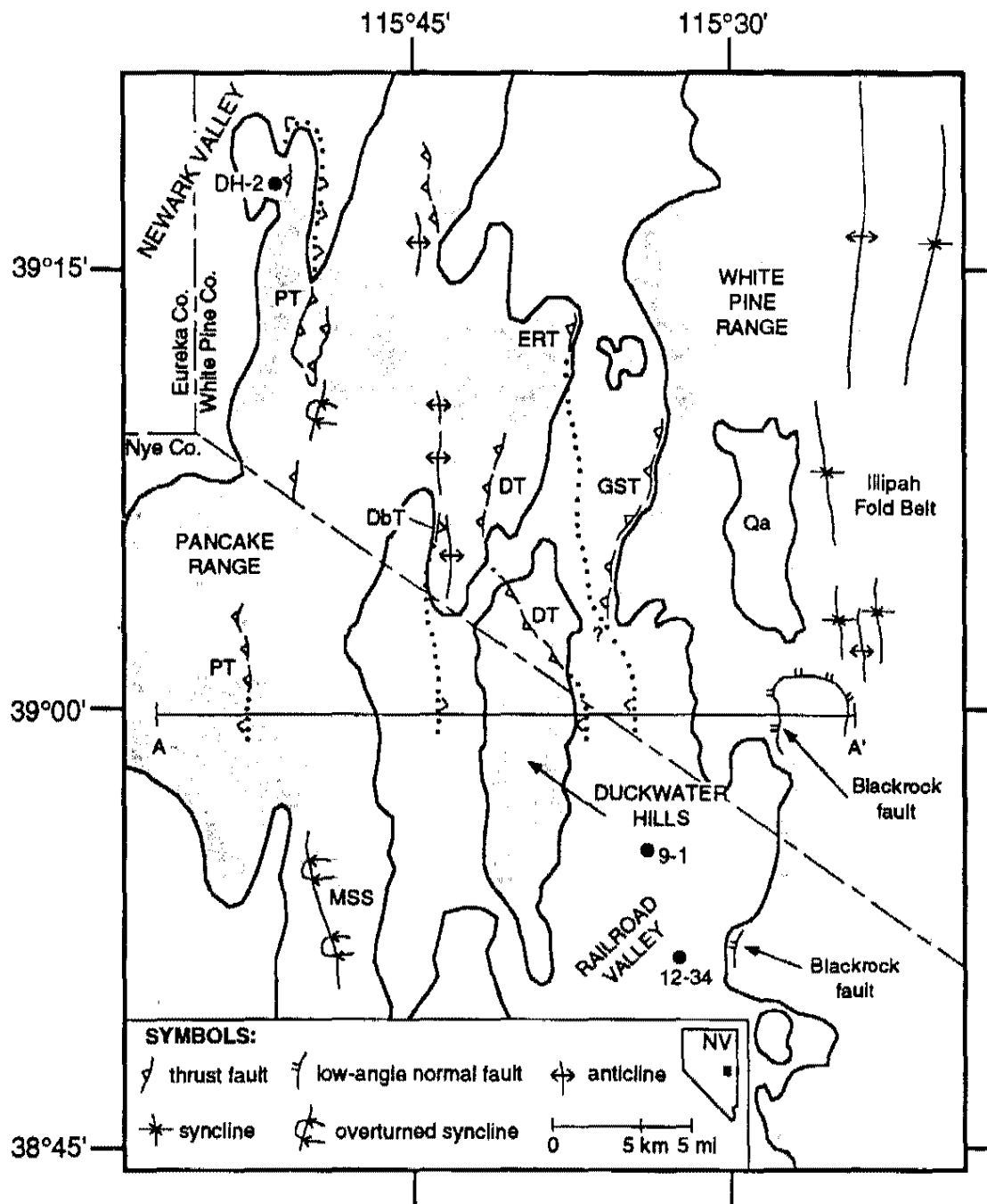


Figure 22. Map showing the location of structures shown on the regional cross section (Plate 3). Thrust faults and folds discussed in chapter 6 are labeled: PT= Pancake thrust; MSS= McClure Spring syncline; DT= Duckwater thrust; DbT= Duckwater backthrust; ERT= Easy Ridge thrust; GST= Green Springs thrust. The locations of these structures were obtained from Pipkin (1956), Hose and Blake (1976), Kleinhampl and Ziony (1985), and Carpenter and others (1993). Structures concealed and/or inferred along the cross-section line are dotted. Drill holes (black circles) discussed in text are labeled. Qa= Quaternary alluvium.

CHAPTER 7

PETROLEUM POTENTIAL

Between 1954 and 1994, 12 oil fields in Railroad and Pine Valleys, Nevada (Figure 23) produced over 35 million barrels of oil (Goff and others, 1994). The most prolific fields are in central Railroad Valley, just 45 km (30 mi) southwest of the Blackrock Canyon area. Bouguer gravity anomalies (Saltus, 1988) suggest that Railroad Valley comprises three subbasins: the southern, central, and northern subbasins (Grabb, 1994). The petroleum potential of the northern subbasin, located just west of the Blackrock Canyon area remains largely unexplored. However, the strata and structure of the Blackrock Canyon area, which presumably are down dropped to the west beneath Railroad Valley, are analogous to several of Nevada's producing oil fields. Collectively, the stratigraphy, structure, and temperature gradient of the Blackrock Canyon area suggest that the petroleum generation and accumulation potential just west of this area is quite high.

Hydrocarbon Occurrence in the Great Basin

In the Great Basin, source and reservoir rocks are the Paleozoic miogeoclinal succession, Eocene sedimentary rocks, and Tertiary volcanic rocks (reservoir only) (Bortz, 1994; Flanigan, 1994; French, 1994; McCutcheon and Zogg, 1994). Oil is generated from the Mississippian Chainman Shale, Devonian Pilot Shale, Late Cretaceous-Eocene Sheep Pass Formation, and the Eocene Elko Formation (Inan and Davis, 1994). The most common source rock, the Chainman Shale, has a regional

average total organic carbon (TOC) content of >1 weight percent with dominantly oil-prone kerogen (Inan and Davis, 1994).

Extensional structures primarily control the generation, migration, and trapping of hydrocarbons, in Nevada. In Railroad Valley, peak oil generation began in the Miocene (~11 Ma), after the onset of significant amounts of extension and basin subsidence (Barrett, 1987; Inan and Davis, 1994). Increased permeability due to extension-related fracturing and faulting caused the subsequent migration of this oil. Trapping of petroleum commonly occurs in structural culminations that are products of extension (e.g., Bortz, 1994; Flanigan, 1994; McCutcheon and Zogg, 1994).

The Grant Canyon Field: A Structural and Stratigraphic Analog

The structural style and stratigraphy of the Blackrock Canyon area is similar to several prolific oil fields in Nevada (e.g., Grant Canyon, Eagle Springs, Blackburn), but it most closely resembles the Grant Canyon field. The Grant Canyon field, the most productive oil field to date in the Great Basin, produced over 19.3 million barrels of oil (as of 1994) from five wells in fractured Devonian carbonates (McCutcheon and Zogg, 1994).

Stratigraphy

The stratigraphy above the Grant Canyon field comprises Devonian carbonates, Mississippian Chainman Shale, Late Cretaceous - Eocene Sheep Pass Formation, Oligocene volcanic rocks, and a thick (1829 m or 6000 ft) accumulation of Tertiary and Quaternary valley fill (McCutcheon and Zogg, 1994). In this field, the Chainman Shale generates petroleum at a burial depth of ~1842 m (7000 ft) and reservoirs in highly fractured Devonian carbonates produce hydrocarbons.

Structure

The structural development of the Grant Canyon field resembles the structural evolution of the adjacent Grant Range; pre-Tertiary folding and thrusting with later widespread extensional faulting and fracturing. In this field, low- and high-angle normal faults of multiple orientations serve as migration pathways, increase permeability of reservoir rocks, and localize oil accumulations in different fault blocks. Also, movement along these normal faults results in extension-related folds that entrap hydrocarbons (McCutcheon and Zogg, 1994).

The Grant Canyon field lies in a highly faulted hangingwall of a low-angle normal-fault system that consists of the active, range-bounding Railroad Valley fault and the inactive Guilmette fault. The pre-Quaternary Guilmette fault, exposed ~1 to 3 km east of the Railroad Valley fault, is the youngest of a stacked set of low-angle normal faults documented in the Grant Range (Fryxell, 1988, 1991; Camilleri, 1989, 1992; Lund and others, 1991; Lund and Beard, 1992; McCutcheon and Zogg, 1994). The high-angle Railroad Valley fault appears to sole into the low-angle Guilmette fault (Figure 24) (Lund and others, 1991; Lund and Beard, 1992; Grow and others, 1993; McCutcheon and Zogg, 1994). In the upper plate of this fault system, high-angle normal faults cut valley fill, Tertiary volcanic and sedimentary rocks, and pre-Tertiary contractile structures.

The fault geometries of the Guilmette and Railroad Valley faults profoundly influenced the formation of the dominant structural traps in the field. These dominant traps consist of two extensional folds observed in valley-fill deposits. The largest of the folds is a fault-bend anticline that formed in response to motion along the Railroad Valley fault. Several productive wells lie along the fold axis that trends N55°W and plunges gently northwest (Figure 25). The second fold is a monocline that occurs across a pronounced lateral ramp in both the Railroad Valley and Guilmette faults (McCutcheon

and Zogg, 1994). Structure contour maps of these faults (e.g., Figure 26) show that this lateral ramp persists to depths of greater than 1524 m (5000 ft) below the fault surface trace. Fault-related monoclines also crop out in Paleozoic rocks within the upper plate of the Guilmette fault (Fryxell, 1988; McCutcheon and Zogg, 1994).

Petroleum Potential of the Blackrock Canyon Area

The northern subbasin of Railroad Valley, located just west of the Blackrock Canyon area, remains largely unexplored and therefore, knowledge of the subsurface geology is limited. However, geologic mapping, a regional retrodeformable cross section, and sparse drill hole data south of the Blackrock Canyon area suggest that the structural and stratigraphic evolution of the subbasin relates closely to that of the Blackrock Canyon area. These data, when combined with the local geothermal gradient, suggest favorable conditions for the generation and accumulation of petroleum within the subbasin.

Stratigraphy

The stratigraphy of the Blackrock Canyon area is similar to that of the Grant Canyon field and elsewhere in and along Railroad Valley. In the study area, Paleozoic miogeoclinal rocks are unconformably overlain by a thick sequence of Oligocene volcanic and sedimentary units that, in Railroad Valley, are then unconformably overlain by Tertiary and Quaternary valley fill. A combination of surface geology and drill-hole data suggest that various reservoir rocks and a source rock (Chainman Shale) lie within the basin (Plate 3a).

The stratigraphy differs slightly from that of the Grant Canyon field. For example, the valley-fill thickness is ~1829 m (6000 ft) in the Grant Canyon field, but does not exceed 1220 m (4000 ft) in the northern subbasin (Apache Corporation well 12-34, Celsius Energy well 9-1). Conversely, the thickness of Oligocene volcanic rocks

(~1460 m or 4800 ft), in the study area, is much greater than in the Grant Canyon field (<263 m or 1000 ft) (McCutcheon and Zogg, 1994). One other significant difference is the absence of the Late Cretaceous - Eocene Sheep Pass Formation in the study area and in the Duckwater Hills, due to either erosion or non-deposition (Pipkin, 1956; Kleinhampl and Ziony, 1985). It is possible that this area was a topographic high during the time of its deposition.

Structure

Structures in the Blackrock Canyon area are strikingly similar to those in the Grant Canyon field (see Chapter 4). A low-angle normal fault and its associated hangingwall faults (Plate 1, Figure 7) cut both Oligocene volcanic rocks and pre-Tertiary contractile structures.

In the Blackrock Canyon area, the range-bounding Railroad Valley fault is interpreted to lie ~2 km west of the Blackrock-fault surface trace. Constraints from a regional retrodeformable cross section (Plate 3) and drill-hole data from a well located 3 km south of the cross-section line, suggest that the steeply dipping (70°W) Railroad Valley fault cuts the Blackrock fault (Celsius Energy well 9-1). Therefore, the basin just west of the Blackrock Canyon area presumably contains the down-dropped highly faulted Blackrock hangingwall. In this subbasin, these faults and fractures most likely enhance reservoir potential and entrap oil in different fault blocks.

The complex pattern of deformation in the Blackrock hangingwall results from slip along the geometrically irregular Blackrock fault (see Chapter 4). The northern part of the Bull Spring corrugation is a moderately dipping (42°SW) lateral ramp (Plate 1, Figures 7 and 8). This lateral ramp could cause the formation of an extensional fold, similar to the fold in the Grant Canyon field. Without adequate subsurface data, it is difficult to know if such a fold exists across this lateral ramp. Reverse faults, however, which cut the volcanic rocks and crop out near this corrugation, suggest that this part of

the Blackrock fault accommodated post-Oligocene shortening and consequently may have a fold or folds within the hangingwall (Plate 1, Figure 12).

Dissected valley-fill deposits just north and south of the study area (in Freeland and Broom Canyons, respectively) display broad anticlines (Langrock and Taylor, unpublished data). These folds most likely formed as rollover anticlines related to the Railroad Valley fault. The valley fill, within the Blackrock Canyon area, remains undissected so it is impossible to determine from field observation whether or not this type of fold is present. Nevertheless, because such folds crop out nearby, the occurrence of such a fold in the basin proximal to the Blackrock Canyon area is quite probable.

Oil Generation Potential

Constraints from drill-hole data south of the Blackrock Canyon area combined with surface geology north of the area suggest that the burial depth of the Chainman Shale, where it is down dropped by the Railroad Valley fault, is ~2195 to 2287 m (7200 to 7500 ft) (Plate 3a). This depth is just within the upper limit (2195 to 3003 m or 7200 to 9850 ft) of the Chainman oil window in parts of Railroad Valley (Barrett, 1987). However, a 1677-m (5500 ft) -deep well drilled ~13 km (8 mi) south of the Blackrock Canyon area reported bottom-hole temperatures ranging from 68° to 73° C (154° to 162° F) (Apache Corporation well 12-34, Stahl, personal communication). This temperature range at this depth suggests that the geothermal gradient in the vicinity of the Blackrock Canyon area is ~19° C/km (2° F/100 ft). This gradient is consistent with the temperature gradient reported for the Eagle Springs and Kate Springs fields, where the Chainman Shale generates oil at a burial depth of 2134 to 2439 m (7000 to 8000 ft) (Duey, 1983; Bortz, 1994). Therefore, based on these data, the Chainman Shale within the basin west of the Blackrock Canyon area, could likely be within the oil window.

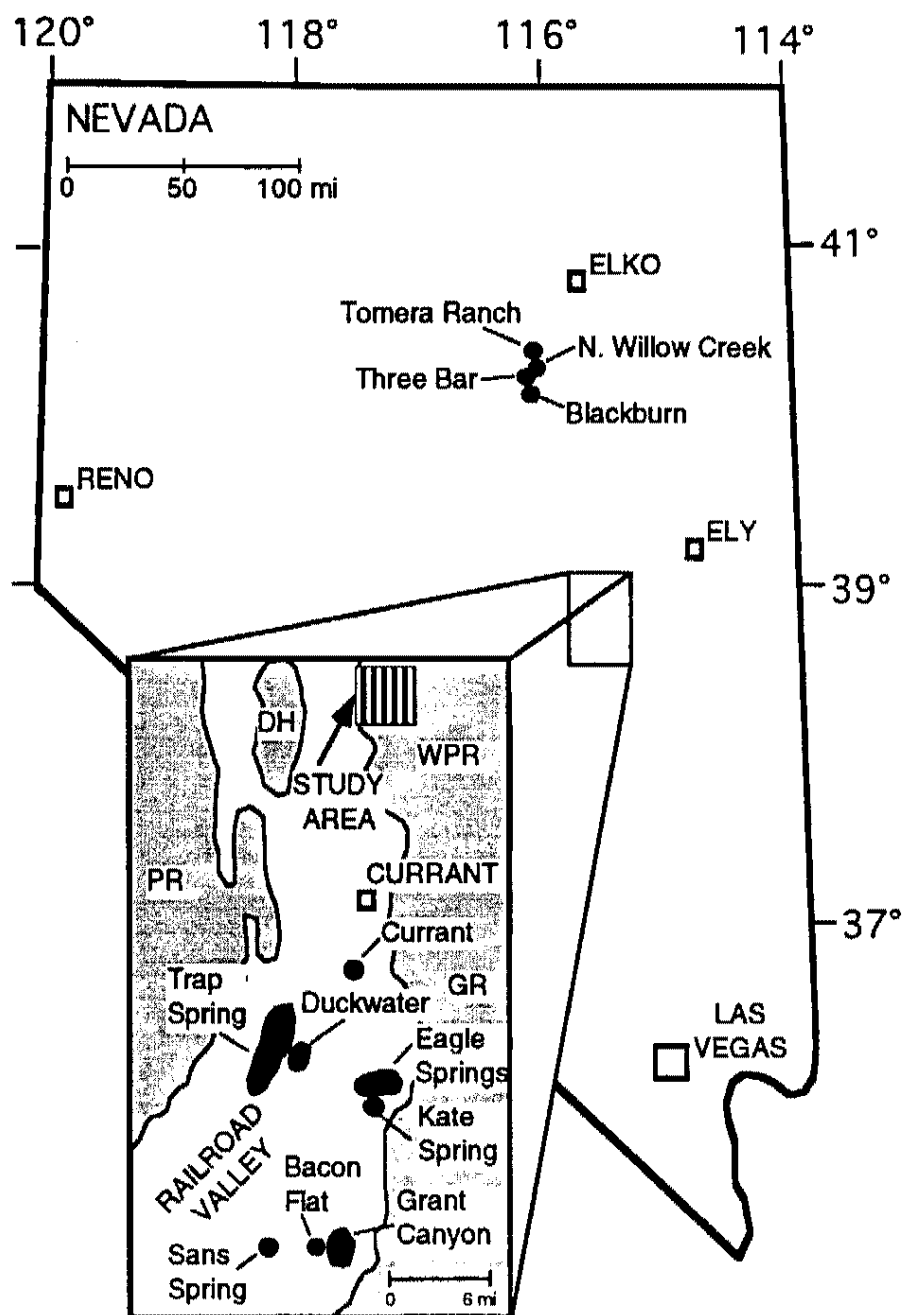


Figure 23. Location map of oil fields (in black) in Nevada. The study area is shown by the vertically ruled box. PR= Pancake Range, DH= Duckwater Hills, WPR= White Pine Range, GR= Grant Range (modified from Schalla and Johnson, 1994).

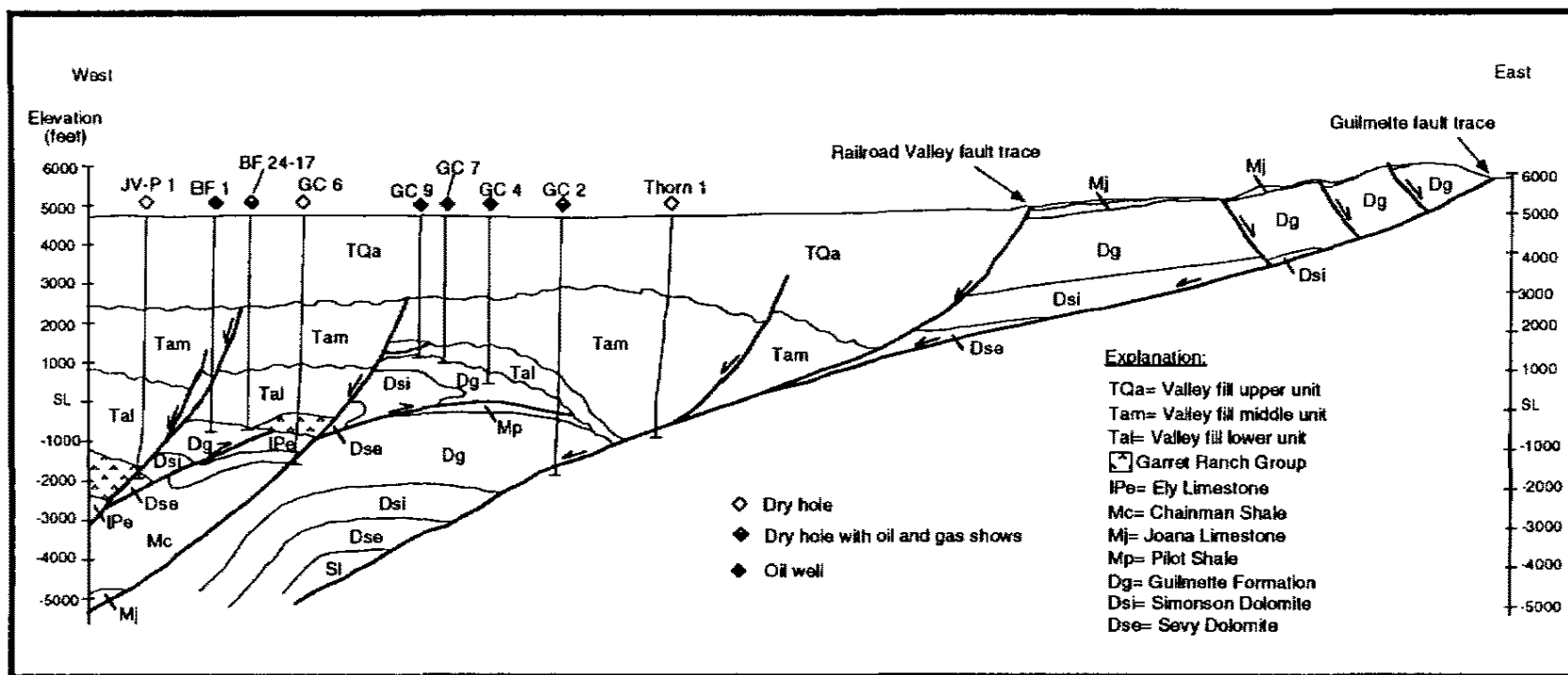


Figure 24. Geologic cross section illustrating the structure and stratigraphy of the Bacon Flat and Grant Canyon fields. Diamonds indicate drill-hole locations (modified from McCutcheon and Zogg, 1994).

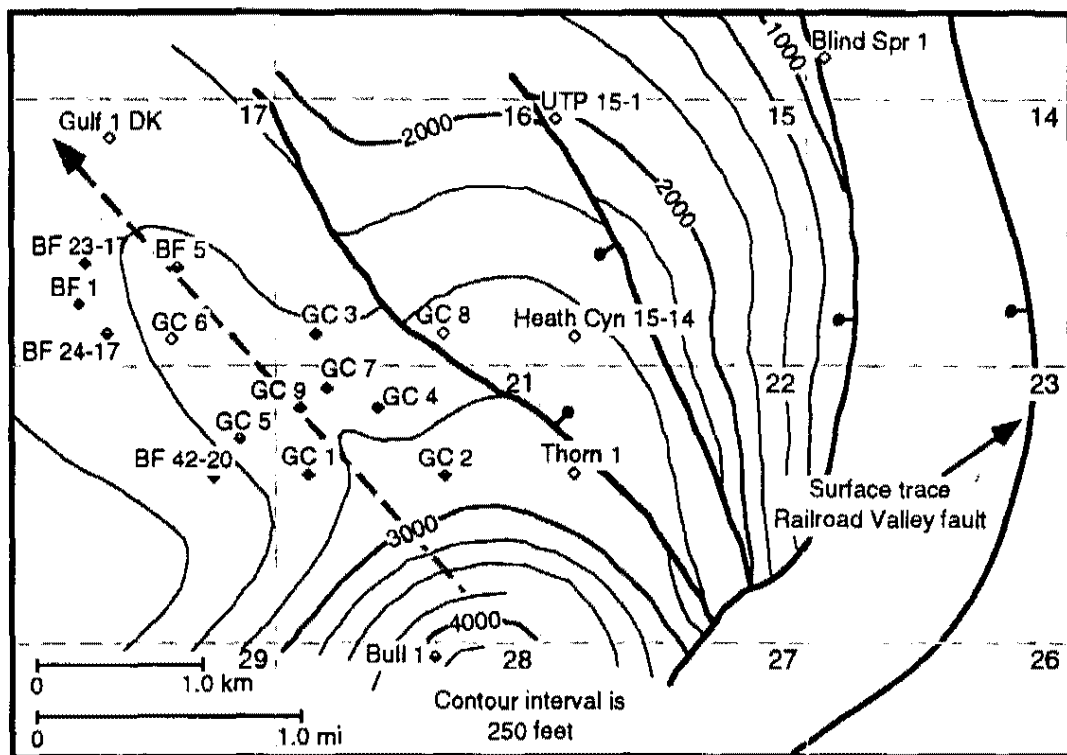


Figure 25. Structure contour map of a middle unit within the valley fill that shows an extensional fault-bend fold across the Railroad Valley fault. The dashed arrow is the approximate trend of the fold axis. Diamonds are locations of drill holes. Dashed, gray lines are section boundaries (modified from McCutcheon and Zogg, 1994).

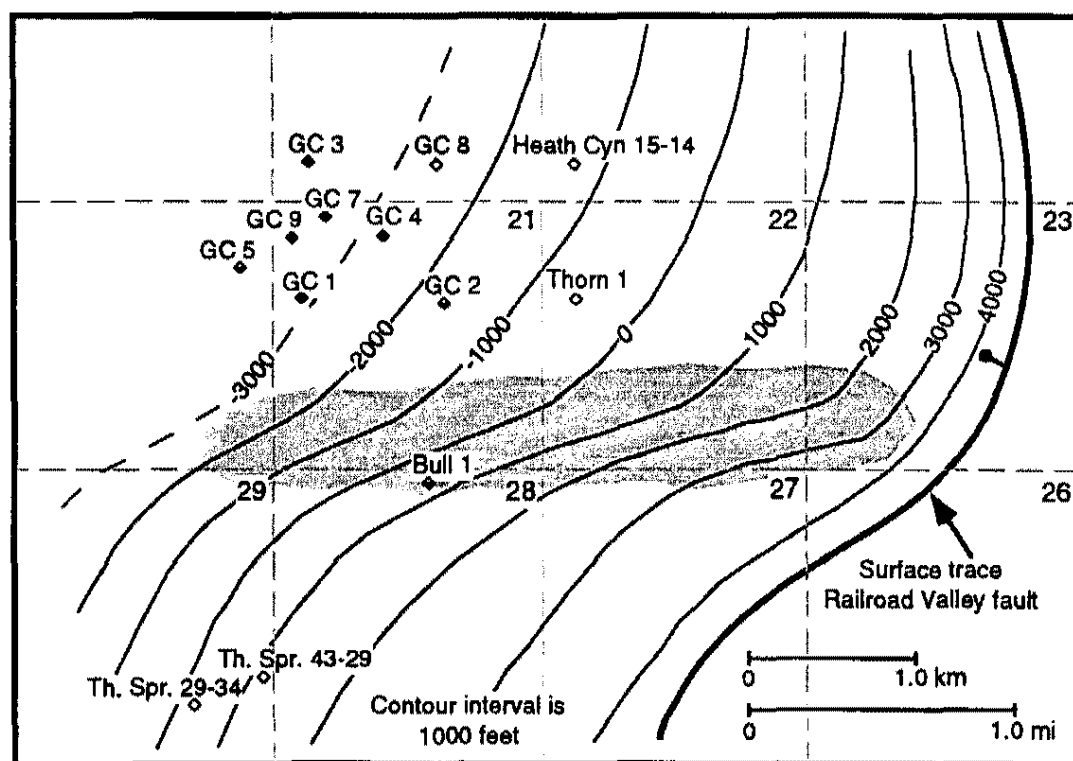


Figure 26. Structure contour map of the Railroad Valley fault, Grant Canyon field. Diamonds are drill-hole locations. Dashed lines are section boundaries. The stipple pattern indicates the approximate location of the north-dipping lateral ramp (modified from McCutcheon and Zogg, 1994).

CHAPTER 8

SUMMARY AND CONCLUSIONS

Mesozoic contraction and Cenozoic extension and volcanism define the tectonic framework of the Blackrock Canyon area in the southern White Pine Range. Detailed geologic mapping, local and regional restored and retrodeformable cross sections, and geometrical and temporal analyses of faults in the study area allow (1) step-wise reconstruction of the Mesozoic contractile structures, (2) documentation of extensional structural style and distribution of extension, and (3) identification of faulting processes that generated the normal faults in the study area.

Restored and retrodeformable cross sections of the study area and a regional cross section that extends from the Pancake Range through the White Pine Range allow reconstruction of a pre-extensional thrust belt. These reconstructions show large-scale folds and thrust faults that are part of the central Nevada thrust belt (CNTB). These thrust faults and folds correlate with the Pancake thrust, McClure Spring syncline, Duckwater thrust, and the Easy Ridge or Green Springs thrust; all of which crop out in surrounding areas. Folds and thrust faults in this part of the CNTB accommodated 6 km and 6.3 km of horizontal and vertical shortening, respectively. The geometries of all of the folds and thrust faults depicted on the cross section suggest that they are part of a single thrust belt. The geometry of this belt, as documented in the cross section, is consistent with the geometry of the CNTB elsewhere. This regional synthesis significantly impacts our present understanding of the area, because only folding and not large-scale thrusting was previously documented here.

At least 4 episodes of normal faulting resulted in 14 km of extension, which nearly doubled the original width of this part of the thrust belt during the Cenozoic. Normal faults in the region consist of (1) moderately to steeply dipping faults, exposed in the ranges, which exhibit moderate amounts of offset; (2) steeply dipping range-bounding faults with significantly larger amounts of offset; and (3) a low-angle normal fault (the Blackrock fault) and associated high-angle faults that crop out in the southern White Pine Range. The individual sets represent different extensional structural styles. Extension across this region is unevenly distributed among these different fault sets with the largest magnitude of extension in the southern White Pine Range.

The balanced and restored regional cross section suggests that the Blackrock fault and its associated hangingwall faults accommodated 55% of the total extension across this part of the belt. The post-Oligocene (post-31.3 Ma) Blackrock fault cuts folds and a previously unrecognized thrust fault, the White Pine thrust, which are interpreted as part of the central Nevada thrust belt. The 15° to 30°W-dipping Blackrock fault is non-planar. The fault consists of two segments; one of which contains a pronounced corrugation: the Bull Spring corrugation. Slip on the Blackrock fault was directed approximately west-northwest. Movement of the hangingwall block over the irregular fault surface resulted in non-conservative deformation in the upper plate.

Temporal and geometric relationships of Blackrock upper plate faults suggest that they represent three-dimensional or non-plane strain. These upper plate faults are roughly synchronous and orthorhombically symmetrical and, thus, did not form by classical conjugate faulting processes. My proposed kinematic model suggests that this non-conservative, three-dimensional deformation results from movement of the upper plate over the non-planar Blackrock fault.

All of these structural elements, when combined with the stratigraphic and thermal evolution of the area, may promote hydrocarbon generation, migration,

entrapment. The study area is located just northeast of Nevada's most productive oil fields, and the strata and structures of many of these fields are similar to those of the study area and adjacent basin. Therefore, the petroleum potential of the area is high.

APPENDIX A

STRATIGRAPHIC DESCRIPTIONS

Stratigraphic units exposed in the study area consist of a thick sequence of Paleozoic carbonates and siliciclastic rocks that are unconformably overlain by Tertiary volcanic and sedimentary units. Not all of the Paleozoic units depicted in Figure 5 are exposed in the study area. Lithologies and textures of only those units that crop out in the study area are described below. Because the White Pine Range is geographically proximal to the Eureka district, equivalent stratigraphic units there are also discussed. Unit thicknesses could not be measured or calculated because either the upper or lower formational boundary of each unit is omitted by a fault. Thus, regional thicknesses for each unit are given (e.g., Langenheim and Larsen, 1973; Hintze, 1985).

Paleozoic Sedimentary Formations

Cambrian through Permian strata crop out in the study area. Units were subdivided and mapped according to stratigraphic succession, textures, rock types, and fossil assemblages. No detailed stratigraphic or sedimentologic analysis of these units was conducted as part of this study, but their general lithology and stratigraphy are described below for field recognition.

Cambrian Windfall Formation

Nolan and others (1956) named the Windfall Formation for Upper Cambrian strata that lie between the Cambrian Dunderberg Shale and the Ordovician Pogonip Group. The type section is in Windfall Canyon in the Diamond Mountains, Nevada. In

the study area, the Windfall Formation is bounded by faults, and recrystallization (particularly at the base of this unit) is common. The 305-m-thick Windfall typically forms cliffs and is well exposed. The unit largely consists of chert-bearing limestones that are medium gray on the fresh and weathered surfaces. Chert occurs throughout the unit as extensive bedding-parallel lenses and is typically dark brown to dark gray. The Windfall contains very few fossils, among which are trilobite fragments and very small (1-2 mm across) crinoids, or eocrinoids (?). Thin-bedded, chert-rich, recrystallized mudstones and wackestones characterize the base of the Windfall. The middle to upper Windfall consists of medium-bedded wackestones and grainstones that are commonly cross-stratified. Some beds contain columnar stromatolites and pisoids. Dark brown-gray, commonly "tiger-striped" dolomites occur in the uppermost Windfall.

Ordovician Pogonip Group

The Pogonip Group, first named by King (1878), included strata between the Cambrian Dunderberg Shale and the Ordovician Eureka Quartzite. Nolan and others (1956) redefined the Pogonip and established the type locality at Pogonip Ridge in the White Pine Range. In the Eureka district, Pogonip subdivisions are the Goodwin Limestone, Ninemile Formation, and Antelope Valley Limestone (Nolan and others, 1956). In the central White Pine Range, Lumsden (1964) mapped six formations in the Pogonip as defined by Hintze (1960): House Limestone, Fillmore Limestone, Wah Wah Limestone, Juab Limestone, Kanosh Shale, and Lehman Formation.

Only a small part of the 1080-m-thick Pogonip Group crops out in the study area, and a description of that part follows. The mapped Pogonip includes the basal part of the Goodwin or House Limestone in fault contact with the upper part of the Ninemile Formation or Kanosh Shale. A change in rock type from silty, thin-bedded wackestones to resistant medium-bedded packstones and grainstones defines the contact between the

Cambrian Windfall Formation and the basal Goodwin or House Limestone. The basal Pogonip packstones and grainstones contain abundant trilobite fragments. Dr. Michael Taylor, U.S. Geological Survey, identified the fragments as asaphid trilobite fragments. Although species identification was difficult because the specimens were greatly fragmented, Dr. Taylor suggested that the trilobites were probably *Symphysurina* sp. The trilobites are Ordovician (Ibexian series) and possibly occur in the *Symphysurina* zone (?). Dr. Taylor stated that these trilobites occur in the Goodwin or House Limestone.

The Goodwin or House Limestone is in fault contact with the uppermost part of the Ninemile Formation or Kanosh Shale. This distinctive unit forms a yellow slope and consists of yellow-and pink-weathering siltstones, shales, and silty limestones with interbeds of more fossiliferous wackestones and packstones. The siliciclastic beds weather into plates and chips, whereas the limestones form medium-bedded, poorly exposed ledges. The limestones are blue-gray on fresh and weathered surfaces and contain abundant intraclasts. A mottled appearance and the presence of yellow silt stringers characterize the Pogonip limestones. Planispiral gastropods, brachiopods, and trilobite fragments are the common fossils within this unit.

Ordovician Eureka Quartzite

Originally, Hague (1883) defined the Eureka Quartzite in the Eureka District, Nevada. Kirk (1933) redesignated the type section at Lone Mountain, Nevada. The Eureka Quartzite is a distinctive resistant, cliff-former that is ~140 m thick. The quartz arenite is milky white on a fresh surface and weathers white to pink. Additionally, red, brown, and purple hematite commonly stains the weathered surface. The Eureka Quartzite comprises well-sorted, well-rounded, highly indurated, fine- to medium-

grained quartz sand. The generally cliffy outcrops are highly fractured and locally brecciated.

Ordovician Fish Haven Dolomite

The Fish Haven Dolomite was described by Richardson (1913) for exposures in the Bear River Range, Idaho. The Eureka district lithologic and temporal equivalent is the Hanson Creek Dolomite (Merriam, 1963). The ~130-m-thick Fish Haven is dark brown-gray on the weathered surface and dark gray on the fresh. In the study area, the Fish Haven is a medium- to coarse-crystalline dolomite that is medium- to thick-bedded. Fish Haven outcrops are typically resistant and cliffy. Fossils within the Fish Haven include small (2 mm across) crinoids, brachiopods, and abundant fossil fragments. The dolomite is laminated, commonly burrow mottled, and contains some brown and red chert lenses near its base.

Silurian Laketown Dolomite

Richardson (1913) described the Laketown Dolomite at the type locality in the Bear River Range, Utah. The stratigraphic equivalent in the Eureka district is the Lone Mountain Dolomite (Merriam, 1963). The Laketown Dolomite in the study area is a light-gray to white, coarse-crystalline dolomite that is ~320 m thick. A distinctive property of the Laketown is its coarse-crystalline, sugary texture. The unit is medium- to thick-bedded and locally contains horizontal algal laminae. No fossils or chert were observed.

Devonian Guilmette Formation

The Guilmette Formation, named by Nolan (1935) for outcrops in the Deep Creek Range, Nevada, consists of interbedded dolomite and limestone. The Eureka district equivalent of the Guilmette Formation is the Devils Gate Limestone (Merriam,

1940; Nolan and others, 1956). In the study area, the Guilmette is a 730-m-thick cliff-former that is bounded entirely by faults and severely brecciated. The Guilmette is chiefly a brown-gray, recrystallized limestone riddled with white calcite veins. Fossils within the Guilmette are sparse and replaced by calcite. The observed fossil assemblage includes high-spined gastropods, planispiral gastropods, and brachiopods. Due to the intense fracturing and veining of the Guilmette, bedding orientation and thickness is not discernible. The absence of chert and the types of fossils in the Guilmette, distinguish the unit from other units that are similar in appearance (e.g., Ely Limestone, Windfall Formation).

Mississippian Diamond Peak Formation

Hague (1883) originally defined the Diamond Peak Formation that Brew (1961) later described for exposures at the type locality in the Diamond Mountains, Nevada. The Diamond Peak Formation in the study area is ~215 m thick and consists principally of medium-grained sandstone and to a lesser extent siltstone and conglomerate. Outcrops of the Diamond Peak are generally resistant and when weathered, form dark-brown soils. The fresh and weathered surfaces of this unit are light brown, mustard yellow, dark brown, and rust-red. The subrounded, moderately sorted, siliceous sandstone contains both quartz and potassium feldspar grains. The sandstone is medium bedded and exhibits trough cross-stratification. Asymmetric ripple marks occur locally on bedding surfaces. The conglomerate consists of pebble-sized clasts of red, brown, green and black chert hosted in a sandy matrix. The chert clasts within the clast-supported conglomerate are subangular to well-rounded and moderately sorted.

Pennsylvanian Ely Limestone

The Ely Limestone was first named by Lawson (1906) and later redefined by both Spencer (1917) and Pennebaker (1932). None of the researchers established a

specific type section. However, Steele (1960) designated a reference section for the Ely Limestone along U.S. Highway 50, between Illipah Creek and Moorman Ranch, Nevada.

The Ely Limestone crops out in numerous localities within the study area and is recognized by a "stair-step" pattern of resistant, ledgy limestone outcrops. Its approximate thickness is 275 m. The bedding thickness in the Ely ranges from platy to very thick bedded, but thick bedding is most common. The Ely is typically light tan-gray on the fresh and weathered surfaces, but locally it is medium- and olive-gray. Chert-bearing mudstones, wackestones, and packstones characterize the Ely Limestone. The chert is light gray or pink and occurs either in nodules or parallel to bedding. The relative abundance of chert appears to decrease upsection. Although much of the limestone is void of clastic material, some beds contain floating sand and chert grains and others are silty and weather into plates. The Ely is typically fossil rich. The observed fossil assemblage includes pelecypods, tabulate corals, solitary corals, stony and lacy bryozoans, several species of brachiopods, small (4 mm across) crinoids, and conispiral gastropods.

Permian Reipe Spring Limestone

Steele (1960) defined the Reipe Spring Limestone for coralline- and fusulinid-bearing limestones that unconformably overlie the Ely Limestone. The type locality for the Reipe Spring is at the north end of Ward Mountain south of Ely, Nevada. A distinctive ledge of chert-pebble conglomerate marks the base of the Reipe Spring Limestone. The conglomerate consists of gravel- to pebble-sized, angular to subrounded chert clasts in a silty carbonate matrix. Black, green, red, and brown chert, as well as some fossil fragments, compose the clasts within the grain-supported conglomerate. In the study area, the conglomerate is discontinuous and approximately 60 cm thick.

An ~310-m-thick succession of medium- to thick-bedded wackestones and packstones overlie the basal conglomerate. Reipe Spring limestones are medium gray on the fresh surface and medium gray to pink-gray on weathered surfaces. The observed fossil assemblage consists of crinoids and brachiopods and an abundance of unidentifiable fossil fragments.

Permian Reipetown Formation

The limestones, sandstones, and shales of the Reipetown Formation were first named the Rib Hill Formation by Pennebaker (1932) for the type locality at Rib Hill in the Ruth mining district, Nevada. In 1960, Steele renamed this unit the Reipetown Sandstone, as a formation in the Carbon Ridge Group. Bissell (1964) changed the name to Reipetown Formation because of its mixed rock types. The Eureka district equivalent of the Reipetown Formation and Reipe Spring Limestone, collectively, is the Carbon Ridge Formation (Nolan and others, 1956). The Reipetown Formation is exposed in the northern part of the study area as a yellow to orange slope former with a few ledge forming beds of bioclastic limestone. It is up to 365 m thick and is composed of yellow and pink-red weathering calcareous siltstones and sandstones that break into thin plates and chips characterize most of the Reipetown. Within these clastic successions, sparse outcrops of medium-gray to brown packstones and fewer grainstones form thin-bedded (6 cm) to thick-bedded ledges. The limestones contain crinoids, brachiopods, pelecypods, lacy bryozoans, planispiral and conispiral gastropods, and large (1 cm long) fusulinids that are typically well preserved.

Tertiary Volcanic Units

Rhyolitic and dacitic ash-flow tuffs, rhyolites, andesite, and volcanoclastic lacustrine and fluvial deposits compose the Tertiary sequence in the study area. Textural and mineralogic features that were observed in the study area are described below.

Modal and volume percentages of constituents in each unit were determined from point count analyses (Table 1).

Tertiary Stone Cabin Formation

The Stone Cabin Formation is the oldest volcanic unit exposed in the study area. An $^{40}\text{Ar}/^{39}\text{Ar}$ radiometric date on the Stone Cabin Formation yielded an age of 35.3 Ma (Radke, 1992; Best and others, 1993). The Stone Cabin Formation was originally defined by Cook (1965) for exposures at the type locality, approximately 13 km (8 mi) southeast of Carrant, Nevada. In the study area, this unit contains generally equigranular (1-2 mm across) phenocrysts of smokey quartz, plagioclase, sanidine and biotite. Orange and pink pumice compose 10 to 20% of the rock, and the unit contains no appreciable lithic fragments (Table 1). The ~365-m-thick Stone Cabin is moderately to densely welded and moderately compacted. Within the study area, a discontinuous black vitrophyre was observed within the unit in one area (T13N, R57E, Sec 13). The Stone Cabin Formation typically weathers to form semi-rounded outcrops that range in color from orange-tan to purple, buff, white, light gray, blue-gray, and rust-red. Fresh surfaces of this tuff vary in color from tan to pink, light purple, white, orange-tan, and light gray.

Tertiary rhyolite of White Pine Range

An ~670-m-thick sequence of rhyolite is exposed throughout the study area. The rhyolite is here informally named the rhyolite of White Pine Range. Due to severe chemical alteration of these rocks, differentiation of the flows was not possible. However, five thin sections were made of samples collected along a transect through a non-faulted section of these flows and point count results indicate that these flows are mineralogically homogeneous (Table 1). This unit is readily recognized by large plagioclase crystals (up to 8 mm long) and sparse quartz, sanidine, and biotite phenocrysts (~1 mm long). Fresh colors of the outcrops vary from dark olive-gray to

light gray, purple, purple-gray, rust-red, and blue-gray. Weathered colors range from rust-red to tan-orange, gray-purple, and dark brown. These flows typically weather to flaggy blocks and commonly exhibit "popcorn texture". Generally, the flows are highly fractured with most fractures subparallel to each other. Outcrops can be very sparse within these rhyolites. Some of the flows are autobrecciated containing pebble to boulder-sized angular clasts. Few flows exhibit well-developed flow banding. The rhyolites also contain black vitrophyres (up to 2 m thick) within them. These rhyolites also underwent considerable amounts of secondary alteration and are riddled with hematite veins.

Tertiary Currant Tuff

The ~185-m-thick Currant Tuff consists of a volcanoclastic sedimentary sequence that is overlain by a poorly welded, pumice-rich tuff. Horizontally laminated and thin-bedded calcareous mudstones, siltstones, and sandstone make up the sedimentary sequence. The sedimentary rocks vary in fresh and weathered color from white to tan, green, blue-gray and yellow-tan. Biotite is conspicuous in nearly all hand samples, and glass shards are apparent in the coarser grained sandstones.

The upper portion of the Currant Tuff is a poorly welded, poorly to moderately compacted tuff that is bright white on both the fresh and weathered surfaces. The tuff consists of abundant clear quartz phenocrysts up to 7 mm in diameter, biotite (4 mm long), plagioclase, and sanidine (5 mm long). Typically large (4 to 30 cm long) pumice (~15 to 25% of the rock) and volcanic and carbonate rock fragments (~5% of the rock) were observed in outcrops. However, a point count analysis of this unit yields ~7% pumice and 0% lithics, which may represent a scale problem (Table 1).

Tertiary Windous Butte Formation

The youngest ash-flow tuff that crops out in the study area is recognized in hand sample by phenocrysts of amethyst to light-gray quartz (~2 mm in diameter); abundant biotite, some of which are up to 3 mm across; and minor phenocrysts of hornblende (2 to 5% of the rock) (Table 1). The tuff is ~120 m thick and consists of a moderately compacted and moderately welded portion overlain by a densely welded, highly compacted, fine-grained cap. Locally, a black vitrophyre crops out between the moderately welded and densely welded portions. The moderately welded portion contains ~10% white pumice and the densely welded part locally contains black fiamme. The tuff contains 0 to 5% volcanic rock fragments and is red-brown to light brown on the fresh surface and red-brown to tan-orange on the weathered surface.

Texturally and mineralogically, this unit appears to correlate with the rhyolitic Windous Butte Formation, except the unit contains a higher percentage of hornblende (Table 1) than is typically reported by workers in other areas (e.g., Cook, 1965; Quinlivan and others, 1974). An $^{40}\text{Ar}/^{39}\text{Ar}$ laser date on sanidine yielded an age of 31.31 ± 0.04 Ma (Table 2). Other researchers report $^{40}\text{Ar}/^{39}\text{Ar}$ incremental release ages of 31.3 Ma for the Windous Butte Formation (e.g., Radke, 1992; Best and others, 1993). Therefore, recognizing that phenocryst compositions of distal outflow sheets vary, this unit is interpreted to correlate with the Windous Butte Formation. Furthermore, the Windous Butte Formation crops out on the eastern side of the range (W.J. Taylor, unpublished mapping) and the Windous Butte type section lies only 30 km southeast of the study area, thus, suggesting that the Windous Butte Formation could occur in the area.

Tertiary andesite of Blackrock Canyon

The youngest volcanic unit exposed in the study area is an aphanitic andesite containing plagioclase and clinopyroxene phenocrysts <0.5 mm in diameter (Table 1).

In the study area, the andesite is exposed in only one locality; the unit caps a hill located along the range front, near the entrance to Blackrock Canyon. The andesite is black on a fresh surface and weathers to brown-black. It weathers to large, angular blocks that exhibit pervasive weathering rinds and form blocky talus slopes.

Previously, this unit was called a basalt (Lumsden, 1964; Pipkin, 1956). The percentage of SiO_2 in the rock, determined by X-ray Fluorescence (XRF), however, indicates that this unit is an andesite (Figure 27; Table 3). Therefore, the ~120-m-thick unit is here informally named the andesite of Blackrock Canyon.

An unnamed andesite also crops out in the Duckwater Hills, just west of the study area (Figure 1) (Pipkin, 1956; Langrock and Taylor, unpublished data). XRF analyses of samples from the andesite in the Duckwater Hills (L94DH-3) and the andesite of Blackrock Canyon in the study area (L95WP-1) suggest that the two andesites are cogenetic. Geochemical plots of incompatible element ratios suggest that the two rocks are very similar in composition and that one could not have been produced from the other via fractional crystallization. A plot of Nb/Rb vs. Sr shows that the “Duckwater Hills” andesite is slightly more enriched with respect to these incompatible elements (Figure 28a) than the andesite of Blackrock Canyon. However, crystal fractionation models, show that the more depleted Blackrock andesite was not produced from the Duckwater Hills andesite by fractionating either plagioclase or clinopyroxene (Figure 28a).

Another incompatible element ratio plot of Nb/Rb vs. Zr/Y shows that the geochemical differences between the two andesites is negligible (Figure 28b). The data are compared with data from cogenetic Pleistocene basalts of the Crater Flat volcanic field, Nevada (Bradshaw and Smith, 1994). Based on both isotopic and geochemical data, the Crater Flat basalts define three cogenetic magma types, each erupted from a different volcano. This plot illustrates that the clustering of the Blackrock andesite data

points lies well within the spread of precisely known fields of cogenetic rocks, thus, suggesting that the two andesites were generated from the same source (Figure 28b). They are considered lithological correlatives and may be temporally correlative as well.

Table 1a. Modal percentages of constituents in each of the volcanic units determined from point count analysis. Numbers are percentages of the entire rock and numbers in parentheses are relative percentages of phenocrysts.

Unit Name/ Sample #	Quartz	Sanidine	Plagioclase	CPX	Biotite	Horn- blende	Fe-oxides	Phenocrysts	Matrix	Pumice	Spherio- lites	Lithics	Total
Stone Cabin Fm:													
L94WP-Tsc	16.1 (43)	14.8 (40)	5.1 (14)	0	0.5 (1)	0	0.7 (2)	37.3	45.2	17.3	0	0.2	100
L94WP-314	12.9 (34)	6.2 (17)	16.2 (43)	0	2.3 (6)	0	0	37.5	49.2	13.3	0	0	100
Rhyolite of White Pine Range:													
L94WP-309	0.4 (2.5)	0.4 (2.5)	14.2 (88)	0	0	0	1.2 (7)	16.1	83.9	0	0	0	100
L94WP-310	0.7 (6)	0.4 (3)	11 (87)	0	0	0	0.5 (4)	12.6	87.4	0	0	0	100
L94WP-311	0.4 (3)	0.4 (3)	11.9 (91)	0	0	0	0.4 (3)	13	87	0	0	0	100
L94WP-312	0.5 (4)	0.2 (1)	13.6 (95)	0	0	0	0	14.3	85.7	0	0	0	100
L94WP-313	1.1 (7)	0.4 (3)	14.1 (90)	0	0	0	0	15.6	84.4	0	0	0	100
Current Tuff:													
L94WP-1	4.9 (18)	2.6 (9)	15.9 (58)	0	3.3 (12)	0	0.7 (3)	27.4	66	6.6	0	0	100
Window Butte Formation:													
L94WP-234	1.2 (8)	3.1 (20)	8.6 (55)	0	1.9 (12)	0.7 (5)	0	15.5	84.3	0.2	0	0	100
L94WP-220	9 (23)	7.2 (18)	15.4 (40)	0	4.6 (12)	2.6 (7)	0	38.8	51.8	6.6	2.8	0	100
Andesite of Blackrock Canyon:													
L94WP-Ta	0	0	30.3 (62)	18.9 (38)	0	0	0	49.2	50.8	0	0	0	100

Table 1b. Volume percentages of constituents in each of the volcanic units determined from point count analysis. Numbers are percentages of the entire rock and numbers in parentheses are relative percentages of phenocrysts.

Unit Name/ Sample #	Quartz	Sanidine	Plagioclase	CPX	Biotite	Horn- blende	Fe-oxides	Phenocrysts	Matrix	Pumice	Spherio- lites	Lithics	Total
Stone Cabin Fm:													
L94WP-Tsc	19.3 (47)	14.7 (36)	5.7 (14)	0	0.5 (1)	0	0.7 (2)	40.8	42.7	16.3	0	0.2	100
L94WP-314	17.7 (43)	6 (14)	15.8 (38)	0	2 (5)	0	0	41.5	42.7	15.8	0	0	100
Rhyolite of White Pine Range:													
L94WP-309	0.3 (1.5)	0.3 (1.5)	17.2 (91)	0	0	0	1.2 (6)	19	81	0	0	0	100
L94WP-310	1.2 (6)	0.5 (3)	15.8 (88)	0	0	0	0.5 (3)	18	82	0	0	0	100
L94WP-311	0.5 (3)	0.7 (4)	15.8 (91)	0	0	0	0.3 (2)	17.3	82.7	0	0	0	100
L94WP-312	0.8 (5)	0.2 (1)	16.3 (94)	0	0	0	0	17.3	82.7	0	0	0	100
L94WP-313	2 (9)	0.3 (1)	20.8 (90)	0	0	0	0	23.2	76.8	0	0	0	100
Current Tuff:													
L94WP-1	6.5 (21)	3 (10)	17.2 (56)	0	3.2 (11)	0	0.7 (2)	30.5	63.2	6.3	0	0	100
Window Butte Formation:													
L94WP-234	1.2 (6)	3.3 (18)	11.3 (62)	0	1.8 (10)	0.7 (4)	0	18.3	81.5	0.2	0	0	100
L94WP-220	12.5 (28)	8.3 (19)	17.2 (39)	0	4.2 (9)	2.3 (5)	0	44.5	47	6	2.5	0	100
Anesite of Blackrock Canyon:													
L94WP-Ta	0	0	30.2 (59)	21 (41)	0	0	0	51.2	48.8	0	0	0	100

Table 2. $^{40}\text{Ar}/^{39}\text{Ar}$ data of sanidine crystals from the Window Butte Formation, sample L94WP-307.

Run ID#	40/39	37/39	36/39	^{39}K moles	K/Ca	%40*	Age	\pm Error
3138-10	11.96	5.97×10^{-3}	4.12×10^{-4}	6.3×10^{-15}	85.4	99.0	31.252	0.084
3138-01	11.89	7.74×10^{-3}	1.73×10^{-4}	5.1×10^{-15}	65.9	99.6	31.255	0.087
3138-08	12.02	6.39×10^{-3}	5.63×10^{-4}	7.8×10^{-15}	79.9	98.6	31.298	0.077
3138-04	11.96	5.36×10^{-3}	3.13×10^{-4}	6.6×10^{-15}	95.1	99.2	31.331	0.075
3138-07	11.91	5.26×10^{-3}	1.53×10^{-4}	6.2×10^{-15}	97.1	99.6	31.335	0.081
3138-06	11.90	5.26×10^{-3}	1.11×10^{-4}	6.0×10^{-15}	96.9	99.7	31.342	0.083
3138-03	11.92	5.68×10^{-3}	1.63×10^{-4}	9.1×10^{-15}	89.8	99.6	31.355	0.075
3138-09	12.08	6.33×10^{-3}	4.54×10^{-4}	3.5×10^{-15}	80.6	98.9	31.545	0.095
3138-05	12.00	5.13×10^{-3}	1.54×10^{-4}	3.6×10^{-15}	99.4	99.6	31.574	0.093
3138-02	11.88	6.22×10^{-3}	-4.02×10^{-4}	1.7×10^{-15}	82.0	101.0	31.674	0.135
mean: n=7							31.310	0.042
standard error of the mean= 0.016								

$D = 1.00890$ 0.00180
 $^{39}\text{Ca}/^{37}\text{Ca} = 0.00070$ 0.00005
 $^{36}\text{Ca}/^{37}\text{Ca} = 0.00026$ 0.00002
 $^{38}\text{K}/^{39}\text{K} = 0.01190$
 $^{40}\text{K}/^{39}\text{K} = 0.00020$ 0.00030

$J = 0.0014765 + 0.000002$

Analyses performed by Dr. W.C. McIntosh, New Mexico Institute of Mining and Technology.

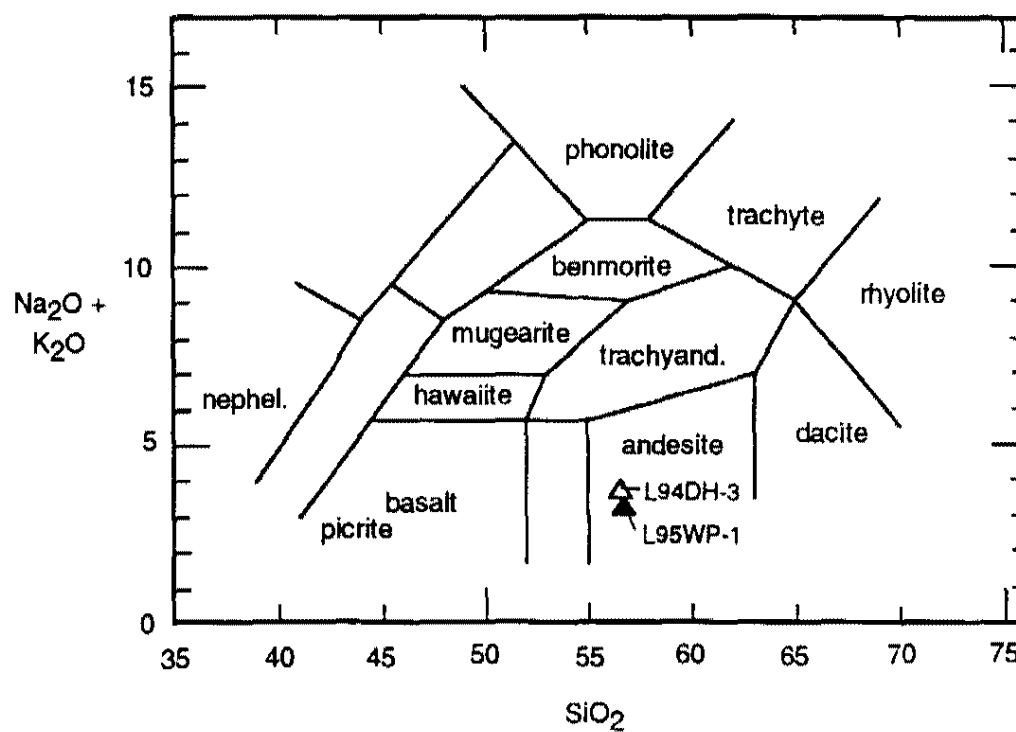


Figure 27. Cox igneous classification diagram illustrating that the black lavas in the White Pine Range (L95WP-1) and Duckwater Hills (L94DH-3) are andesites.

Table 3. Major and trace element concentrations of andesite collected in the Duckwater Hills (L94DH-3) and the Blackrock Canyon area (L95WP-1).

Sample #	L94DH-3	L95WP-1
Major Elements:		
Concentration (wt%)		
SiO ₂	56.6	56.8
Al ₂ O ₃	13.8	13.6
TiO ₂	1.24	1.29
FeO*	8.3	9.0
MgO	5.1	5.2
CaO	7.7	8.2
Na ₂ O	1.87	1.80
K ₂ O	1.82	1.43
MnO	0.13	0.13
P ₂ O ₅	0.21	0.29
Total wt. % ¹	96.79	97.72
Trace Elements:		
Concentration (ppm)		
Rb	51.1	56.4
Sr	501	458
Ba	530	396
Nb	16.4	15.3
Y	29.9	24.7
Zr	263	233

¹Totals do not include loss on ignition (LOI).

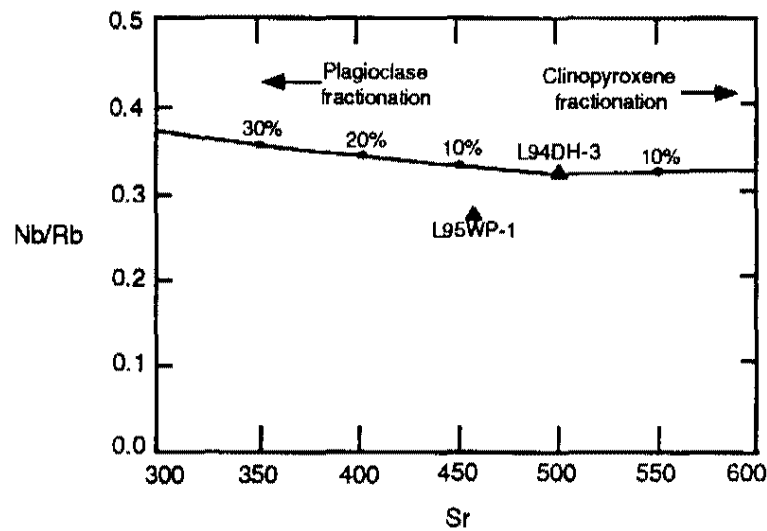


Figure 28a. Nb/Rb vs. Sr plot illustrating that the more depleted andesite of Blackrock Canyon (L95WP-1) cannot be produced from the "Duckwater Hills" andesite (L94DH-3) via fractional crystallization of either plagioclase or clinopyroxene. The following bulk distribution coefficients (D_o) are used in the model: in plagioclase, (Sr) $D_o = 0.1$; (Nb) $D_o = 0.01$; (Rb) $D_o = 0.031$ and in clino-pyroxene, (Sr) $D_o = 2$; (Nb) $D_o = 0.1$; (Rb) $D_o = 0.39$ (Larsen and Smith, 1990).

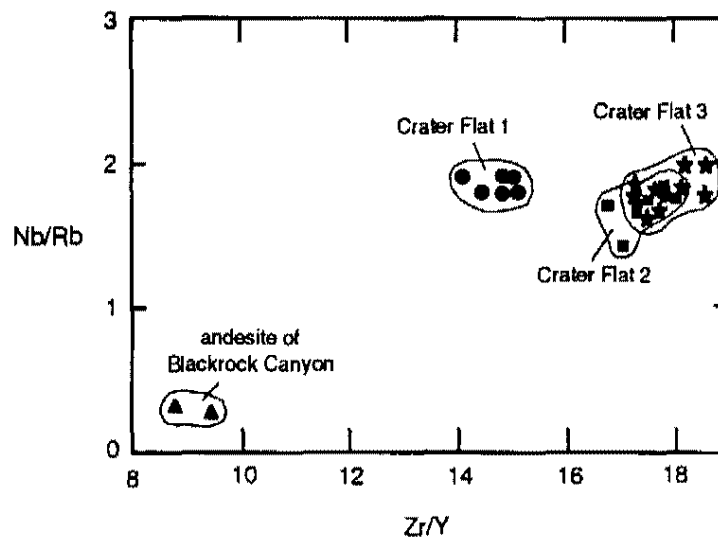


Figure 28b. Nb/Rb vs. Zr/Y plot of cogenetic groups of Crater Flat basalts (Bradshaw and Smith, 1994) and andesite samples from Blackrock Canyon and the Duckwater Hills. This plot shows that the two andesites are probably cogenetic. The data points lie within the "spread" of well-constrained cogenetic rocks.

APPENDIX B

METHODS

The methodology of data collection and analyses includes geologic mapping, stereonet analyses, balanced cross section techniques, point counts, x-ray fluorescence, and $^{40}\text{Ar}/^{39}\text{Ar}$ radiometric dating. All of these techniques collectively resulted in the analysis and interpretation of the data and each technique is briefly discussed below.

Geologic Mapping

Geologic mapping at a scale of 1:24,000 was conducted during the summer of 1994. Standard field mapping techniques were employed. A geologic map was created on the Duckwater N.E., Currant Mtn., Green Springs, and Indian Garden Mtn. U.S.G.S. 7.5' topographic quadrangles. Aerial photographs served as an aid, but the mapping was performed on foot.

Cross Section Techniques

Deformed-state cross sections of the study area were created using basic kink-method cross section techniques (Suppe, 1983). The kink-method was used consistently throughout the cross section except where there are fault propagation folds. For fault propagation folds, the Busk method (Rowland and Duebendorfer, 1994) is used because it is easier to maintain constant unit thickness. Only one fault yielded a measurable surface in the field area, therefore fault attitudes were calculated using either the three-point or structure contour method. Both the bedding and fault orientations were

corrected for apparent dips. Constant thickness of units is maintained and are based on regional thicknesses (Langenheim and Larson, 1973; Hintze, 1985).

Deformed-state cross sections were restored by a step-wise process. Tertiary normal faults were restored first, followed by the restoration of pre-Tertiary normal faults and contractile structures. Separate, but related cross-section balancing techniques were used for normal faults (e.g., Davison, 1986; Wheeler, 1987; Groshong, 1989; Rowan and Kligfield, 1989; White, 1992) and contractile structures (e.g., Dahlstrom, 1969; Suppe, 1983; Woodward and others, 1989).

$^{40}\text{Ar}/^{39}\text{Ar}$ Methods

One $^{40}\text{Ar}/^{39}\text{Ar}$ date (L94WP-307) on the Windous Butte Formation was obtained as part of this study. Approximately 2 kg of vitrophyre was collected and trimmed of all weathered surfaces. The sample was crushed and sieved to uniform grain sizes and a size range was chosen that yielded the largest possible individual grains. Mineral separates of sanidine were removed using standard physical methods including frantzing, heavy liquids separation, and hand picking. The physical mineral separations were completed by the author at separation facilities at the University of Nevada, Las Vegas.

Ten single sanidine grains were analyzed by W.C. McIntosh, using the $^{40}\text{Ar}/^{39}\text{Ar}$ laser technique, at New Mexico Institute of Mining and Technology. Methods of isotope measurements and data reductions are described by (McIntosh and Quade, 1995). The 27.84 Ma Fish Canyon Tuff (age relative to the Minnesota Hornblende) was used as a standard. The data is presented in Table 2.

X-ray Fluorescence Techniques

X-ray fluorescence spectrometry (XRF) was conducted on two samples of the Blackrock andesite, L94DH-3 and L95WP-1. Approximately 1/2 kg of sample was collected and trimmed of all weathered surfaces in the field. The samples were then

crushed to <325 mesh using a Bico jaw crusher and shatterbox. Trace element analyses were completed on pressed pellets using 0.6 g of methyl cellulose and 3.00 g of sample (Hutchison, 1974). Major element analyses were completed on fused glass disks using 9.00 g of lithium tetraborate, 0.16 g of ammonium nitrate, and 1.00 g of sample. The disks were heated to 1100° C in Au-Pt crucibles and allowed to cool in Au-Pt molds (Noorish and Hutton, 1969).

The samples were analyzed for trace elements (Zr, Rb, Sr, Nb, Y, Ba) and major elements (Si, Al, Ti, Fe, Mg, Ca, Na, K, Mn, P). Shirley A. Morikawa and Alex J. Sanchez completed the analyses on a Rigaku 3030 spectrometer at the University of Nevada, Las Vegas. The following standards were used to establish accuracy and precision of the spectrometer: U.S.G.S. MAG-1 (trace elements) and U.S.G.S. BIR-1 and GIT-IWG BE-N (major elements). Table 3 shows the accuracy and precision for major and trace elements.

Point Count Analysis

Thin sections of each volcanic unit exposed in the study area were examined using a petrographic microscope. Six hundred points were counted per sample using a fixed-grid spacing. For most samples, two thin sections, oriented mutually perpendicular, were counted (300 points each) to minimize any differences in grain distribution throughout the rock. Both volume and modal percentages of all constituents were determined (Table 1).

Table 4. Standard deviation, precision and accuracy of measurements using standards U.S.G.S. BIR-1, GIT-IWG BE-N, and U.S.G.S. MAG-1.

Element	Standard/ Published Value	Mean of replicate analyses	Standard Deviation ($\pm 1\sigma$)	% Precision	% Accuracy
	BIR-1	n=16			
SiO ₂	47.77	47.13	0.52	1.11	1.33
Al ₂ O ₃	15.35	15.16	0.17	1.10	3.13
TiO ₂	0.96	0.95	0.02	1.80	1.24
Fe ₂ O ₃	11.26	11.14	0.10	0.89	1.05
CaO	13.24	13.05	0.09	0.69	1.43
MnO	0.17	1.68	0.10	5.84	4.15
NaO	1.75	0.17	0.00	2.64	0.21
MgO	9.68	9.61	0.25	2.62	0.70
	BE-N	n=15			
K ₂ O	1.39	1.42	0.02	1.17	2.11
P ₂ O ₅	1.05	1.01	0.02	1.82	4.25
	MAG-1	n=15			
Zr	149	130.34	3.03	2.3	3.4
Sr	146	174.88	3.54	2.4	1.3
Nb	12	16.82	0.79	4.7	40.2
Y	28	29.28	1.24	4.2	4.6
Rb	149	151.93	3.48	2.3	5.3
Ba	479	493.27	26.30	5.3	3.0

REFERENCES CITED

- Allmendinger, R.W., 1989, Stereonet v. 4.3, a program for the Macintosh computer, copyrighted software.
- Allmendinger, R.W., 1992, Fold and thrust tectonics of the western United States exclusive of the accreted terranes, *in* Burchfiel, B.C., Lipman, P.W., and Zoback, M.L., eds., *The Cordilleran orogen: conterminous U.S.*: Geological Society of America, *The Geology of North America*, v. G-3, Boulder, p. 583-608.
- Anderson, E.M., 1951, *The Dynamics of Faulting*: Oliver and Boyd, London, 206 p.
- Armstrong, P.A., and Bartley, J.M., 1993, Displacement and deformation associated with a lateral thrust termination, southern Golden Gate Range, southern Nevada, U.S.A.: *Journal of Structural Geology*, v. 15, no. 6, p. 721-735.
- Armstrong, R.L., 1968, Sevier orogenic belt in Nevada and Utah: *Geological Society of America Bulletin*, v. 79, p. 429-458.
- Armstrong, R.L., and Oriel, S.S., 1965, Tectonic development of Idaho-Wyoming thrust belt: *American Association of Petroleum Geologists Bulletin*, v. 48, p. 1847-1866.
- Axen, G.J., Wernicke, B.P., Skelly, M.J., and Taylor, W.J., 1990, Mesozoic and Cenozoic tectonics of the Sevier thrust belt in the Virgin River Valley area, southern Nevada, *in* Wernicke, B.P., ed., *Basin and Range extensional tectonics near the latitude of Las Vegas, Nevada*: Geological Society of America Memoir 176, p. 123-154.
- Axen, G.J., Taylor, W.J., and Bartley, J.M., 1993, Space-time patterns and tectonic controls of Tertiary extension and magmatism in the Great Basin of the western United States: *Geological Society of America Bulletin*, v. 105, p. 56-76.
- Aydin, A., 1977, *Faulting in Sandstone*: Ph.D. Dissertation, Stanford University, Stanford, 246 p.
- Aydin, A., and Reches, Z., 1982, Number and orientations of fault sets in the field and in experiments: *Geology*, v. 10, p. 107-112.
- Bartley, J.M., Axen, G.J., Taylor, W.J., and Fryxell, J.E., 1988, Cenozoic Tectonics of a transect through eastern Nevada near 38° N latitude, *in* Weide, D.L., and Faber, M.L., *This extended land; geological journeys in the southern Basin and Range*: Geological Society of America Field Trip Guidebook, p. 1-20.

- Bartley, J.M., and Gleason, G.C., 1990, Tertiary normal faults superimposed on Mesozoic thrusts, northern Quinn Canyon and southern Grant Ranges, Nye County, Nevada, *in* Wernicke, B.P., ed., Basin and Range extensional tectonics near the latitude of Las Vegas, Nevada: Geological Society of America Memoir 176, p. 195-212.
- Bartley, J.M., and Taylor, W.J., 1991, Central Nevada thrust belt formed in the Jurassic Elko Orogeny?: Geological Society of America Abstracts with Programs, v. 23, no. 5, p. A192.
- Bartley, J.M., Taylor, W.J., Fryxell, J.E., Schmitt, J.G., Vandervoort, D.S., and Walker, J.D., 1993, Tectonic style and regional relations of the Central Nevada Thrust Belt: Geological Society of America Abstracts with Programs, v. 25, no. 5, p. A7.
- Barrett, R.A., 1987, The maturation of the Mississippian Chainman Shale in Railroad Valley, Nye county, Nevada: M.S. Thesis, University of Wyoming, Laramie, 82 p.
- Best, M.G., Christiansen, E.H., Deino, A.L., Grommé, C.S., McKee, E.H., and Noble, D.C., 1989, Eocene through Miocene volcanism in the Great Basin of the western United States: New Mexico Bureau of Mines and Mineral Resources Memoir 47, p. 91-133.
- Best, M.G., Scott, R.B., Rowley, P.D., Swadley, W.C., Anderson, R.E., Grommé, C.S., Harding, A.E., Deino, A.L., Christiansen, E.H., Tingey, D.G., and Sullivan, K.R., 1993, Oligocene-Miocene caldera complexes, ash-flow sheets, and tectonism in the central and southeastern Great Basin, *in* Lahren, M.M., Trexler, J.H., Jr., and Spinosa, C., eds., Crustal evolution of the Great Basin and Sierra Nevada: Cordilleran/Rocky Mountain Section, Geological Society of America Guidebook, Department of Geological Sciences, University of Nevada, Reno, p. 285-311.
- Bissell, H.J., 1964, Ely, Arcturus, and Park City Groups (Pennsylvanian-Permian) in eastern Nevada and western Utah: American Association of Petroleum Geologists Bulletin, v. 48, no. 5, p. 565-636.
- Bortz, L.C., 1994, Petroleum geology of the Eagle Springs oil field, Nye County, Nevada, *in* Schalla, R.A., and Johnson, E.H., eds., Oil Fields of the Great Basin: Nevada Petroleum Society, p. 289-298.
- Boyer, S.E., and Elliot, D., 1982, Thrust systems: American Association of Petroleum Geologists Bulletin, v. 66, p. 1196-1230.
- Bradshaw, T.K., and Smith, E.I., 1994, Polygenetic Quaternary volcanism in Crater Flat, Nevada: Journal of Volcanology and Geothermal Research, v. 63, p. 165-182.
- Brew, D.A., 1961, Lithologic character of the Diamond Peak Formation (Mississippian) at the type locality, Eureka and White Pine Counties, Nevada: U.S. Geological Survey Paper 424-C, p. 110-112.

- Burchfiel, B.C., and Davis, G.A., 1972, Structural framework and evolution of the southern part of the Cordilleran orogen, western United States: *American Journal of Science*, v. 272, p. 97-118.
- Burchfiel, B.C., Cowan, D.S., and Davis, G.A., 1992, Tectonic overview of the Cordilleran orogen in the western United States, *in* Burchfiel, B.C., Lipman, P.W., and Zoback, M.L., eds., *The Cordilleran orogen: conterminous U.S.*: Geological Society of America, *The Geology of North America*, v. G-3, Boulder, p. 407-480.
- Burchfiel, B.C., Molnar, P., Zhang, P., Deng, Q., Zhang, W., and Wang, Y., 1995, Example of a supradetachment basin within a pull-apart tectonic setting: Mormon Point, Death Valley, California: *Basin Research*, v. 7, p. 199-214.
- Camilleri, P.A., 1989, Superposed compressional and extensional strain in metamorphosed lower Paleozoic rocks of the northwestern Grant Range, Nevada: M.S. Thesis, Oregon State University, Corvallis, 84 p.
- Camilleri, P.A., 1992, Extensional Geometry of a part of the northwestern flank of the northern Grant Range, Nevada: inferences of its evolution: *The Mountain Geologist*, v. 29, no. 3, p. 75-84.
- Carpenter, D.G., Carpenter, J.A., Dobbs, S.W., and Stuart, C.K., 1993, Regional structural synthesis of Eureka fold-and-thrust-belt, east-central Nevada, *in* Gillespie, C.W., ed., *Structural and Stratigraphic Relationships of Devonian Reservoir Rocks, East-Central Nevada*: Nevada Petroleum Society 1993 Field Conference Guidebook, p. 59-72.
- Carr, M.D., Poole, F.G., and Christiansen, R.L., 1984, Pre-Cenozoic geology of the el Paso Mountains, southwestern Great Basin, California; A summary, *in* Lintz, J. Jr., ed., *Western geological excursions: Geological society of America 1984 Annual Meeting Field Trip Guide*: University of Nevada Mackay School of Mines, v. 4, p. 84-93.
- Cook, E.H., 1965, Stratigraphy of Tertiary volcanic rocks in eastern Nevada: Nevada Bureau of Mines, Report 11, 61 p.
- Crone, A.J., and Harding, S.T., 1984, Relationships of late Quaternary fault scarps to subsequent faults, eastern Great Basin: *Geology*, v. 12, p. 292-295.
- Dahlstrom, D.C.A., 1969, Balanced cross sections: *Canadian Journal of Earth Sciences*, v. 6, p. 743-757.
- Davis, G.A., and Lister, G.S., 1988, Detachment faulting in continental extension; Perspectives from the southwestern U.S. Cordillera, *in* Clark, S.P., Jr., Burchfiel, B.C., and Suppe, J., eds., *Processes in continental lithospheric deformation*: Geological Society of America Special Paper 218, p. 133-160.
- Davison, I., 1986, Listric normal fault profiles: calculation using bed-length balance and fault displacement: *Journal of Structural Geology*, v. 5, p. 209-210.

- Drewes, H., and Palmer, A.R., 1957, Cambrian rocks of the southern Snake Range, Nevada: Geological Society of America Bulletin, v. 69, p. 221-240.
- Dohrenwend, J.C., Schell, B.A., and Moring, B.C., 1991, Reconnaissance photogeologic map of young faults in the Ely 1° by 2° Quadrangle, Nevada and Utah: U.S. Geological Survey Map MF-2181.
- Dohrenwend, J.C., Schell, B.A., and Moring, B.C., 1991, Reconnaissance photogeologic map of young faults in the Lund 1° by 2° Quadrangle, Nevada and Utah: U.S. Geological Survey Map MF-2180.
- Donath, F.A., 1962, Analysis of basin-range structure, south-central Oregon: Geological Society of America Bulletin, v. 73, p. 1-16.
- Duey, H.D., 1983, Oil generation and entrapment in Railroad Valley, Nye County, Nevada, *in* The role of heat in the development of energy and mineral resources in the northern Basin and Range Province: Geothermal Resources Council Special Report n. 13, p. 199-205.
- Flanigan, T.E., 1994, Blackburn field: Oil above a low-angle detachment fault in Eureka County, Nevada, *in* Schalla, R.A., and Johnson, E.H., eds., Oil Fields of the Great Basin: Nevada Petroleum Society, p. 343-364.
- French, D.E., and Freeman, K.J., 1979, Tertiary volcanic stratigraphy and reservoir characteristics of Trap Spring field, Nye County, Nevada, *in* Newman, G.W., and Goode, H.D., eds., 1979 Basin and Range Symposium: Rocky Mountain Association of Geologists and Utah Geological Association, p. 487-502.
- French, D.E., 1994, Petroleum geology of Trap Spring oil field, Nye County, Nevada, *in* Schalla, R.A., and Johnson, E.H., eds., Oil Fields of the Great Basin: Nevada Petroleum Society, p. 259-274.
- Fryxell, J.E., 1988, Geologic map and descriptions of stratigraphy and structure of the west-central Grant Range, Nye County, Nevada: Geological Society of America Map and Chart Series MCH064.
- Fryxell, J.E., 1991, Tertiary tectonic denudation of an igneous and metamorphic complex, west-central Grant Range, Nye County, Nevada, *in* Raines, G.H., Lisle, R.E., Schafer, R.W., and Wilkinson, W.H., eds., Geology and ore deposits of the Great Basin: Symposium Proceedings, Geological Society of Nevada, p. 87-92.
- Gabrielse, H., Snyder, W.S., and Stewart, J.H., 1983, Sonoma orogeny and Permian to Triassic tectonism in western North America: Geology, v. 11, p. 484-486.
- Gleason, G.C., 1989, Structural geology of the east flank of the southern Grant Range, Nye County, Nevada: M.S. Thesis, University of Utah, Salt Lake City, 114 p.
- Goff, F., Hulen, J.B., Adams, A.I., Trujillo, P.E., Counce, D., and Evans, W.C., 1994, Geothermal characteristics of some oil field waters in the Great Basin, Nevada, *in* Schalla, R.A., and Johnson, E.H., eds., Oil Fields of the Great Basin: Nevada Petroleum Society, p. 93-106.

- Grabb, R.F., 1994, Extensional tectonics and petroleum accumulations in the Great Basin, *in* Schalla, R.A., and Johnson, E.H., eds., *Oil Fields of the Great Basin*: Nevada Petroleum Society, p. 41-56.
- Groshong, R.H.J., 1989, Half-graben structures: Balanced models of extensional fault-bend folds: *Geological Society of America Bulletin*, v. 101, p. 96-105.
- Grow, J.A., Potter, C.J., and Miller, J.J., 1993, Seismic constraints on fault angles in Railroad Valley, Nevada: *Geological Society of America Abstracts with Programs*, v. 25, n. 5, p. 45.
- Guerrero, J.A., 1983, *Geology of the northern White Pine Range, east-central Nevada*: M.S. Thesis, California State University, Long Beach, 105 p.
- Hague, A., 1883, Abstract of report on the geology of the Eureka district, Nevada: U.S. Geological Survey Third Annual Report, 1881-1882, p. 237-290.
- Heller, P.L., Bowdler, S.S., Chambers, H.P., Coogan, J.C., Hagen, E.S., Shuster, M.W., Winslow, N.S., and Lawton, T.F., 1986, Time of initial thrusting in the Sevier orogenic belt, Idaho-Wyoming and Utah: *Geology*, v. 14, p. 388-391.
- Hintze, L.F., 1960, Ordovician of the Utah-Nevada Great Basin, *in* Boettcher, J.W., and Sloan, W.W., Jr., eds., *Geology of east central Nevada: Intermountain Association of Petroleum Geologists Guidebook, 11th Annual Field Conference*, p. 59-62.
- Hintze, L.F., 1985, Great Basin Region: Correlation of Stratigraphic Units of North America (COSUNA) Project: *American Association of Petroleum Geologists*, 1 plate.
- Hose, R.K., and Blake, M.C., Jr., 1976, *Geology and Mineral Resources of White Pine County, Nevada*: Nevada Bureau of Mines and Geology Bulletin 85, Part 1, 35 p.
- Humphrey, F.L., 1960, *Geology of the White Pine mining district, White Pine County, Nevada*: Nevada Bureau of Mines Bulletin 57, 119 p.
- Hutchison, C.S., 1974, *Laboratory Handbook of Petrographic Techniques*: John Wiley and Sons, New York, 527 p.
- Inan, S., and Davis, A., 1994, The history of oil generation in Pine and Railroad Valleys, eastern Nevada, *in* Schalla, R.A., and Johnson, E.H., eds., *Oil Fields of the Great Basin*: Nevada Petroleum Society, p. 57-84.
- Jordan, T.E., 1981, Thrust loads and foreland basin evolution, Cretaceous, western United States: *American Association of Petroleum Geologists Bulletin*, v. 65, p. 2506-2520.
- Kellogg, H.E., 1963, Paleozoic stratigraphy of the southern Egan Range, Nevada: *Geological Society of American Bulletin*, v. 74, p. 685-708.

- King, C., 1878, Systematic geology: U.S. Geological Exploration 40th Parallel, v.1.
- Kirk, E., 1933, The Eureka quartzite of the Great Basin region: American Journal of Science, 5th series, v. 26, p. 27-44.
- Kleinhampl, F.J., and Ziony, J.I., 1985, Geology of northern Nye County, Nevada: Nevada Bureau of Mines and Geology Bulletin 99A, 172 p.
- Krantz, R.W., 1988, Multiple fault sets and three-dimensional strain: Theory and application: Journal of Structural Geology, v. 10, p. 225-237.
- Krantz, R.W., 1989, Orthorhombic fault patterns: The odd axis model and slip vector orientations: Tectonics, v. 8, no. 3, p. 483-495.
- Langenheim, R.L., Jr., and Larson, E.R., 1973, Correlation of Great Basin Stratigraphic Units, Nevada Bureau of Mines and Geology Bulletin 72, 36 p.
- Langrock, H., and Taylor, W.J., 1995, Extensional tectonics of a part of the southwestern White Pine Range, Nevada: Implications for petroleum occurrence in Railroad Valley: 1995 AAPG Rocky Mountain Section Meeting Official Program, p. A7.
- Larsen, L.L., and Smith, E.I., 1990, Mafic enclaves in the Wilson Ridge pluton, northwestern Arizona: Implications for the generation of a calc-alkaline intermediate pluton in an extensional environment: Journal of Geophysical Research, v. 95, n. B11, p. 17693-17716.
- Lawson, A.C., 1906, The copper deposits of the Robinson mining district, Nevada: University of California Department of Geology Bulletin 4, p. 287-357.
- Levy, M., and Christie-Blick, N., 1991, Tectonic subsidence of the early Paleozoic passive continental margin in eastern California and southern Nevada: Geological Society of America Bulletin, v. 103, p. 1590-1606.
- Lumsden, W.W., Jr., 1964, Geology of the southern White Pine Range and northern Horse Range, Nye and White Pine Counties, Nevada: Ph.D. dissertation, University of California, Los Angeles, 249 p.
- Lund K., Beard, L.S., and Perry, W.J., Jr., 1991, Structures of the northern Grant Range and Railroad Valley, Nye County, Nevada: Implications for oil occurrences *in* Flanigan, D.M.H., Hansen, M., and Flanigan, T.E., eds., Geology of White River Valley, the Grant Range, eastern Railroad Valley and western Egan Range, Nevada: 1991 Nevada Petroleum Society Fieldtrip Guidebook, p. 1-6.
- Lund, K. and Beard, L.S., 1992, Extensional Geometry in the northern Grant Range, east-central Nevada-- implications for oil deposits in Railroad Valley, *in* Thorman C.H., ed., Application of Structural Geology to Mineral and Energy Resources of the Central and Western United States: U.S. Geological Survey Bulletin 2012, p. 11-19.
- Malone, S.D., Rothe, G.H., and Smith, S.W., 1975, Details of microearthquake swarms in the Columbia Basin, Washington: Seismological Society of America Bulletin, v. 65, p. 844-864.

- McCutcheon, T.J., and Zogg, W.D., 1994, Structural geology of the Grant Canyon-Bacon Flat field area, Nye County, Nevada: Implications for hydrocarbon exploration in the Great Basin, *in* Schalla, R.A., and Johnson, E.H., eds., *Oil Fields of the Great Basin: Nevada Petroleum Society*, p. 201-226.
- McIntosh, W.C., and Quade, J., 1995, $^{40}\text{Ar}/^{39}\text{Ar}$ geochronology of tephra layers in the Santa Fe Group, Española Basin, New Mexico, *Geology of the Santa Fe Region: New Mexico Geological Society Guidebook, 46th Field Conference*, p. 279-287.
- Merriam, C.W., 1940, Devonian stratigraphy and paleontology of the Roberts Mountain region, Nevada: *Geological Society of America Special Paper 25*, 114 p.
- Merriam, C.W., 1963, Paleozoic rocks of Antelope Valley Eureka and Nye Counties, Nevada: *U.S. Geological Survey Professional Paper 423*, 62 p.
- Miller, E.L., Gans, P.B., and Garing, J., 1983, The Snake Range decollement: An exhumed mid-Tertiary ductile-brittle transition: *Tectonics*, v. 2, p. 239-263.
- Miller, E.L., Miller, M.M., Stevens, C.H., Wright, J.E., and Madrid, R., 1992, Late Paleozoic paleogeographic and tectonic evolution, *in* Burchfiel, B.C., Lipman, P.W., and Zoback, M.L., eds., *The Cordilleran orogen: conterminous U.S.: Geological Society of America, The Geology of North America*, v. G-3, Boulder, p. 57-106.
- Misch, P., 1960, Regional structural reconnaissance in central-northeast Nevada and some adjacent areas: observations and interpretations *in* Boettcher, J.W., and Sloan, W.W., Jr., eds., *Geology of east central Nevada: Intermountain Association of Petroleum Geologists Guidebook, 11th Annual Field Conference*, p. 17-42.
- Moore, E.M., Scott, R.B., and Lumsden, W.W., 1968, Tertiary tectonics of the White Pine-Grant Range region, east-central Nevada: *Geological Society of America Bulletin*, v. 79, p. 1703-1726.
- Nolan, T.B., 1930, Paleozoic formations in the Gold Hill quadrangle, Utah: *Journal of Washington Academy of Science*, v. 20, no. 17, p. 421-432.
- Nolan, T.B., 1935, The Gold Hill mining district, Utah: *U.S. Geological Survey Professional Paper 177*, 172 p.
- Nolan, T.B., Merriam, C.W., and Williams, J.S., 1956, The stratigraphic section in the vicinity of Eureka, Nevada: *U.S. Geological Survey Professional Paper 276*, 77 p.
- Nolan, T.B., Merriam, C.W., and Blake, M.C., 1974, Geologic map of the Pinto Summit Quadrangle, Eureka and White Pine Counties, Nevada: *U.S. Geological Survey Miscellaneous Investigation Series Map I-793*.
- Noorish, K., and Hutton, J.T., 1969, An accurate X-ray spectrographic method for the analysis of a wide range of geological samples: *Geochimica et Cosmochimica Acta*, v. 33, p. 431-453.

- Ode', H., 1960, Faulting as a velocity discontinuity in plastic deformation: Geological Society of America Memoir 79, p. 293-321.
- Oertel, G., 1965, The mechanics of faulting in clay experiments: Tectonophysics, v. 2, p. 343-393.
- Oldow, J.S., 1983, Tectonic implication of a late Mesozoic fold and thrust belt in northwestern Nevada: Geology, v. 11, p. 542-546.
- Oldow, J.S., 1984, Spatial variability in the structure of the Roberts Mountains allochthon, western Nevada: Geological Society of America Bulletin, v. 95, p. 174-185.
- Pennebaker, E.N., 1932, Geology of the Robinson (Ely) mining district in Nevada: Mining and Metallurgy, v. 13, p. 163-168.
- Perry, W.J., Jr., 1992, Structure of the northern Pancake Range, Nevada; a progress report: Geological Society of America Abstracts with Programs, v. 24, no. 6, p. A57.
- Perry, W.J., Jr., 1994, Pre-Oligocene structure of central Railroad Valley area and adjacent Pancake Range, Nevada - western margin of the Paleogene Sheep Pass basin: AAPG 1994 Annual Convention Program, v. 3, p. 233.
- Perry, W.J., Jr., and Dixon, G.J., 1993, Structure and time of deformation in the central Pancake Range, *in* Gillespie, C.W., ed., Structural and stratigraphic relationships of Devonian reservoir rocks, east-central Nevada: 1993 Field Conference Guidebook, Nevada Petroleum Society, p. 123-132.
- Pipkin, B.W., 1956, Geology of the south third of the Green Springs quadrangle, Nevada: M.A. Thesis, University of Southern California, Los Angeles, 82 p.
- Poole, F.G., and Sandberg, C.A., 1977, Mississippian Paleogeography and conodont biostratigraphy of the western United States, *in* Cooper, J.D., and Stevens, C.H., eds., Paleozoic Paleogeography of the Western United States II: Pacific Section Society Economic Paleontologists and Mineralogists, v. 67, p. 107-136.
- Quinlivan, W.D., Rogers, C.L., and Dodge, H.W., Jr., 1974, Geologic map of the Portuguese Mountain quadrangle, Nye County, Nevada: U.S. Geological Survey Miscellaneous Investigations Series map I-804.
- Radke, L.E., 1992, Petrology and temporal evolution of the rhyolite ash-flow tuffs of the 35.3 Ma Stone Cabin Formation, Central Nevada: M.S. Thesis, Brigham Young University, Provo, 65 p.
- Reches, Z., 1978, Analysis of faulting in three-dimensional strain field: Tectonophysics, v. 47, p. 109-129.
- Reches, Z., 1983, Faulting of rocks in three-dimensional strain fields. II. Theoretical analysis: Tectonophysics, v. 95, p. 133-156.

- Reches, Z., and Dieterich, J.H., 1983, Faulting of rocks in three-dimensional strain fields I. Failure of rocks in polyaxial servo-control experiments: *Tectonophysics*, v. 95, p. 111-132.
- Richardson, G.B., 1913, The Paleozoic section in northern Utah: *American Journal of Science*, 4th series, v. 36, p. 406-416.
- Roberts, R.J., Hotz, P.E., Gilluly, J., and Ferguson, H.G., 1958, Paleozoic rocks of north-central Nevada: *American Association of Petroleum Geologists Bulletin*, v. 49, p. 1926-1956.
- Rowan, M.G., and Kligfield, R., 1989, Cross section restoration and balancing as aid to seismic interpretation in extensional terranes: *American Association of Petroleum Geologists Bulletin*, v. 73, p. 955-966.
- Rowland, S.M., and Deubendorfer, E.M., 1994, Structural analysis and synthesis, a laboratory course in structural geology, 2nd edition: Blackwell Scientific Publications, Boston, 279 p.
- Sadlick, W., 1960, Some preliminary aspects of Chainman stratigraphy, in Boettcher, J.W., and Sloan, W.W., Jr., eds., *Geology of east central Nevada: Intermountain Association of Petroleum Geologists Guidebook*, 11th Annual Field Conference, p. 81-90.
- Saleeby, J.B., and Busby-Spera, C., 1992, Early Mesozoic tectonic evolution of the western U.S. Cordillera, in Burchfiel, B.C., Lipman, P.W., and Zoback, M.L., eds., *The Cordilleran orogen: conterminous U.S.: Geological Society of America, The Geology of North America*, v. G-3, Boulder, p. 107-168.
- Saltus, R.W., 1988, Bouguer gravity anomaly map of Nevada: Nevada Bureau of Mines and Geology Map 94A.
- Schalla, R.A., and Johnson, E.H., 1994, Introduction, in Schalla, R.A., and Johnson, E.H., eds., *Oil Fields of the Great Basin: Nevada Petroleum Society*, p. ix-xii.
- Scott, D.L., Etheridge, M.A., and Rosendahl, B.R., 1992, Oblique-slip deformation in extensional terrains: A case study of the Lakes Tanganyika and Malawi rift zones: *Tectonics*, v. 11, n. 5, p. 998-1009.
- Scott, R.B., 1965, The Tertiary geology and ignimbrite petrology of the Grant Range, east central Nevada: Ph.D. thesis (with appendix), Rice University, Houston, 241 p.
- Silberling, N.J., and Roberts, R.J., 1962, Pretertiary stratigraphy and structure of northwestern Nevada: *Geological Society of America Special Paper* 72, 58 p.
- Smith, E.I., 1984, Geologic map of the Boulder City quadrangle, Nevada: Nevada Bureau of Mines and Geology, Map 81.
- Speed, R.C., 1979, Collided Paleozoic microplate in the western United States: *Journal of Geology*, v. 87, p. 279-292.

- Speed, R.C., 1983, Evolution of the sialic margin in the central-western United States, *in* Watkins, J.S., and Drake, C.L., eds., *Studies in Continental Margin Geology: American Association of Petroleum Geologists Memoir 34, Hedburg Volume*, p. 457-468.
- Speed, R.C., Elison, M.W., and Heck, F.R., 1988, Phanerozoic history of the western Great Basin, *in* Ernst, W.G., ed., *Metamorphism and crustal evolution, western United States: Rubey Volume VII*, p. 573-605.
- Spencer, A.C., 1917, Geology and ore deposits of Ely, Nevada: U.S. Geological Survey Professional Paper 96, 189 p.
- Spencer, J.E., 1984, Role of tectonic denudation in warping and uplift of low-angle normal faults: *Geology*, v. 12, p. 95-98.
- Spencer, J.E., and Reynolds, S.J., 1990, Relationship between Mesozoic and Cenozoic tectonic features in west central Arizona and adjacent southeastern California: *Journal of Geophysical Research*, v. 95, p. 539-555.
- Steele, G., 1960, Pennsylvanian-Permian stratigraphy of east-central Nevada and adjacent Utah, *in* Boettcher, J.W., and Sloan, W.W., Jr., eds., *Geology of east central Nevada: Intermountain Association of Petroleum Geologists Guidebook, 11th Annual Field Conference*, p. 91-113.
- Stevens, C.H., 1977, Mississippian Paleogeography and conodont biostratigraphy of the western United States, *in* Cooper, J.D., and Stevens, C.H., eds., *Paleozoic Paleogeography of the Western United States II: Pacific Section Society of Economic Paleontologists and Mineralogists*, v. 67, p. 149-166.
- Stewart, J.H., and Poole, F.G., 1974, Lower Paleozoic and uppermost Precambrian cordilleran miogeocline, Great Basin, western United States, *in* Dickinson, W.R. ed., *Tectonics and Sedimentation: Society of Economic Paleontologists and Mineralogists Special Publication 22*, p. 28-57.
- Stewart, J.H., and Carlson, J.E., 1976, Cenozoic Rocks of Nevada-Four maps and brief description of distribution, lithology, age, and centers of volcanism: Nevada Bureau of Mines and Geology Map 52.
- Stewart, J.H., and Suczek, C.A., 1977, Cambrian and latest Precambrian paleogeography and tectonics in the western United States, *in* Stewart, J.H., Stevens, C.H., and Fritsche, A.E., eds, *Paleozoic paleogeography of the western United States, Pacific Coast Paleogeogeography Symposium 1: Society of Economic Mineralogists and Paleontologists*, p. 1-17.
- Stone, P., and Stevens, C.H., 1984, Stratigraphy and depositional history of Pennsylvanian and Permian rocks in the Owens Valley, Death Valley region, eastern California, *in* Lintz, J. Jr., ed., *Western geological excursions: Geological society of America 1984 Annual Meeting Field Trip Guide: University of Nevada Mackay School of Mines*, v. 4, p. 94-118.

- Suppe, J., 1983, Geometry and kinematics of fault-bend folding: *American Journal of Science*, v. 283, p. 684-721.
- Taylor, W.J., Bartley, J.M., Lux, D.R., and Axen, G.J., 1989, Timing of Tertiary extension in the Railroad Valley-Pioche transect, Nevada: Constraints from $^{40}\text{Ar}/^{39}\text{Ar}$ ages of volcanic rocks: *Journal of Geophysical Research*, v. 94, p. 7757-7774.
- Taylor, W.J., Bartley, J.M., Fryxell, J.E., Schmitt, J.G., and Vandervoort, D.S., 1993, Tectonic style and regional relations of the Central Nevada thrust belt, *in* Lahren, M.M., Trexler, J.H., Jr. and Spinosa, C., eds., *Crustal Evolution of the Great Basin and Sierra Nevada: Cordilleran/Rocky Mountain Section*, Geological Society of America Guidebook, Department of Geological Sciences, University of Nevada, Reno, p. 57-96.
- Thompson, G.A., and Burke, D.B., 1973, Rate and direction of spreading in Dixie Valley, Basin and Range province, Nevada: *Geological Society of America Bulletin*, v. 84, p. 627-632.
- Tracy, W.C., 1980, Structure and stratigraphy of the central White Pine Range, east-central Nevada: M.S. Thesis, California State University, Long Beach, 70 p.
- Varnes, D.J., 1962, Analysis of plastic deformation according to Von Mises' theory with application to the south Silverton area, San Juan County, Colorado: U.S. Geological Survey Professional Paper 378-B, 49 p.
- Walcott, C.D., 1908, Nomenclature of some Cambrian Cordilleran formations: *Smithsonian Miscellaneous Collections*, v. 53, no. 5, p. 1-12.
- Wernicke, B., 1981, Low-angle normal faults in the Basin and Range province: nappe tectonics in an extending orogen: *Nature*, v. 291, no. 5817, p. 645-648.
- Wernicke, B., 1992, Cenozoic extensional tectonics of the U.S. Cordillera, *in* Burchfiel, B.C., Lipman, P.W., and Zoback, M.L., eds., *The Cordilleran orogen: conterminous U.S.: Geological Society of America, The Geology of North America*, v. G-3, Boulder, p. 553-582.
- Wheeler, J., 1987, Variable-heave models of deformation above listric normal faults: the importance of area conservation: *Journal of Structural Geology*, v. 9, p. 1047-1049.
- White, N., 1992, A method for automatically determining normal fault geometries at depth: *Journal of Geophysical Research*, v. 97, p. 1715-1733.
- Winfrey, W.M., Jr., 1960, Stratigraphy, correlation, and oil potential of the Sheep Pass Formation, east-central Nevada, *in* Boettcher, J.W., and Sloan, W.W., Jr., eds., *Geology of east central Nevada: Intermountain Association of Petroleum Geologists Guidebook*, 11th Annual Field Conference, p. 126-133.

Woodward, N.B., Boyer, S.E., and Suppe, J., 1989, Balanced geological cross-sections: an essential technique in geological research and exploration: American Geophysical Union, Short Courses in Geology, v. 6, 132 p.